Spring 5-10-2019

ROLE OF PKCBETA AND OXIDANT SIGNALING IN NEONATAL PULMONARY HYPERTENSION

Joshua R. Sheak

Joshua R. Sheak

Candidate

Biomedical Sciences Graduate Program: Cell Biology and Physiology

Department

This dissertation is approved, and it is acceptable in quality and form for publication:

Approved by the Dissertation Committee:

Thomas C. Resta, Ph.D. , Chairperson

Mary Beth Goens, M.D.

Nancy L. Kanagy, Ph. D.

Nikki L. Jernigan, Ph. D.

Diane S. Lidke, Ph. D.

ROLE OF PKCBETA AND OXIDANT SIGNALING IN NEONATAL PULMONARY HYPERTENSION

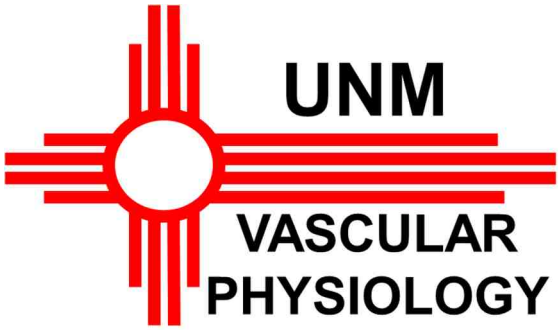

by

JOSHUA R. SHEAK

B.S., Biochemistry, University of New Mexico, 2010

DISSERTATION

Submitted in Partial Fulfillment of the
Requirements for the Degree of

Doctor of Philosophy
Biomedical Sciences

The University of New Mexico
Albuquerque, New Mexico

May 2019

DEDICATION

To mom and dad

Thank you for inspiring me to work hard for the things I love.

ACKNOWLEDGEMENTS

Thank you, Dr. Tom Resta, for your mentorship, encouragement, and support over the last five years. You have helped me build a foundation for scientific inquiry and hypothesis-driven research that will be with me throughout my career.

Thank you to my committee members Dr. Nancy Kanagy, Dr. Nikki Jernigan, Dr. Diane Lidke, and Dr. M. Beth Goens. I would also like to thank Dr. Benjimen Walker for his work on my Committee on Studies and his role in helping to shape this dissertation.

Additional thanks to the Vascular Physiology Group, members past and present, for their contributions during lab meetings, journal clubs, and during experiments in the laboratory. I am lucky to have been part of a positive, collaborative, and productive work environment.

Thanks to my parents for their support and encouragement. Finally, and most importantly, thank you Kenna for your love and support. I would not be the person I am today without you.

ROLE OF PKCBETA AND OXIDANT SIGNALING

IN NEONATAL PULMONARY HYPERTENSION

By

Joshua R. Sheak

B.S. Biochemistry, University of New Mexico, 2010

Ph.D., Biomedical Sciences, University of New Mexico, 2019

ABSTRACT

Chronic hypoxia (CH)-induced vasoconstriction has been implicated in the pathogenesis of pulmonary hypertension (pHTN) in infants with chronic cardiorespiratory disorders. Although endothelial dysfunction, reduced nitric oxide (NO) bioavailability and oxidative stress contribute to a variety of cardiovascular disorders, their contribution to enhanced vasoconstrictor reactivity in neonatal pHTN is poorly understood. We therefore hypothesized that neonatal CH augments pulmonary vasoconstrictor reactivity by limiting NO-dependent pulmonary vasodilation and by promoting the generation of reactive oxygen species (ROS).

Enzymatic sources of ROS in the vasculature include NADPH oxidase isoforms, xanthine oxidase, and uncoupled endothelial nitric oxide synthase (eNOS). The mitochondria are also a major source of cellular ROS, but surprisingly little is known about the role of mitochondrial-derived ROS (mitoROS) in neonatal pHTN. Based on preliminary studies from our laboratory and evidence that protein kinase Cβ (PKC_{β}) mediates mitochondrial dysfunction and oxidative stress in neurodegenerative diseases, we further hypothesized that neonatal CH enhances pulmonary vasoconstrictor sensitivity via PKC_{β}-dependent activation of mitoROS generation.

To test these hypotheses, we employed pharmacologic approaches to assess the role of NO, mitoROS and PKC_{β} on basal vascular tone and agonist-induced vasoconstrictor sensitivity in both isolated (*in situ*) lungs and pressurized pulmonary arteries (~150 μm) from control and CH (2 weeks at 380 mmHg) neonatal rats. CH neonates displayed elevated right ventricular (RV) systolic pressure (*in vivo*) and RV hypertrophy, indicative of pHTN. CH increased both basal pulmonary arterial tone and vasoconstrictor reactivity to the thromboxane analog, U-46619. Interestingly, we observed that endogenous NO limits CH-dependent increases in pulmonary vasoconstriction. Exposure to CH also enhanced NO-dependent vasodilation to arginine vasopressin (AVP), pulmonary expression of NOS III (eNOS), and eNOS phosphorylation at activation residue serine-1177. Additional studies using *in situ* lungs revealed an effect of scavenging ROS or inhibition of PKC_{β} to attenuate CH-dependent increases in basal tone and agonist-induced pulmonary vasoconstrictor sensitivity. Selective inhibitors of PKC_{β} or mitoROS similarly reduced basal tone in arteries from CH rats, while having no effect in control arteries.

We conclude that, in contrast to our hypothesis, enhanced basal tone and agonist-induced vasoconstriction following neonatal CH is limited by increased NO-dependent pulmonary vasodilation resulting from greater eNOS expression and phosphorylation at activation residue serine-1177. Furthermore, both PKC_{β} and mitoROS contribute to enhanced pulmonary vasoconstrictor sensitivity following CH in neonates. These signaling mediators represent new potential therapeutic targets in the treatment of neonatal pHTN.

TABLE OF CONTENTS

LIST OF FIGURES

LIST OF TABLES

CHAPTER 1 – INTRODUCTION

Pulmonary hypertension (pHTN) in newborns results from the failure of the pulmonary circulation to dilate after birth (4, 6). Elevated pulmonary arterial pressure during infancy or childhood contributes significantly to death and disability (5, 14, 27). Current therapies depend on strategies to lower pulmonary arterial pressure, such as inhaled nitric oxide (NO, a potent vasodilator), but have not been demonstrated to improve mortality or length/cost of hospital stay (27, 191, 204, 273). Advances in our understanding of neonatal pHTN are therefore needed to facilitate newer, mechanistically targeted therapies.

Chronic hypoxia (CH) is a common cause of neonatal pHTN and can negatively impact the developing pulmonary circulation (120). CH is a term used to describe chronic reductions in arterial oxygen available to the body (general hypoxia) or to a specific region (tissue hypoxia). Chronic reductions in arterial oxygen levels (hypoxemia) can result from complications occurring during prenatal and antenatal pulmonary development. Reduced fetal oxygen supply resulting from limited maternal oxygen supply (as can occur during exposure to high altitude) or reduced uterine blood flow (found in placental insufficiency) can lead to pHTN (120). Exposure to CH can also occur intrapartum, during labor. Intermittent episodes of interrupted fetal oxygenation can occur during human labor due to uterine contraction, compression of the umbilical cord, head compression, placental abruption, or rupture of fetal vessels (231, 267). Most fetuses tolerate these moments of hypoxia, but some do not and hypoxia-associated disorders such as persistent pHTN of the newborn can result (120). Post-natal exposure to CH usually occurs in newborn babies suffering from parenchymal lung disease such as bronchopulmonary dysplasia (27, 30), meconium aspiration pneumonia

(5, 152), or pulmonary hypoplasia resulting from conditions such as congenital diaphragmatic hernia (249, 260).

Neonatal pHTN resulting from CH exposure is associated with elevated pulmonary vascular resistance (PVR) that is attributed to luminal narrowing of the pulmonary arterial circulation resulting from arterial remodeling and vasoconstriction. Several studies have evaluated factors that influence the degree of pulmonary arterial remodeling that occurs in the setting of neonatal pHTN (19, 33, 142). Therapy for neonates with pHTN aims to reduce and perhaps reverse remodeling of the pulmonary vasculature to facilitate long-term reductions in PVR. Therapies aimed at selective pulmonary vasodilation however are important for the acute management of neonates with pHTN. Enhanced pulmonary vasoconstriction following neonatal CH may result from impaired endothelium-dependent pulmonary vasodilation (19, 87, 89, 129) and increased production of or sensitivity to vasoconstrictor agonists (15, 40, 91, 233). The relative contribution of diminished endothelium-dependent pulmonary vasodilation and enhanced pulmonary vasoconstriction related to increases in basal tone as well as augmented reactivity to endogenous vasoconstrictor agonists has not been fully investigated. The following sections outline the normal development and physiology of the fetal and neonatal pulmonary vasculature and mechanisms contributing to the development of CH-induced neonatal pHTN.

Development of the Pulmonary Vasculature In Utero

Structure of Arteries. Fetal development of the pulmonary vasculature begins near the 5th week of gestation and continues after birth, well into the postnatal period (212). The pulmonary circulation is characterized by three structural motifs for arteries – fully muscular, partially muscular, and nonmuscular (263). In the fetal lung, the muscularization of arteries is dependent on vascular external diameter. Based on

microscopic evaluation of the fetal pulmonary vasculature, Hislop and Reid observed, “In all arteries over 200 μm external diameter the wall is muscular. Below 200 μm partially muscular arteries appear and increase until, in the diameter range 100-75 μm, they comprise 68% of the population of arteries. Non-muscular arteries appear between 125 and 100 μm and below 37 μm all arteries have this structure,” (127). This size-dependent breakdown of fully to nonmuscularized arteries is present throughout gestation and is similar to that observed in the pulmonary circulation of adults (127, 263).

Although arteries of similar size have comparable muscularization patterns (fully, partially, and nonmuscularized vessels) between the fetal and adult pulmonary circulation, the fetal pulmonary arterial circulation is more muscular and has a larger percent wall thickness (127). Percent wall thickness represents the thickness of the arterial wall as a percentage of the external diameter of the vessel (127). The wall of a given arterial size is twice as muscular in the fetus compared to the adult (127). In the fetus, when the artery contains muscle, wall thickness is inversely proportional to vessel diameter with smaller vessels having the highest percentage wall thickness (127).

Hemodynamic Components of Fetal Pulmonary Circulation. Fetal blood is oxygenated at the placenta and circulated to the fetus (212). A major characteristic of the fetal cardiopulmonary circulation is that more than 90% of cardiac output is diverted away from the lungs to other organs via fetal shunts like the foramen ovale and the ductus arteriosus (153). Shunting of cardiac output away from the lungs *in utero* is accomplished by elevated PVR. *In utero*, fetal PVR is greater when compared to the systemic circulation (3, 187). Elevated PVR is uncharacteristic for the post-natal pulmonary circulation, which is characterized by low pressure and low resistance under normoxic conditions in otherwise healthy adult individuals. Poiseuille’s equation

describes elements that impact arterial resistance. Per this equation, we expect that increases in blood viscosity and decreases in luminal radius of the vessel increase PVR.

Increased blood viscosity occurs when hematocrit, or the ratio of the volume of red blood cells to the total volume of blood, increases. *In utero*, circulating red blood cell concentrations gradually increase during the second trimester (weeks 13 – 28), increasing hematocrit values from 30 – 40%. From the second trimester to term (week 40) the red cell content of blood continues to increase to bring fetal hematocrit to an average of around 50% (97). The increase in fetal hematocrit occurring during gestation similarly increases vascular resistance in the pulmonary and systemic circulations. Considering that PVR is so much greater than systemic vascular resistance *in utero*, gestational increase in hematocrit is unlikely to account for enhanced PVR observed in the fetus.

Decreases in radius of the vessel may account for increased fetal PVR. In Poiseuille's equation resistance is inversely proportional to radius to the fourth power, meaning that halving the radius would increase resistance by 16-fold. As mentioned above, arteries in the fetal lung are more muscularized relative to the lungs of adults. This heightened degree of muscularization narrows the lumen of the vessel and contributes to enhanced fetal PVR (212). Small vessels in the fetal lungs have the thickest muscular walls and are believed to contribute to the elevation of PVR *in utero* (127, 212). Early studies evaluating pulmonary vascular structure in the antenatal period demonstrate that these smallest vessels dilate at birth and contribute to an immediate drop in PVR (127). The impact of pulmonary vasodilation occurring at birth suggests that mechanisms of vasoconstriction contribute to enhanced PVR *in utero*.

Mechanisms of Fetal Pulmonary Vasoconstriction.

Increased PVR *in utero* is due to several mechanisms such as mechanical compression of pulmonary vessels by fluid-filled airways in the lungs and vasoconstriction of fetal pulmonary arteries (102, 104).

Fluid-filled airways. Fluid-filled airways are part of gestational lung development with fetal lung fluid formed by the oncotic force generated by chloride secretion of the respiratory epithelium into the lumen of the airway (39, 178). In late gestation fetal lambs, the volume of lung liquid contained in potential airspaces was greater than the volume of air (functional residual capacity) in newborn lambs (131), indicating that fetal lungs are hyperexpanded relative to neonatal lungs. Draining lung liquid increased pulmonary blood flow, whereas tracheal obstruction limited pulmonary blood flow in these fetal lambs (131). These observations suggest that overexpansion of the fluid-filled airway adds extraluminal pressure on the pulmonary vasculature (266) and contributes to increased PVR in the fetus (131).

Hypoxic pulmonary vasoconstriction (HPV). Increase of fetal blood oxygen tension in chronically instrumented lambs either by exposure of pregnant ewes to hyperbaric hyperoxia or *in utero* fetal ventilation with 100% oxygen reduces fetal PVR and increases pulmonary blood flow (24, 26, 188). The pulmonary vasculature is sensitive to changes in blood oxygen tension in near-term fetal lambs, but due to the hypoxic nature of the fetal circulation (57), oxygen-dependent vasodilation is absent (275) and pulmonary arteries demonstrate HPV (77, 78).

HPV describes a physiologic response whereby contraction of pulmonary VSM increases due to both airway and blood-borne hypoxia, with airway hypoxia as the more potent stimulus. Hypoxia exposure has been shown to contract isolated VSM cells from medium and small diameter pulmonary arteries collected from cats, whereas hypoxia-

dependent contraction of VSM cells from cerebral (systemic) arteries was absent (169). In addition to the hypoxia sensitivity of isolated VSM cells, HPV can be demonstrated in isolated, *ex vivo*, perfused lungs (113, 168). Hypoxic sensitivity of isolated VSM cells and lungs indicates that HPV is a local response to hypoxia and not mediated by neurovascular reflexes.

HPV typically occurs in two phases with the rapid, first phase intrinsic to the VSM and the second slower, sustained phase due to the contribution of an endothelium-derived contractile factor (2, 275). The mechanisms that mediate phase 1 of HPV are controversial. One hypothesis proposes that hypoxia decreases the open probability of voltage-gated potassium channels (K_v) present on VSM (282). Hypoxia-dependent reduction of K_v channel open probability can depolarize the VSM membrane (282) and activate voltage-dependent calcium channels (VDCC) leading to entry of extracellular calcium (Ca^{2+}) (179). The resulting increase in intracellular Ca^{2+} concentration ($[Ca^{2+}]_i$) leads to Ca^{2+}-dependent pulmonary VSM contraction (1, 2, 179). Hypoxia-dependent inhibition of K_v channels has been linked to decreased production of mitochondrial-derived reactive oxygen species (mitoROS), including superoxide (O_2^-) anion, as oxygen becomes rate-limiting for ROS generation by the mitochondrial electron transport chain (1). Decreases in mitoROS shift the balance of cellular redox state to favor net reduction which further inhibits the K_v channel (282).

An alternative hypothesis for phase 1 of HPV suggests that hypoxia increases mitoROS levels which shifts the cellular redox state to being more oxidized (78, 275). An oxidized cellular state triggers VSM cell contraction through the release of Ca^{2+} from intracellular stores such as the sarcoplasmic reticulum (SR) and subsequent store-operated Ca^{2+} entry (SOCE) (275). Ca^{2+} flux across the plasma membrane secondary to depletion of SR Ca^{2+} stores is termed SOCE. Several studies have shown that phase 1 of HPV is suppressed by depletion of SR Ca^{2+} stores with cyclopiazonic acid, lanthanum

(La^{3+}, a blocker of SOCE), and psalmotoxin (an inhibitor of the store-operated channel, acid sensing ion channel 1) (1, 195, 227).

Mechanisms regulating phase 2 of HPV involve release of an endothelium-derived contractile factor. Removal of the endothelium of pulmonary arteries either eliminates or greatly reduces phase 2 of HPV (2, 275). Vasoconstriction occurring during phase 2 of HPV relies on endothelin-1 (ET-1)-dependent contractile responses in VSM and increases in myofilament Ca^{2+} sensitivity due to signaling involving RhoA and Rho kinase (ROK) (2, 51, 275).

HPV occurring during gestation contributes to elevated PVR and shunting of cardiac output from the lungs to other organs (77, 78). Of interest, conditions of hypoxia *in utero* maintain vasodilation of the ductus arteriosus and the increase in blood oxygen tension occurring with birth has a direct effect to constrict and close the ductus (121). In addition to HPV, other mechanisms of vasoconstriction contribute to enhanced PVR in the fetal pulmonary circulation.

Myogenic response. Unlike the mature pulmonary circulation in adults, the fetal pulmonary vasculature appears to regulate flow through a myogenic response (251, 262). Acute increases in pulmonary arterial pressure *in vivo* accomplished by occlusion of the ductus arteriosus in fetal lambs fitted with an inflatable vascular occluder increased PVR in the presence of NOS inhibition (251). The pressure-dependent increase in pulmonary vasoconstriction suggests myogenic regulation. The myogenic response represents vasoconstriction observed in certain vascular beds that occurs due to an increase in intraluminal pressure. The response is intrinsic to the VSM (69) and although observed in the fetal pulmonary circulation, is better characterized in studies of arteries in the systemic circulation (65, 69, 70, 256).

In studies of the myogenic response in the systemic circulation, increased pressure of an isolated blood vessel elicits VSM depolarization (69). Depolarization opens VDCCs which increases Ca^{2+} influx and leads to subsequent VSM cell contraction (69, 123, 294). Stretch-sensitive, non-selective cation channels such as transient receptor potential channels (TRPs) (64, 123, 192) and epithelial sodium channels (123) have been proposed to mediate depolarization in the myogenic response. Intracellular signaling such as the release of Ca^{2+} from intracellular stores (69, 123) and activation of kinases, ROK (44, 186) and PKC (186), also contribute to myogenic tone.

TRP channels are expressed in the pulmonary circulation of the fetus, however their direct contribution to the fetal pulmonary myogenic response has not been evaluated (40, 102, 108, 203). ROK signaling contributes to the fetal pulmonary vascular myogenic response (262). Signaling of both ROK (202, 262) and PKC (56) are important to pulmonary arterial constriction in the fetus.

Agonist-induced pulmonary vasoconstriction. In the fetal pulmonary circulation, agonist-dependent pulmonary vasoconstriction contributes to fetal PVR (71, 132, 137). Vasoconstrictive agonists such as ET-1, platelet activating factor (PAF), and serotonin (5-HT) have been linked to pulmonary vasoconstriction *in utero* (71, 132, 137). Vasoconstrictive agonists such as ET-1, PAF, and 5-HT promote VSM contraction by binding a g-protein coupled receptor on the VSM membrane (133, 274, 290). When bound to agonist, the receptor's g-protein subunit disassociates and breaks into G_{α} and $G_{\beta\gamma}$ subunits (17). The subunit G_{α} activates phospholipase C (PLC) which cleaves membrane phospholipids into diacylglycerol (DAG) and inositol triphosphate (IP_3) (162). DAG has second-messenger properties associated with activation of some downstream kinases such as PKC and is important for 5-HT-induced intracellular signaling (110). IP_3 can bind the IP_3-receptor on the SR which leads to Ca^{2+} release, increased $[Ca^{2+}]_i$, and

VSM contraction (133). Vasoconstrictive agonists can also promote G_{α}-dependent activation of Rho A/ROK signaling in VSM (145, 167), a response that can contribute to enhanced myofilament Ca^{2+} sensitivity (17, 145).

In late-gestation fetal lambs, treatment of chronically instrumented near-term fetal lambs with ET-1 infusion increases PVR in a manner sensitive to ET_A (ET-1 receptor linked to VSM contraction) receptor blocker, BQ-123 (136). However in other reports, administration of ET-1 to either chronically instrumented near-term lambs or isolated, perfused lungs from late gestation fetal sheep lead to dose-dependent pulmonary vasodilation (48, 50). These findings suggest that the contribution of ET-1 to regulate fetal pulmonary vascular tone is controversial.

In contrast to the controversial role of ET-1 in the fetal pulmonary circulation, selective inhibition of the PAF receptor with WEB-2170, in near term fetal lambs, facilitated a 68% reduction in fetal PVR, suggesting that PAF contributes to elevated pulmonary vascular tone *in utero* (132). PAF is synthesized from membrane phospholipids by phospholipase A_2 (PLA_2) (132) in a variety of cell types, such as platelets, macrophages, endothelial cells, and VSM (29, 134). The levels of PAF and PAF-receptor (PAF-R) in lung tissue are higher in the fetus than in newborn lambs (133, 134). The relatively hypoxic fetal pulmonary circulation may, in part, account for the increase in both PAF and PAF-R (29, 134). In response to hypoxia, transiently cultured pulmonary arterial smooth muscle cells (PASMC) collected from fetal lambs increase protein expression of both PAF-R and PAF (133, 134). Treatment of transiently cultured PASMCs with PAF facilitated IP_3-dependent increases in intracellular Ca^{2+} that were augmented following exposure to hypoxia (133). Taken together, these results suggest that the hypoxic environment of the fetal pulmonary vasculature may facilitate high PVR through PAF-dependent pulmonary vasoconstriction.

5-HT is another vasoconstrictor agonist that may contribute to enhanced PVR *in utero* (71, 72). 5-HT infusion causes dose-dependent pulmonary vasoconstriction *in vivo* in chronically instrumented late-gestation fetal lambs (71). Interestingly, in near-term fetal lambs, acute infusion of ketanserin, a selective antagonist of a subtype of 5-HT receptors, 5-HT_{2A}, decreases basal PVR (71) suggesting that 5-HT contributes to enhanced PVR *in utero*. Furthermore, selective serotonin reuptake inhibitors (SSRIs), drugs that prolong 5-HT signaling, such as sertraline and fluoxetine also increase PVR in late-gestation fetal sheep (71). SSRI-induced fetal pulmonary vasoconstriction is important because maternal SSRI use in humans has been associated with enhanced newborn PVR in the antenatal period (49). SSRI-dependent increases in antenatal PVR may be due to direct actions on the developing pulmonary circulation considering that SSRIs can cross the placenta (219). Material fluoxetine and sertraline exposure in mice leads to premature closure of the ductus arteriosus (130). Fetal closure of the ductus increases PVR in fetal lambs and facilitates persistent elevations of PVR even after delivery (6, 181). Taken together, these studies indicate that 5-HT is an important mediator of enhanced PVR *in utero*.

In summary, enhanced PVR in the fetus is due to several mechanisms: fluid-filled lungs, HPV, myogenic tone, and agonist-induced pulmonary vasoconstriction. These mechanisms are important in maintaining shunting of cardiac output from developing fetal lungs and are vital to the healthy maturation of the pulmonary circulation. High PVR and shunting of blood from the lungs *in utero* is possible due to the role of the placenta in fetal blood oxygenation. After birth, the newborn infant must rely on its lungs for blood oxygenation. This requirement is associated with a massive shift in cardiopulmonary perfusion with cardiac output of the right ventricle no longer shunted from the lungs, but redistributed to them (126). This shift to allow for increased

pulmonary blood flow is associated with profound pulmonary vasodilation and is discussed in following sections.

Adaptation of the Pulmonary Vasculature After Birth

Studies investigating the adaptation that occurs in the pulmonary circulation to allow a newborn to transition from fetal to antenatal life have indicated roles for both reduced arterial muscularity and vasodilation.

Branching Pattern and Structure. Following birth, new arteries and alveoli develop within the acinus (128). Neonatal rats, like humans, undergo the alveolar stage of lung development after birth (61, 260). In rats, the alveolar wall thins, the surface areas of alveoli expand by 20-fold, and capillary surface area expands by 35-fold (260). In the preacinar region, the relative percent wall thickness of arteries gradually decreases throughout infancy. Hislop and Reid compared percent wall thickness in pulmonary arteries from a three-day old child to the mean for children aged 10 months to 10 years and noted, "[In the child aged 3 days], while the arteries over 200 μm external diameter still had a percentage wall thickness in the range of the fetal ages, for those below 200 μm the adult range has been reached. Thinning of the small vessels had been immediate, probably due to dilation. Only after 4 months had the larger vessels lost their fetal wall thickness," (128). From this study and others, it is clear that initial, rapid reductions in arterial diameter are due to vasodilation and that long-term reductions in percent wall thickness are due to changes in cytoskeletal structure and proliferation (114, 118, 126, 128).

Birth-Related Pulmonary Vasodilation. Pulmonary vasodilation occurring after birth has a rapid onset. In chronically instrumented fetal lambs, pulmonary arterial

pressure decreases and pulmonary blood flow increases within minutes of birth (4, 164). After delivery, the mean pulmonary arterial blood pressure decreases to a value lower than mean arterial blood pressure in the systemic circulation. Greater systemic blood pressure leads to pressure-dependent closure of the foramen ovale (102). The ductus arteriosus begins to close within minutes after birth, but does not fully close for several weeks. Despite the delay in full closure of the ductus, blood flow through the structure stops within 15 hours after birth (190). Reductions of PVR and closure of fetal shunts occurring at birth increase pulmonary blood flow to include total cardiac output in the human infant (102). This is important because at birth the lungs replace the placenta as the organ of gas exchange and blood oxygenation (126).

Mechanisms of Endothelium-Dependent Pulmonary Vasodilation. The anatomy of the blood vessel places the endothelium directly adjacent to the layer of VSM cells and therefore can rapidly influence the tone of VSM cells (95). The endothelium is also luminally positioned and in direct contact with the blood and can therefore detect birth-related increases in shear stress related to increased pulmonary blood flow (3) and increased oxygen tension (47, 68, 122). Following detection of these birth-related stimuli, the endothelium releases vasoactive mediators such as prostacyclin (164, 165) and NO (4, 46, 100) to facilitate pulmonary vasodilation and decreases in PVR.

Prostacyclin. Endothelial cell prostacyclin production is stimulated by shear stress, changes in blood oxygen tension, and receptor-dependent agonists (164, 235). In response to these stimuli, Ca^{2+}-dependent activation of phospholipase A_2 (PLA_2) generates arachidonic acid (AA) through cleavage of membrane phospholipids. Prostacyclin is a product of cyclooxygenase (COX)-dependent metabolism of AA.

Prostacyclin can leave the endothelial cell and bind to the prostacyclin receptor on VSM cells, leading to VSM relaxation through a mechanism reliant on stimulation of adenylyl cyclase and production of cyclic adenosine monophosphate (cAMP) (112). COX expression and the synthesis of prostacyclin are developmentally regulated (42, 164). The increase in blood oxygenation that occurs with the onset of ventilation at birth stimulates prostacyclin synthesis (164). In response to the initiation of ventilation, the decrease in PVR of chronically instrumented newborn lambs occurs in two phases: 1) A rapid decline (< 30 seconds) and; 2) A slower, more gradual decline that occurs during the first 10-20 minutes of ventilation (165). Treatment of these lambs with infusions of indomethacin, an inhibitor of COX, limits only the gradual second phase of ventilation-dependent decrease in PVR (165). Thus, the stimulus of ventilation on prostacyclin release may contribute to postnatal pulmonary vasodilation.

NO. NO derived from the endothelium (100) leads to vasodilation in the perinatal pulmonary circulation (4). NO is produced during the conversion of L-arginine to L-citrulline. The conversion is catalyzed by nitric oxide synthase (NOS) (96, 98). There are three NOS isoforms that contribute to NO formation in the pulmonary circulation of the fetus and neonate, NOS I (neuronal NOS or nNOS), NOS II (inducible NOS or iNOS), and NOS III (endothelial NOS or eNOS).

In whole lung tissue collected from fetal rats, nNOS mRNA and protein expression are increased throughout gestation and then fall rapidly after birth (196). In chronically instrumented fetal lambs, selective nNOS inhibition increases PVR without affecting acetylcholine-induced pulmonary vasodilation (217). Moreover, nNOS protein expression was identified in pulmonary arteries, both with and without the endothelium, collected from late gestation fetal sheep, suggesting that nNOS may be expressed in the VSM or adventitial layer of the pulmonary artery during gestation in sheep (217).

Experiments investigating the contribution of iNOS to PVR in newborn lambs, demonstrated that selective iNOS inhibition mitigates the ventilation- and oxygen-dependent fall in PVR that occurs during early postnatal life (215). However, selective iNOS inhibition in chronically instrumented late gestation fetal lambs only partially inhibited shear stress dependent increases in pulmonary vasodilation (216). Data from these studies is consistent with findings in baboons, where iNOS appears to take on a larger role to impact PVR only after birth (236).

In whole lung tissue collected from fetal rats, both mRNA and protein expression of eNOS are detectable in late stage gestation and near term at their highest levels (196). In a separate study using whole lung tissue from neonatal rats, eNOS mRNA and protein expression were detected at their highest levels within 24 hours after birth with increased eNOS mRNA persisting for 16 days post-partum (150). Additionally, as newborn rats age from one to two weeks eNOS protein expression and NO-dependent regulation of pulmonary vascular tone are increased (53).

Birth-related stimuli such as increases in blood oxygenation (35, 188) and shear stress (96) stimulate eNOS dependent pulmonary vasodilation. In near term lambs, ventilation with 100% O_2 increases eNOS mRNA and protein expression more than ventilation with a gas mixture of $N_2/O_2/CO_2$ (35). In a study of near-term lambs, raising fetal arterial oxygen tension by exposing pregnant ewes to 100% oxygen at 3 atmospheres of pressure increased the proportion of the right ventricular output distributed to fetal lungs from 8 to 59% (188). Increased pulmonary blood flow occurring at birth would likewise increase shear stress on the endothelium. In isolated pulmonary arterial endothelial cells transiently cultured from late gestation fetal lambs, exposure to shear stress in vitro increased eNOS mRNA and protein expression (35, 276, 279). In chronically instrumented, near term fetal lambs fitted with an inflatable vascular occluder around the ductus arteriosus, compression of the ductus increased pulmonary blood flow

by 300% and decreased PVR (57). These responses were significantly blunted when NOS was inhibited by infusions of nitro-L-arginine (57), an L-arginine analog unavailable for NO production (185). These findings suggest that eNOS contributes to the normal fall in elevated PVR occurring at birth.

Neonatal Pulmonary Hypertension

Newborn pHTN commonly results from the failure of the pulmonary circulation to dilate at birth (6). Elevated PVR impedes blood flow through the pulmonary circulation by remaining greater than systemic vascular resistance (5, 249). This differential leads to right-to-left shunting of unoxygenated blood across the ductus arteriosus and foramen ovale and consequential severe hypoxemia (249). Life-threatening circulatory failure can also result from pHTN (66, 102, 249). Neonatal pHTN resulting from a failure of post-natal pulmonary vasodilation affects 1.9 per 1000 live births in the United States and can complicate the course of up to 10% of all infants admitted to the NICU (246).

Mechanisms of Neonatal Pulmonary Hypertension

There are several elements that mediate increased in PVR observed in the setting of neonatal pHTN and are diagramed in **Figure 1** and discussed below.

Polycythemia. Increased circulating concentration of red blood cells has the potential to increase the viscosity of blood and therefore vascular resistance in a manner described by Poiseuille's equation. Erythropoietin is a hormone that stimulates production of red blood cells in response to either global or tissue hypoxia. Exposure to fetal hypoxia increases erythropoietin concentration (231). Erythropoietin does not cross the placenta and therefore, tissue hypoxia stimulates erythropoietin production in the fetus (283). The liver is the primary site for fetal erythropoietin synthesis and is

Figure

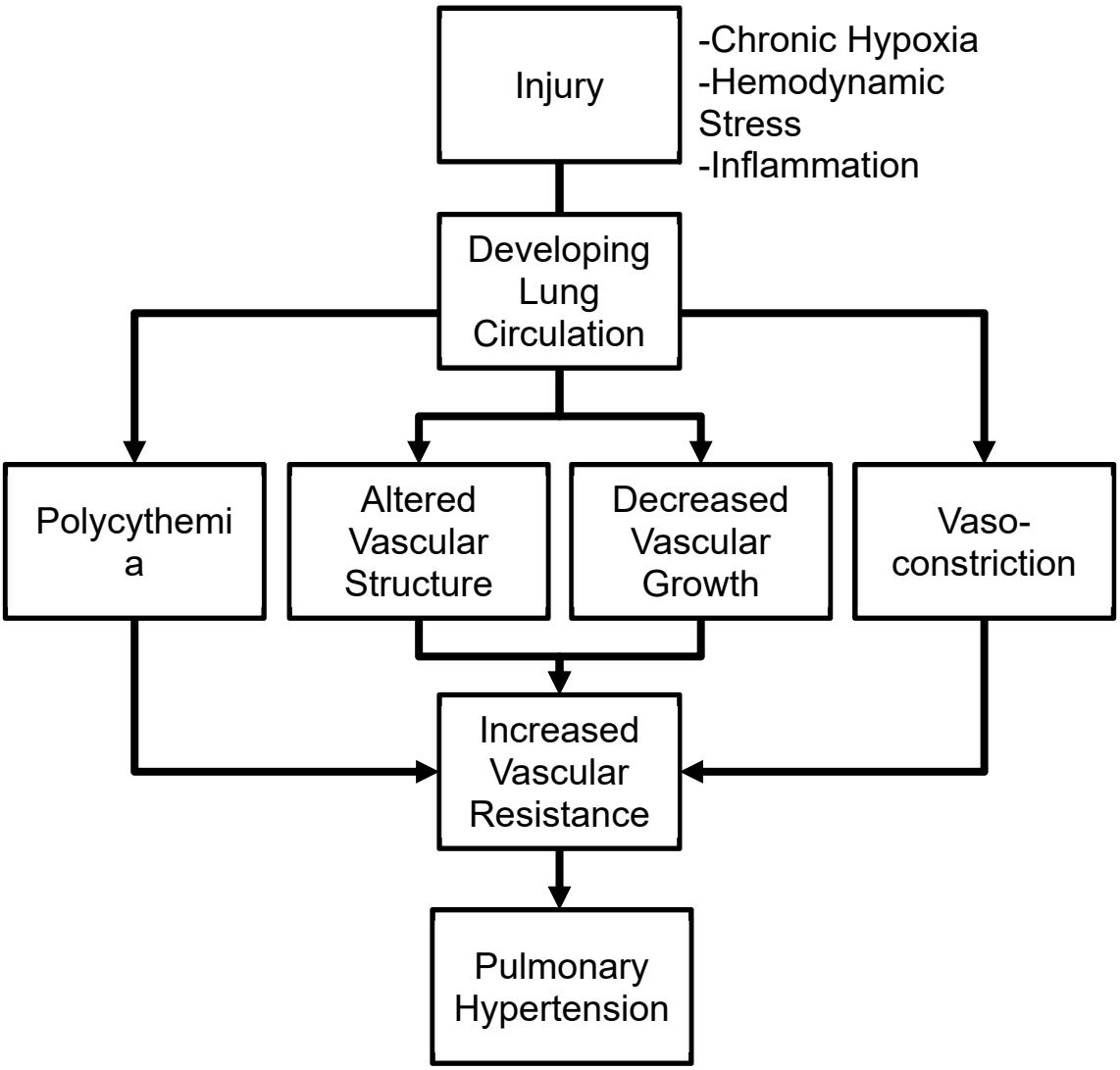

Figure 1. Development of Neonatal Pulmonary Hypertension.
Chronic hypoxia (CH) increases pulmonary vascular resistance via polycythemia, altered vascular structure, decreased vascular growth, and vasoconstriction, all of which may contribute to neonatal pHTN.

considered to be the sensor organ for the erythropoietin response to hypoxia (240). Infants with fetal exposure to CH associated with maternal preeclampsia had elevated erythropoietin concentrations in amniotic fluid, cord blood (231), and in serum (232). However, erythropoietin returned to near normal levels within 8 hours of delivery (232).

Hypoxia-dependent changes in erythropoietin expression may impact red blood cell concentrations. In animal models of neonatal pHTN involving exposure to CH, hematocrit values in CH exposed neonates are elevated relative to normoxic controls (52, 148). In neonatal rats exposed to 2 weeks of CH, mean hematocrit values for CH exposed rats were approximately 40% whereas mean hematocrit values were 30% in normoxic controls (52, 148). Exposure of adult rats to CH for the same length of time leads to hematocrit values of 61% for CH and 46% for normoxic controls (52). Although hematocrit increases in both newborn and adult rats exposed to CH, the hematocrit of CH exposed neonatal rats equals hematocrit for normoxic adult rats. Modest increases in hematocrit are also observed in newborn piglets (89) and calves (79) with CH-induced pHTN. Due to the small size of the increase in hematocrit, it is unlikely that CH-dependent polycythemia alone is sufficient to explain elevations in PVR observed in neonates with pHTN. In a study involving human infants whether either acute or CH exposure, polycythemia (venous hematocrit >65%) occurred in some patients, but those infants did not require ventilator support or oxygen treatment (232) whereas infants with pHTN do require therapeutic interventions (5, 138, 246).

Altered Vascular Structure. The histology of neonatal pHTN is characterized by thick walled pulmonary arteries (61, 79) that, if untreated, can persist into adulthood (60, 61, 214). The fully muscularized thick arterial wall observed in neonates with pHTN is, in part, due to extension of muscle down the arterial tree into previously partial or non-muscularized arteries (212). The initial thickening of the medial layer of pulmonary

arteries is due to smooth muscle cell hypertrophy and increases in extracellular connective tissue (184). VSM cells in the medial layer of pulmonary arteries from newborn calves and rats show increased cell proliferation and DNA synthesis (183). Extension of smooth muscle down the vascular tree is thought to be due to proliferation of smooth muscle cells as well as differentiation of precursor cells such as pericytes in the non-muscular region of the artery or intermediate cells (fibroblasts) in the partially muscular region to mature VSM cells (184).

Increased circulating levels of ET-1 in human infants with pHTN (228) and in various animal models of neonatal pHTN (20, 143, 144, 247) may promote VSM proliferation and hypertrophy and facilitate arterial remodeling in neonates with pHTN (20, 143, 144). ET-1 signaling also promotes activity of other growth factors like platelet-derived growth factor (141), transforming growth factor-β (139), and nuclear factor of activated T cells isoform c3 (99) that may additionally play a role in vascular remodeling occurring in the setting of neonatal pHTN (21, 25, 33, 117). In a study that compared neonatal fawn-hooded rats (a genetic rat strain that develops pHTN after exposure to mild CH) to Sprague-Dawley rats (a genetic strain that requires exposure to more severe CH to develop pHTN), whole lung ET-1 mRNA expression (preproET-1 mRNA) is elevated 5 days after birth in fawn-hooded rats with no change observed in Sprague-Dawley rats (247). This elevation occurs before pHTN develops, suggesting that ET-1 may play a role in the development of neonatal pHTN (247). Consistent with this possibility, chronic ET_A receptor (ET-1 receptor present on VSM and endothelial cells) blockade prevents and partially reverses arterial remodeling occurring in neonatal rats with CH-induced pHTN (19).

In addition to the role of ET-1 to promote VSM proliferation to vascular remodeling observed in the setting of neonatal pHTN, it may also contribute to reductions in VSM apoptosis. In a study of neonatal rats with pHTN, ET-1 signaling can

limit apoptosis observed in the arterial wall of lungs from neonates with pHTN (140). Additionally, pulmonary arterial expression of Bax, a proapoptotic factor was decreased while that of Bcl-xL, an antiapoptotic factor, was increased in lung sections from neonatal rats with pHTN (140). These results suggests that, in addition to enhanced proliferation, ET-1 may inhibit apoptosis and promote vascular wall thickening.

Decreased Vascular Growth. In human infants with congenital heart disease and subsequent pHTN, the number of peripheral arteries is reduced (184, 213). In models of neonatal pHTN associated with CH such as bronchopulmonary dysplasia (BPD), reduced numbers of small arteries and an abnormal distribution of vessels within the distal lung have been described (60, 61). Neonates who survive neonatal pHTN seem to have a permanent decrease in the number of pulmonary arteries (61). Neonatal fawn-hooded rats show reduced vessel density and alveolar simplification when raised at a high altitude in Denver, CO (60). Housing of neonatal rats in hyperbaric chambers to bring the animals to barometric pressures occurring at sea-level increases vessel number and promotes alveolar septation and development (60).

Reduced signaling of vascular endothelial growth factor (VEGF) may contribute to reduced vascular growth in the setting of neonatal pHTN. VEGF is an important hormone that promotes development and growth of the pulmonary vasculature and airways (201, 261). The addition of a VEGF receptor inhibitor leads to a reduction in artery formation and a failure of alveolar septation in growing rats (61). Human infants and newborn baboons with BPD have reduced lung levels of VEGF and VEGF receptors (32, 170). Neonatal rats with pHTN also have reduced VEGF levels (173, 261) and intratracheal adenovirus-mediated VEGF gene therapy increased survival and promoted development of the lung vasculature and alveoli in these animals (261).

Vasoconstriction. In additional to the role of polycythemia, altered vascular structure, and decreased vascular growth described above, enhanced pulmonary vasoconstriction contributes to increased PVR in neonates with pHTN (88, 180, 250). Indeed, enhanced PVR occurring in animal models of neonatal pHTN can be significantly reduced if not fully alleviated by limiting mechanisms of enhanced pulmonary vasoconstriction (88, 180). In neonatal piglets exposed to CH, elevated PVR is sensitive to exogenous vasodilator treatment with papaverine (88). Additionally, acute inhibition of ROK with fasudil alleviates increased PVR observed in neonates with pHTN (180). In human neonates with pHTN, small precapillary arteries remain undilated after birth with VSM cells containing more contractile elements such as actin and myosin heavy chain isoforms (114, 119). This observation is also true in piglets with CH-induced neonatal pHTN (115). These findings in neonates with pHTN suggests that the VSM of pulmonary arteries is equipped to facilitate more robust VSM contraction and potentially enhanced pulmonary arterial vasoconstriction.

Mechanisms of Enhanced Vasoconstriction in Neonatal Pulmonary Hypertension

Both basal tone and enhanced pulmonary vasoconstrictor agonist sensitivity contribute to enhanced pulmonary vasoconstriction in neonates with pHTN (7, 157, 228, 250). A potential mechanism for enhanced basal tone involves the myogenic response. After birth, the fetal pulmonary myogenic response and subsequent vascular tone is limited by mechanisms of pulmonary vasodilation (53, 250) and, over time, the pulmonary circulation becomes a more passive vascular bed not classically associated with myogenic regulation (44). In newborn lambs fitted with an inflatable vascular occluder around the ductus arteriosus, acute compression of the ductus leads to NO-dependent pulmonary vasodilation (250). In lambs with pHTN however, occluder

inflation increases in PVR and limits pulmonary arterial blood flow in a manner consistent with the myogenic response (250).

Enhanced pulmonary vasoconstriction occurring in neonatal pHTN may also be attributed to increased activity of pulmonary vasoconstrictor agonists. Indeed, in human infants with pHTN, circulating levels of vasoconstrictor agonists such as ET-1 and thromboxane A_2 are increased (7, 8, 157, 228). Additionally, young children with congenital heart disease and pHTN demonstrate an imbalance in the biosynthesis of thromboxane A_2 and prostacyclin (both COX products) with greater urinary excretion of metabolic products of thromboxane A_2 and fewer of prostacyclin (7). The regulation of COX products appears to be important in the development of neonatal pHTN because babies born to mothers who report high NSAID (inhibitors of COX) use in pregnancy are at elevated risk of neonatal pHTN (171).

In animal models of neonatal pHTN, the pulmonary vasoconstrictor agonists 5-HT and thromboxane A_2 contribute to enhanced PVR (72, 90, 93). Acute inhibition of 5-HT signaling alleviates enhanced PVR in lambs with pHTN (72) and administration of an SSRI further increases PVR in these lambs (72) thereby demonstrating that 5-HT enhances basal pulmonary vascular tone, a response that enhances PVR and perhaps contributes to pHTN in neonates. Furthermore, acute inhibition of COX-2 (the enzyme responsible for thromboxane A_2 synthesis from AA) augmented AA-induced pulmonary vasodilation in isolated pulmonary arterial rings from piglets with CH-induced pHTN (90) suggesting that thromboxane A_2 potentiates pulmonary arterial vasoconstriction in neonates with pHTN. Taken together, these results suggest that vasoconstrictor agonists contribute to enhanced vasoconstriction in neonates with pHTN.

There are two potential pathways for enhanced basal tone and pulmonary vasoconstrictor reactivity. The first involves reduced production of vasodilatory compounds that allows fetal pulmonary arterial tone to be uncovered and persist into

antenatal life. The second potential mechanism involves enhanced VSM contractility that may contribute to an augmented myogenic response or augment the action of a vasoconstrictor agonist. In the literature, evidence to support the existence of both possibilities is present and discussed below.

Role of Endothelial Dysfunction. Endothelial production of vasodilatory factors, prostacyclin and NO is limited in the setting of neonatal pHTN (7, 238). In human infants with pHTN, urinary excretion of prostacyclin metabolites is decreased (7). In pulmonary arteries of newborn pigs with CH-induced pHTN, the production of prostacyclin is attenuated (90, 93). In newborn lambs with pHTN, intratracheal administration of prostacyclin decreased PVR and increased pulmonary arterial blood flow (221). Moreover, infusion of milrinone, an inhibitor of phosphodiesterase type 3 (an enzyme that limits prostacyclin-induced vasodilation), decreased baseline PVR and potentiated the therapeutic effect of intratracheal prostacyclin (221). These findings support a role for diminished prostacyclin-dependent pulmonary vasodilation to permit enhanced vasoconstriction in neonates with pHTN.

Limitations on NO-dependent pulmonary vasodilation may additionally contribute to diminished pulmonary vasodilation observed in neonates with pHTN. Indeed, decreased eNOS mRNA and protein expression, reduced production of endothelial-derived NO (EDNO), and impaired NO-dependent pulmonary vasodilation have all been documented in animal models of neonatal pHTN (11, 52, 89, 238). Endogenous inhibitors of eNOS, such as asymmetric dimethylarginine (ADMA) can reduce EDNO production (23, 264). In human infants with pHTN, urinary ADMA levels are elevated relative to healthy control infants (205, 264).

In addition to ADMA-dependent reductions in eNOS-derived NO, other factors that influence eNOS NO production are also altered in neonatal pHTN. Association of

eNOS with heat shock protein 90 (HSP-90) is correlated with increased NO production and decreased superoxide anion (O_2^-) generation (159, 254). Examination of transiently cultured pulmonary arterial endothelial cells from lambs with pHTN noted decreased HSP90-eNOS interaction relative to levels observed in cells from healthy neonates (254). In addition to lower levels of interaction, decreased eNOS-dependent NO production and elevated O_2^- generation was also observed (159, 254). This result suggests that in neonatal pHTN, eNOS association with HSP90 is decreased and eNOS switches from generation of NO to O_2^-, thus limiting NO levels.

To promote VSM relaxation, NO stimulates VSM soluble guanylyl cyclase (sGC)-dependent production of cyclic guanine monophosphate (cGMP) which in turn activates protein kinase G (PKG). PKG causes VSM relaxation in two ways, first by decreasing $[Ca^{2+}]_i$ in the VSM and by decreasing Ca^{2+}-sensitivity of the contractile apparatus (149). In fetal lambs with pHTN, cGMP content and protein expression of sGC is decreased (36, 281). Additionally, increased pulmonary levels of H_2O_2 in lambs with pHTN have been proposed to attenuate both sGC protein expression and activity in pulmonary arterial VSM (281). Increased expression PKG was observed in neonatal lambs with CH-induced pHTN, but activity of PKG was decreased in isolated pulmonary arteries from these lambs (101). These findings suggest that in addition to reduced NO production, the downstream signaling mechanisms that promote NO-induced VSM relaxation are also impaired in neonates with pHTN.

In addition to limitations on factors that promote NO-induced VSM relaxation, there is evidence for augmented levels of enzymes that limit the activity of NO. In studies of lambs with pHTN, protein expression PDE5 is increased (37). Activity of PDE5 in VSM is also increased and acute treatment with PDE5 inhibitors decreased baseline PVR in lambs with pHTN (116) suggesting that PDE5 may potentiate the

limitation on what small amount of NO-dependent pulmonary vasodilation is present in neonates with pHTN.

Decreased production of endogenous NO may also contribute to elevated ET-1 levels observed in neonates with pHTN. NO can limit ET-1 production by inhibition of preproET-1 transcription (151), possibly by decreasing NF- κB activity, an important transcription factor for ET-1 production (229). ET-1 also regulates NO levels by downregulation of the expression of eNOS and thus may further potentiate ET-1-mediated pulmonary vasoconstriction (277). These studies suggest that reductions in NO not only limit pulmonary vasodilation, but also increase the amount of the contractile factor, ET-1 thereby promoting enhanced vasoconstriction in neonates with pHTN.

Role of Enhanced VSM Contractility. An additional contributor to enhanced pulmonary vasoconstriction in neonatal pHTN is an increase contractility of VSM, independent of changes in vasodilator levels. Potential contributors to enhanced VSM contractility in neonates with pHTN include enhanced Ca^{2+} signaling and increased myofilament Ca^{2+} sensitivity.

In studies of neonatal lambs with pHTN, acute treatment with the VDCC inhibitor nifedipine limits the pulmonary arterial myogenic response (250) suggesting that enhanced Ca^{2+} entry contributes to that response in neonates with pHTN. Nifedipine administration in isolated lungs from piglets exposed to CH leads to profound reductions in pulmonary arterial pressure with little effect in lungs from control piglets (125), suggesting that VDCC are important for elevated pulmonary arterial basal tone. Moreover, isolated pulmonary arterial rings from piglets exposed to CH demonstrate robust reactivity to the Ca^{2+} channel agonist, Bay K 8644, a response that is absent in rings from control neonates (125). Whole cell, voltage-dependent Ca^{2+} currents are also exaggerated in isolated VSM from piglets exposed to CH (125). Taken together, these

studies support a role for VDCC to mediate enhanced pulmonary arterial tone in neonates with pHTN.

One potential explanation for the increased role of VDCC in mediating enhanced VSM contractility can be found in the pathway for HPV. HPV can involve the hypoxia-dependent reduction of the open probability of voltage-gated potassium channels (K_v) present on VSM (282). Reduced K_v channel open probability following exposure to acute hypoxia can depolarize the VSM membrane (282) and activate VDCC leading to entry of extracellular Ca^{2+} (179) and Ca^{2+}-dependent pulmonary VSM contraction (1, 2, 179). K_v channel activity is reduced in neonatal lambs with pHTN in a manner that depends on O_2^- signaling (158). Additionally, O_2^- scavengers restore K_v channel function in isolated arteries from neonatal piglets with CH-induced pHTN (86). Taken together, these findings indicate that neonatal animals with pHTN demonstrate reduced K_v channel activity. This impairment of K_v channels may allow for increased VDCC-induced VSM contractility in neonates with pHTN.

In addition to VDCCs, Ca^{2+} influx through other Ca^{2+} permeable ion channels contributes to increased Ca^{2+} signaling in VSM of neonates with pHTN (203, 223). Enhanced contraction of isolated pulmonary arterial rings from lambs with either pre- or perinatal CH-induced pHTN, is sensitive to inhibitors of TRP channel family members (40, 108, 203). Enhanced protein expression of TRPC4 (203) and TRPC6 (223) may contribute to enhanced SOCE-dependent pulmonary arterial vasoconstriction in neonatal lambs with pHTN (203, 223).

In addition to altered Ca^{2+}-signaling, increased myofilament Ca^{2+} sensitization may contribute to enhanced vasoconstriction observed in neonates with pHTN. Classically, there are two pathways thought to influence myofilament Ca^{2+} sensitization. One pathway involves RhoA/ROK-dependent signaling and the other involves activity of PKC/CPI17. In animal models of neonatal pHTN, levels of activated RhoA are elevated

(105, 180). Increased ROK protein expression and activity is observed in adult and neonatal animals with pHTN, assessed by MYPT1 phosphorylation, a downstream phosphorylation target of ROK (101, 145, 180). These results suggest that increased RhoA/ROK signaling contributes to increased myofilament Ca^{2+} sensitivity due to ROK-dependent MYPT1 phosphorylation. Indeed, ROK contributes to enhanced PVR observed in neonates with pHTN and therapeutic inhibition of ROK normalizes PVR to that of control neonates (180, 250). These results demonstrate that ROK contributes to pHTN in neonates, perhaps through promotion of myofilament Ca^{2+} sensitization.

A separate pathway that promotes myofilament Ca^{2+} sensitization in the setting of pHTN involves PKC-dependent activation of CPI-17 that in turn inhibits activity of myosin light chain phosphatase (242). In studies of isolated lungs from healthy newborn piglets, PKC inhibition with chelerythrine limits ET-1-dependent pulmonary vasoconstrictor activity, but has no effect on baseline pulmonary arterial pressure (31). Moreover, PKC activation with either 1-oleyl-2-acetyl-sn-glycerol (OAG) or phorbol 12,13-dibutyrate (PDBu) leads to dose-dependent pulmonary vasoconstriction in lungs from control piglets (31). Lungs from piglets with CH-induced pHTN showed enhanced baseline pulmonary arterial pressure that was reduced after chelerythrine treatment, suggesting that CH-dependent increases in PVR, in part, depend on PKC signaling (31).

Role of ROS in Vascular Signaling and Pathology

Considering the role of ROK and PKC in mediating enhanced pulmonary vasoconstriction occurring in the setting of neonatal pHTN, it is important to consider how their activity may be stimulated. In models of pHTN in adult animals, both ROK and PKC activity is stimulated by signaling involving reactive oxygen species (ROS) (145, 242). ROS-dependent activation of ROK and PKC signaling may also be occurring in neonates with pHTN. In transiently cultured pulmonary arterial endothelial cells from

neonatal piglets with pHTN, activation of Rac1, an enzymatic subunit of NADPH oxidase (NOX) important for NOX-derived superoxide O_2^- production (55), leads to downstream activation of RhoA/ROK signaling (284).

Several PKC isoforms are activated by oxidant stress (16, 54, 155) and contribute to VSM contraction by increasing $[Ca^{2+}]_i$ (193) and enhancing Ca^{2+} sensitivity of the myofilament contractile apparatus (172, 186, 194). Studies from adult rats with pHTN induced by exposure to intermittent hypoxia, demonstrate augmented agonist-dependent pulmonary vasoconstrictor reactivity through PKC_β-mediated VSM Ca^{2+} sensitization (242). PKC also contributes to enhanced pulmonary vasoconstriction and mediates the vasoconstrictor activity of ET-1 in the hypertensive neonatal pulmonary circulation of piglets (31). Taken together, these results suggest that oxidant-dependent activation of Ca^{2+} sensitization pathways involving ROK and PKC contribute to enhanced pulmonary vasoconstriction observed in neonatal pHTN.

Considering the oxidant-dependent stimulation of ROK and PKC dependent Ca^{2+} sensitization, it is interesting to note that in many animal models of neonatal pHTN, enhanced pulmonary levels of ROS are documented from various subcellular sources (9, 111, 144). In newborn rats with pHTN, lung levels of lipid peroxidation products such as 8-isoprostane are elevated and stimulate enhanced pulmonary vascular ET-1 production (144). In newborn lamb models of neonatal pHTN, O_2^- levels in pulmonary vessels are increased (9, 111). In addition to promotion of enhanced VSM contractility through activation of ROK and PKC signaling, increased lung levels of ROS limit the bioavailability of NO due to scavenging and can thus potentiate vasoconstriction (43, 142). Intratracheal treatment of pulmonary hypertensive lambs with recombinant human SOD reduces the high levels of pulmonary ROS observed in these animals, increases eNOS protein expression, and restores NO-dependent pulmonary arterial vasorelaxation (82). This result suggests that lung production of ROS may contribute to enhanced PVR

observed in neonates with pHTN through promotion of enhanced VSM contractility and reductions in NO-dependent pulmonary vasodilation.

Sources of Cellular ROS

A variety of subcellular sources for ROS may contribute to the enhanced level observed in the pulmonary vasculature of neonates with pHTN. Those sources include NOX (43, 92, 111), xanthine oxidase (142), uncoupled eNOS (eNOS-dependent O_2^- production instead of NO) (163), and the mitochondria (9, 234).

The mitochondria are a major source of cellular ROS in VSM, but seldom investigated in the setting of neonatal pHTN (177). MitoROS have been implicated in the development of pulmonary arterial hypertension in adult rats (22). Additionally, lung levels of mitoROS are elevated in neonatal sheep with pHTN (9, 83, 234, 280). Potential stimuli for mitoROS generation in neonates with pHTN includes stretch of VSM cells (278), as might occur in pulmonary arteries of neonates with increased luminal pressures and pHTN (6). Transiently cultured PASMC from lambs with pHTN and healthy controls demonstrated that cyclic stretching increased mitochondrial complex III-dependent production of O_2^- (278). Signaling leading to mitoROS production in the pulmonary circulation has been attributed to uncoupled eNOS (234, 255), reduced SOD2 (the SOD isoform present in the mitochondria) levels (9), and PKC (222). Increased mitoROS levels can lead to diminished NO-dependent pulmonary vasodilation by uncoupling eNOS (234) and promoting the activity of PDE5 (83).

Mitochondrial dysfunction occurring in a number of disease states such as ischemia-reperfusion injury (270), atherosclerosis (210), diabetic cardiomyopathy (244), and multiple sclerosis (252) depends on upstream signaling of PKC_β. PKC_β is an isoform of PKC activated by $[Ca^{2+}]_i$ (268) and cellular redox state (106). Despite the link between PKC_β and mitoROS indicated in a variety of disease states and cell types, the

contribution of PKC_{β} to mitoROS generation in the neonatal pulmonary circulation has not yet been studied.

It is evident that enhanced vasoconstriction plays an important role in mediating pHTN in neonates and reduced NO-dependent vasodilation and enhanced VSM contractility contribute to that enhanced vasoconstriction. However, the relative contribution of both to augmented pulmonary vasoconstriction is unclear. Therefore, the series of experiments described in this dissertation were designed to examine the roles of diminished NO-dependent vasodilation and enhanced VSM contractility as well as the potential contributory signaling mechanisms occurring in neonatal CH-induced pHTN.

Rationale and Specific Aims

Neonatal pHTN affects 1-2 of every 1000 live births in the United States with 20% of cases being fatal. Surviving patients face significant morbidity associated with detriments to neural development and chronic lung disease (5, 246). CH is implicated in the pathogenesis of pHTN (14, 120) and thought to elevate postnatal PVR by increasing basal arterial tone and by augmenting reactivity to endogenous vasoconstrictor agonists (15, 40, 233). Enhanced pulmonary vasoconstriction following neonatal CH may result from a limitation on the production of endothelium-derived relaxing factors or increases in VSM contractility (19, 87, 89, 114, 119, 129). To investigate the relative contribution of each, we first investigated mechanisms of reduced endothelium-dependent pulmonary vasodilation and the contribution of those mechanisms to enhanced vasoconstriction occurring in neonatal rats with pHTN. ROS mediate reduced NO-dependent vasodilation in neonates with pHTN (43, 234) and promote VSM contraction by increasing $[Ca^{2+}]_i$ (51) and enhancing myofilament Ca^{2+} sensitivity (51, 145, 156). Therefore, we next sought to evaluate the role of ROS in enhanced pulmonary vasoconstriction occurring in neonates with CH-induced pHTN. Finally, PKC_β contributes to augmented pulmonary arterial vasoconstriction in adult rodents with pHTN (242) and leads to mitoROS production in a variety of disorders (210, 244, 252, 270). Understanding that mitoROS contribute to neonatal pHTN (9, 10, 83), we set out to investigate the role of PKC_β in stimulating mitoROS production in neonatal PASMC and the contribution of this signaling pathway to enhanced pulmonary vasoconstriction in neonates with CH-induced pHTN.

<u>Specific Aim 1</u>: Determine the contribution of endothelial dysfunction to enhanced basal tone and agonist-induced vasoconstriction in neonatal pHTN.

Hypothesis: Neonatal CH increases basal tone and pulmonary vasoconstrictor sensitivity by attenuating NO-dependent pulmonary vasodilation.

1. Assess effects of neonatal CH on regulation of basal tone and agonist-induced vasoconstriction by endogenous NO.
2. Evaluate the effect of CH on NO-dependent pulmonary vasodilation in neonatal rats.
3. Assess the effect of neonatal CH on expression of pulmonary NOS.

Approach

To test our hypothesis, we used an isolated (*in situ*) perfused lung preparation to evaluate the contribution of endogenous NO to basal and agonist-induced pulmonary vasoconstriction in normoxic and CH neonatal (2 week old) rats. Additional experiments examined vasodilatory responsiveness to the receptor-mediated, NO-dependent pulmonary vasodilator arginine vasopressin (AVP), and assessed pulmonary eNOS expression and phosphorylation status by western blotting. Our findings demonstrate a novel effect of neonatal CH to augment NO-dependent vasodilation and to increase pulmonary eNOS expression and phosphorylation at activation residue Ser-1177, responses that lessen enhanced basal tone and vasoconstrictor sensitivity to the thromboxane analog U-46619.

<u>Specific Aim 2</u>: Establish the contribution of ROS to enhanced vasoconstriction in CH-induced neonatal pHTN.

Hypothesis: MitoROS contribute to enhanced pulmonary arterial vasoconstriction in neonates with CH-induced pHTN.

1. Determine the contribution of ROS to enhanced basal tone and vasoconstrictor reactivity following CH in isolated *(in situ)* lungs.
2. Evaluate the role of mitoROS in enhanced pulmonary arterial vasoconstriction following CH in isolated pulmonary arteries.

Approach

To evaluate the hypothesis, we used scavengers of cytosolic ROS in an isolated (*in situ*) lung preparation to investigate the role of pulmonary ROS to mediate enhanced basal tone and agonist-induced vasoconstriction observed in neonates exposed to CH. In addition to *in situ* lung experiments, this study included protocols featuring isolated, pressurized small pulmonary arteries (100-200 μm) from control and CH neonates to evaluate the contribution of mitoROS to arterial tone. We observed that ROS contribute to enhanced basal tone and agonist-induced vasoconstriction in lungs from neonatal rats with pHTN. We additionally found that mitoROS contribute to enhanced tone in isolated pulmonary arteries from CH-exposed neonates. Our findings demonstrate that mitoROS contribute to enhanced pulmonary arterial tone in neonates with CH-induced pHTN.

<u>Specific Aim 3</u>: Define the contribution of PKC$_\beta$-signaling to enhanced vascular reactivity following CH exposure in neonates.

Hypothesis: PKC$_\beta$-dependent mitoROS generation in pulmonary vascular smooth muscle contributes to enhanced pulmonary arterial tone following neonatal CH.

1. Determine the contribution of PKC$_\beta$ to CH-dependent increases in vasoconstriction in both isolated (*in situ*) lungs and isolated pulmonary arteries.
2. Determine the effect of PKC$_\beta$ stimulation on mitoROS generation in neonatal pulmonary VSM.
3. Assess the effect of neonatal CH on PKC$_\beta$ expression.

Approach

To address our hypothesis, we used both isolated (*in situ*) lungs and pulmonary arteries to study the contribution of PKC$_\beta$ to enhanced pulmonary vasoconstriction observed in neonates following CH exposure. Additional studies examined PKC$_\beta$-dependent mitoROS generation in transiently cultured PASMCs from control neonates and assessed PKC$_\beta$ protein expression using western blotting. Our findings suggest that neonatal CH leads to PKC$_\beta$–dependent increases in pulmonary arterial tone and increased agonist-induced vasoconstriction without increasing PKC$_\beta$ protein expression. Additionally, PKC$_\beta$ promotes mitoROS production in pulmonary VSM of neonatal rats, a response that may contribute to PKC$_\beta$-dependent enhancement of pulmonary vasoconstriction following CH exposure.

CHAPTER 2 – METHODS

General Methods

All protocols used in this study were reviewed and approved by the Institutional Animal Care and Use Committee of the University of New Mexico Health Sciences Center.

Experimental Groups and Hypoxic Exposure Protocol

Timed-pregnant Sprague-Dawley (Harlan Industries) rats were allowed to acclimate for 1 wk before giving birth at ambient normobaric pressure (~630 mmHg in Albuquerque, NM). Litters selected for exposure to CH were housed in a hypobaric hypoxic chamber with barometric pressure maintained at 380 ± 5 mmHg for 12 days [beginning on postnatal day 2 of life]. Age-matched normoxic controls were housed in similar sham conditions at ambient barometric pressure. Neonates were housed with their birthing dam. The chamber was opened two times per wk to provide animals with food, water, and clean bedding. Animals were housed on a 12:12 hour light-dark cycle.

Assessment of Right Ventricular Systolic Pressure (RVSP), Right Ventricular Weight, and Hematocrit

RVSP and RV hypertrophy were evaluated as indices of pHTN (33, 248). Rats from each group were anesthetized with ketamine (40 mg/kg) and xylazine (6 mg/kg) (180). An upper transverse laparotomy was performed, and RVSP was assessed using a closed-chest transdiaphragmatic approach with a 25-gauge needle attached to a pressure transducer (Hugo Sachs Electronik-Harvard Apparatus). Entry into the right ventricle (RV) was confirmed by monitoring the pressure waveform. RVSP and heart rate were obtained using AT-CODAS data-acquisition software (Dataq Instruments). Fulton's index, expressed as the percent ratio of RV to left ventricle and interventricular

septum (LV+S) weight was used to assess the degree of CH-induced RV hypertrophy. The polycythemic response to CH was determined by measuring hematocrit (Hct) from blood samples taken by direct cardiac puncture at the time of lung isolation.

Isolated (in situ) Perfused Rat Lung Preparation

To evaluate the effect of neonatal CH on baseline as well as agonist-dependent changes in PVR, neonatal rats were anesthetized with pentobarbital sodium (200 mg/kg, i.p.). The animal was placed on a heating block, the trachea was cannulated and lungs were ventilated with a positive-pressure mouse ventilator (Hugo Sachs Electronik-Harvard Apparatus) at a tidal volume of 5 ml/kg body wt. and a rate of 100 breaths/min with a warmed and humidified gas mixture (21% O_2/6% CO_2/balance N_2). End-expiratory pressure was maintained at 3 cm H_2O. After removal of the frontal ribcage, heparin (5 U, 50 µl) was injected into the RV and the pulmonary artery was cannulated with custom fitted PE-90 tubing (Becton-Dickinson). The preparation was immediately perfused with a peristaltic pump (Ismatec) at a rate of 0.1 ml/min with a physiological saline solution (PSS) containing in mM: 129.8 NaCl, 5.4 KCl, 0.83 $MgSO_4$, 19 $NaHCO_3$, 1.8 $CaCl_2$, and 5.5 glucose with 4% (wt/vol) bovine serum albumin (BSA) (all from Sigma). Following cannulation of the pulmonary artery, the left ventricle was cannulated with custom fitted PE-160 tubing. Perfusion rate (Q) was gradually increased to a maximum of 15 ml/min·kg body wt. Perfusion was non-recirculating until the perfusate exiting the lung was nearly free of blood. Recirculation was then initiated and maintained for the duration of the experiment. Total recirculating volume was ~3.5 ml. Following a 20 min equilibration period, an effluent sample of PSS was collected for determination of pH, Pco_2, and Po_2 using a handheld iSTAT 1 blood gas analyzer (Abbott) and iSTAT test cartridges (G3+, Abbott). Lungs were kept in zone 3 conditions by maintaining venous pressure at 3 mmHg and airway pressure at 1 mmHg (53).

Pulmonary arterial (P_a) and venous (P_v) pressures were recorded continuously. Pressures were measured using a P-75 pressure transducer (Hugo Sachs Electronik-Harvard Apparatus) connected to the pulmonary arterial and venous lines. Data were recorded and processed using data acquisition software and hardware (AT-CODAS, Dataq Instruments). Total PVR was calculated as $(P_a-P_v)/Q$.

Assessment of Segmental Vascular Resistance in Isolated (in situ) Rat Lungs

Effects of neonatal CH on basal and agonist-induced changes in arterial and venous resistance were determined using a double occlusion method as previously reported (80, 226). Briefly, lungs were isolated as described above and inflow and outflow lines were simultaneously occluded, allowing arterial and venous pressures to rapidly equilibrate to an approximation of microvascular capillary pressure (P_c). Pulmonary arterial resistance was calculated using the formula, $(P_a-P_c)/Q$, and pulmonary venous resistance was calculated using, $(P_c-P_v)/Q$.

Western Blot in Whole Lung Homogenates and Isolated Pulmonary Arteries

Western blots were performed as previously reported (52). Whole lungs collected from neonates on post-natal day 14 (P14) were snap-frozen in liquid nitrogen and stored at -80°C. On the day of experimentation, frozen lungs were fragmented with a mortar and pestle pre-cooled in liquid nitrogen.

In experiments requiring investigation of arterial protein content, pulmonary arteries were collected from lungs of P14 neonatal pups and snap frozen in liquid nitrogen and stored at -80°C until assayed.

Frozen lung tissue or pulmonary arteries were added to a Dounce homogenizer containing ice-cold homogenization buffer [10 mM Tris·HCl (pH 7.4), 255 mM sucrose, 2 mM EDTA, 12 μM leupeptin, 4 μM pepstatin A, 1 μM aprotinin, 1% v/v phosphatase

inhibitor cocktail 3 (cantharidin, (-)-p-bromolevamisole oxalate, and calyculin A) from Sigma]. Tissue homogenates were sonicated on ice with an ultrasonic homogenizer (Cole Parmer). Homogenates were then spun at 1500 x g for 10 min in a desktop centrifuge (Beckman) at 4°C. Sample protein concentrations were assessed using a NanoDrop (Thermo Fisher Scientific). Samples (15-45 µg/lane) were resolved by SDS-PAGE using 7.5% acrylamide gels along with molecular-weight standards (Bio-Rad). The separated proteins were transferred to polyvinylidene difluoride membranes (Bio-Rad) and blocked for 1 hour at room temperature with 5% nonfat milk (Carnation) and 0.05% Tween-20 (Bio-Rad) in a Tris-buffered saline solution (TBS) containing 10 mM Tris·HCl and 50 mM NaCl (pH 7.5). Blots were then incubated overnight at 4°C with slight agitation in primary antibody. For each protein of interest, various primary antibodies were used and are indicated in specific methods for each aim of this study.

Blots were then probed with a horseradish peroxidase-conjugated goat secondary antibody raised against the animal of origin for the primary antibody (1:3000; Bio-Rad) in TTBS plus 5% nonfat milk to achieve immunochemical labeling. Chemiluminescence labeling was performed according to manufacturer instructions (ECL substrate, Thermo Scientific). Protein bands were detected using chemiluminescent-sensitive film and band intensity was quantified by densitometric analysis using ImageJ (NIH). To control for protein loading, all membranes were treated with Coomassie Brilliant Blue (Bio-Rad) to stain total protein. All bands were normalized to total protein content in the membrane as assessed by coomassie staining (208).

Calculations and Statistics

Data are expressed as mean ± standard error of the mean (SEM). Values of “n” indicate numbers of animals per experimental group. A t-test, one-way analysis of variance (ANOVA), or two-way ANOVA was used to make comparisons between groups

when appropriate. If differences were detected using ANOVA, individual groups were further evaluated using a Student-Newman-Keuls post-hoc comparison. Percentage data were arcsine transformed before statistical comparison. *P* values of <0.05 were considered significant.

Protocols for Specific Aims

Protocols for Specific Aim 1

Determine the contribution of endothelial dysfunction to enhanced basal tone and agonist-induced vasoconstriction in neonatal pHTN.

Protocol Series 1.1: Assess effects of neonatal CH on regulation of basal tone and agonist-induced vasoconstriction by endogenous NO.

To assess the role of endogenous NO to baseline PVR, lungs from each group were perfused with PSS containing either saline vehicle or the NOS inhibitor, N^{ω}-nitro-L-arginine (L-NNA; 300 μM). We have previously demonstrated that this dose of L-NNA effectively inhibits NO-dependent pulmonary vasodilation in isolated, perfused lungs from adult rats (230). After a 20 min equilibration period, P_c was assessed by double occlusion technique. The contribution of active tone to baseline PVR was assessed by administration of the NO donor, 1,3-propanediamine, *N*-{4-[1-(3-aminopropyl)-2-hydroxy-2-nitro-sohydrazino]butyl} (spermine NONOate; 100 μM) to maximally dilate the pulmonary vasculature. A second double occlusion was performed after stabilization of the response to spermine NONOate. Basal tone is expressed as the change in resistance to spermine NONOate.

The effect of endogenous NO to limit vasoconstrictor reactivity was determined by performing cumulative concentration-response curves to the thromboxane analog 9,11-dideoxy-9α,11α-methanoepoxy prostaglangin $F_{2\alpha}$ (U-46619) in the presence and

absence of L-NNA. Double occlusions were performed to assess P_c under baseline conditions and following development of a stable pressor response to each concentration of U-46619.

Protocol Series 1.2: Evaluate the effect of CH on NO-dependent pulmonary vasodilation in neonatal rats.

Endothelium-Dependent Vasodilatory Responses. Receptor-mediated vasodilation to the endothelium-derived NO (EDNO)-dependent vasodilator, AVP (226), was measured in lungs from control and CH neonatal rats. After a 20 min equilibration period, lungs were preconstricted with the thromboxane analog, U-46619 to achieve a stable arterial pressor response of ~10 mmHg. AVP (25 nM) was then added to the perfusate to induce vasodilation. Parallel protocols were performed in the presence of L-NNA to verify the contribution of endogenous NO to this response. Vasodilatory responses are expressed as a percent reversal of U-46619-mediated constriction.

Responses to Exogenous NO. Considering that EDNO-dependent responses following CH may be influenced by altered NO bioavailability or VSM sensitivity to NO, we assessed concentration-response curves to the NO donor, spermine NONOate, in lungs from each group of rats. After the equilibration period, lungs were preconstricted with U-46619 to ~10 mmHg above baseline P_a. Once the constriction stabilized, a cumulative concentration-response curve to spermine NONOate was performed. Considering that lungs from neonates exposed to CH display greater basal pulmonary arterial constriction than control lungs, we repeated these experiments in lungs preconstricted with U-46619 to achieve similar overall P_a between groups. All experiments were conducted in the presence of L-NNA to eliminate the contribution of

endogenous NO to these responses. Segmental vascular resistances were evaluated by double occlusion technique at baseline, after stabilization of the U-46619 constriction, and following stabilization of the response to each concentration of NONOate.

Protocol Series 1.3: Assess the effect of neonatal CH on expression of pulmonary NOS.

The effect of CH on the expression of NOS isoforms: NOS I (neuronal or nNOS), NOS II (inducible or iNOS), NOS III (endothelial or eNOS), as well as the post-translational phosphorylation of eNOS at serine-1177, a modification associated with increased eNOS-dependent NO production (75), were also investigated. Western blots were performed using whole lung homogenates from both control and CH neonates as outlined above in the general western blot protocol. Samples (45 µg protein/lane) were resolved by SDS-PAGE with 7.5% acrylamide along with molecular-weight standards (Bio-Rad). Antibodies used to probe for NOS isoforms included mouse monoclonal antibodies against nNOS (1:500; BD Biosciences-Transduction Labs), iNOS (1:500; BD Biosciences-Transduction Labs), eNOS (1:1000; BD Biosciences-Transduction Labs), and phospho(Ser-1177)-eNOS (1:1000; BD Biosciences-Transduction Labs). Protein expression was normalized to total protein to account for any variance in protein loading.

Protocols for Specific Aim 2

Establish the contribution of ROS to enhanced vasoconstriction in CH-induced neonatal pHTN.

Protocol Series 2.1: Determine the contribution of ROS to enhanced basal tone and vasoconstrictor reactivity following CH in isolated *(in situ)* lungs.

To evaluate the role of ROS in enhanced vasoconstriction following CH, lung studies similar to those in Protocol Series 1.1 were repeated in the presence of the

superoxide dismutase (SOD) mimetic, 1-oxyl-2,2,6,6-tetramethyl-4-hydroxypiperidine (218) (TEMPOL; 1 mM). All lungs were pretreated with L-NNA (300 μM) to avoid complications of endogenous NO on observed studies. Lungs from P14 neonates in both groups were allowed to equilibrate for 20 minutes, after which a baseline double occlusion was performed. The contribution of vascular tone to baseline PVR was assessed via administration of spermine NONOate. A double occlusion was performed after stabilization of the response to NONOate. Basal tone is expressed as the change in resistance to spermine NONOate.

To determine the effect of ROS on vasoconstrictor sensitivity of the pulmonary vasculature in control and CH pups, a cumulative dose-response curve to U-46619 (50, 100, 150, and 200 nM) was performed in the presence and absence of TEMPOL. A double occlusion was performed after a stabilized pressor response at each concentration.

Protocol Series 2.2: Evaluate the role of mitoROS in enhanced pulmonary arterial vasoconstriction following CH in isolated pulmonary arteries.

We assessed the role of ROS to mediate enhanced pulmonary arterial vasoconstrictor reactivity in pressurized small pulmonary arteries isolated from each group of animals (P14) as previously described (44, 197, 242). Pulmonary arteries [~150-200 μm inner diameter (i.d.)] from the left lung were dissected from surrounding parenchyma and cannulated on glass microcannulae secured in a vessel perfusion chamber (Living Systems Instrumentation). Cannulated, pressurized vessels were superfused with recirculating, heated (37°C) PSS bubbled with a 6% CO_2/10% O_2/balance N_2 gas mixture for a 20 min equilibration period. Vessel i.d. was simultaneously measured using bright-field videomicroscopy. Following a 20 min equilibration period, L-NNA (300 μM) was added to the superfusate. In the presence of

L-NNA, the vessels developed vasomotor tone. Experiments were allowed to progress for a minimum of 20 min or until the vasoconstrictor response stabilized. Following stabilization of basal tone, vessels were superfused with non-recirculating Ca^{2+}-free PSS that contained (in mM) 129.8 NaCl, 5.4 KCl, 0.83 $MgSO_4$, 19 $NaHCO_3$, 5.5 glucose, and 3 ethylene glycol-bis(β-aminoethyl ether)-N,N,N'N'-tetraacetic acid (EGTA) for 30 min. Following a 30 min Ca^{2+}-free PSS washout, recirculation was initiated and ionomycin [3 μM; Ca^{2+} ionophore (198, 243)] was added to maximally dilate the vessel. Basal tone was expressed as % of maximally dilated, Ca^{2+}-free diameter using the formula: [(Ca^{2+}-free i.d. – Constricted i.d.)/Ca^{2+}-free i.d.]*100.

In isolated vessel studies conducted in the presence of ROS inhibitors, the inhibitor was present throughout the experiment – during the vessel dissection, cannulation, equilibration, and L-NNA exposure. Basal tone studies were performed in the presence and absence of the mitochondrial specific SOD mimetic, MitoTEMPO (74) (200 μM), MitoQ (67, 109, 241) (1 μM; restores electron flux through the electron transport chain to lower oxidative stress), or vehicle.

Protocols for Specific Aim 3

Define the contribution of PKC_β-signaling to enhanced vascular reactivity following CH exposure in neonates.

Protocol Series 3.1: Determine the contribution of PKC_β to CH-dependent increases in vasoconstriction.

Isolated (in situ) lung studies

To evaluate the role of PKC_β to mediate enhanced vasoconstriction following CH, lung studies similar to those in Protocol Series 2.1 were repeated in the presence of

either the general PKC inihibitor, Ro 31-8220 (242) (10 μM) or the selective PKC_{β} inhibitor LY-333,531 (84, 146, 242) (10 nM). As in Protocol Series 2.1, all lungs were pretreated with L-NNA (300 μM). Following a 20 minute equilibration period, a baseline double occlusion was performed in all *in situ* lung preparations. The contribution of vascular tone to baseline PVR was assessed through administration of spermine NONOate. A double occlusion was performed after stabilization of the response to NONOate. Basal tone is expressed as the change in resistance to spermine NONOate.

To determine the contribution of PKC and PKC_{β} to vasoconstrictor sensitivity of the pulmonary vasculature in neonates from both groups, a cumulative dose-response curve to U-46619 (50, 100, 150, and 200 nM) was performed in the presence and absence of either Ro 31-8220 (10 μM) or LY-333,531 (10 nM). A double occlusion was performed after a stabilized pressor response at each concentration.

Isolated pulmonary arteries

Parallel to Protocol Series 2.2, we assessed effects of PKC_{β} inhibition with LY-333,531 on basal tone development in isolated, pressurized pulmonary arteries (~150-200 μm i.d.) collected from both control and CH neonates. Similar to Protocol Series 2.2, cannulated arteries were equilibrated in bubbled PSS for 20 min. Following a 20 min equilibration period, L-NNA (300 μM) was added to the superfusate. In the presence of L-NNA, the vessels developed vasomotor tone. Experiments were allowed to progress for a minimum of 20 min or until the vasoconstrictor response stabilized. Following stabilization of tone, vessels were superfused with non-recirculating Ca^{2+}-free PSS for 30 min. Following a 30 min Ca^{2+}-free PSS washout, recirculation was initiated and ionomycin (3 μM) was added to maximally dilate the vessel. Basal tone was expressed as % of maximally dilated, Ca^{2+}-free diameter using the formula: [(Ca^{2+}-free i.d. – Constricted i.d.)/Ca^{2+}-free i.d.]*100.

To evaluate the contribution of PKC_{β} to arterial tone development, isolated pulmonary arteries from both control and CH neonates were evaluated in the presence and absence of LY-333,531 (10 nM). When present, LY-333,531 was maintained throughout the experimental duration – during the vessel dissection, cannulation, equilibration, and L-NNA exposure.

Protocol Series 3.2: Determine the effect of PKC_{β} stimulation on mitoROS generation in neonatal pulmonary VSM.

PKC-dependent increases in levels of mitochondrial ROS (mitoROS) were assessed in transiently cultured, primary PASMCs as previously described (208). Briefly, neonatal rats (P14) from control neonates were anesthetized with pentobarbital sodium (200 mg/kg i.p.) and the heart and lungs were exposed via midline thoracotomy. The left and right lungs were removed and placed in sterile 20 mM Ca^{2+} Hank's buffered saline solution (HBSS) plus 1% (v/v) penicillin/streptomycin (pen/strep). Intrapulmonary arteries (~2^{nd}-5^{th} order) were dissected from surrounding lung parenchyma. To isolate PASMCs, isolated pulmonary arteries from both lungs were enzymatically digested in 20 mM Ca^{2+} HBSS containing papain (9.5 U/ml), type-1 collagenase (1,750 U/ml), and dithiothreitol (1 mM) at 37°C for 15 min. Following enzymatic digestion, collected pulmonary arteries were added to a 70 μm cell strainer and rinsed with 10 mL Ca^{2+}-free HBSS. Pulmonary arteries were then added to a fresh Eppendorf tube containing Ca^{2+}-free HBSS and dispersed with a Pasteur pipette. The cell suspension was then placed on gelatin-coated 25 mm glass coverslips and cultured in Ham's F-12 media supplemented with 5% fetal bovine serum (FBS) and 1% pen/strep for 48 hrs at 37°C.

Cultured PASMCs from control neonates were serum starved for 24 hours in Ham's F-12 media plus 1% FBS and 1% pen/strep prior to experimentation. Cells were then treated with PMA (10 μM) to stimulate PKC-dependent mitoROS production.

Mitochondrial-derived O_2^- was detected with the mitochondrial specific O_2^- indicator MitoSOX (147) (5 μM). Depending on the experimental protocol, cells were pre-treated with scavengers of cellular ROS, 1-oxyl-2,2,6,6-tetramethyl-4-hydroxypiperidine (218) (TEMPOL; 1 mM) and 4,5-Dihydroxy-1,3-benzenedisulfonic acid disodium salt (145) (Tiron, 10 mM). A selective scavenger of mitochondrial O_2^- was also used (2-(2,2,6,6-tetramethylpiperidin-1-oxyl-4-ylamino)-2-oxoethyl)triphenylphosphonium chloride (mitoTEMPO, 200 μM). ROS scavenger pre-treatment occurred for 20 minutes at 37°C and remained throughout the duration of mitoSOX treatment. Following 20 min pre-treatment, PASMCs were then exposed to mitoSOX for 30 min before being fixed with 4% paraformaldehyde (PFA). The coverslips containing mitoSOX labeled PASMCs were then secured to a glass slide using FluoroGel (Electron Microscopy Sciences) and imaged using confocal microscopy.

Fluorescence images were acquired with a x63 80% glycerol immersion objective on a confocal microscope (Leica, TCS SP5, 1.3 numerical aperture). MitoSOX was excited with a DPSS 561 laser and the emission processed through an Acousto-Optical Beam Splitter (AOBS, Leica) crystal set to an emission bandwidth of 570 nm – 620 nm. Images were obtained without an optical zoom (x-y pixel dimensions of 0.49 μm x 0.49 μm), all images were obtained using a 512 x 512 frame, and frame averaging of 2 scans. Scan speed was set to 400 Hz. Laser power was 60% for the DPSS 561 laser. Z-stacks were obtained at z-steps of 0.8 μm. Detector gain and offset setting were held constant for all acquired z-stacks at a gain setting of 985 and an offset of -12 for the photomultiplier tube set to collect bandwidth of 570 nm – 620 nm.

Quantification of fluorescence was performed using SlideBook 6 (3i: Intelligent Imaging Innovations). MitoSOX fluorescence intensity is represented as an average fluorescence intensity using an inclusive threshold of 10,000 to 65,535 (maximum for 16 bit images). Each z-stack was thresholded to select for positive-stained areas with

fluorescence intensity values above background (cells not treated with MitoSOX). Data are reported as mean ± SEM and n represents the number of individual animals that yielded cells for experimentation. Each individual n is an average of 2 technical replicates of cells from the same animal. To explore PKC_{β}-dependent mitoROS production, we conducted studies parallel to Protocol Series 2.2, in the presence and absence of LY-333,531.

Protocol Series 3.3: Assess the effect of neonatal CH on PKC_{β} expression.

Western blots were performed to evaluate protein expression of PKC_{β} splice variants (PKCβI and PKCβII) protein expression in isolated pulmonary arteries from each group of rats (209, 269). The following primary antibodies were used: α-$PKC_{\beta I}$ (1:200, Santa Cruz) and α-$PKC_{\beta II}$ (1:200, Santa Cruz). Protein expression was normalized to total protein, as determined by staining with Coomassie, to account for variance in protein loading.

CHAPTER 3 – RESULTS

General

Evidence for pHTN and Right Ventricular Hypertrophy in Neonatal CH Rats

CH neonates developed higher RVSP compared to normoxic control rats (Figure 2A, B). Heart rate was not significantly different between groups (**Table 1**). Consistent with elevated RVSP, the ratio of RV to LV+S weight was increased by CH exposure, demonstrating RV hypertrophy indicative of pHTN (**Figure 2**C). Similar results were obtained for RV weight normalized to either body weight or total heart weight (**Table 1**). CH also increased LV+S weight normalized to body mass, which may reflect a lower body weight of CH neonates compared to age-matched controls (**Table 1**). Hematocrit was greater in rats exposed to CH compared to controls, reflecting the polycythemic response to CH (**Table 1**).

Saline gases in isolated (in situ) lung experiments

Effluent collected from both control and CH rats and analyzed by iStat demonstrtated that pH, P_{CO2}, and P_{02} did not differ between groups (**Table 2**).

Specific Aim 1

Determine the contribution of endothelial dysfunction to enhanced basal tone and agonist-induced vasoconstriction in neonatal pHTN.

Hypothesis:

We hypothesized that neonatal CH enhances basal tone and pulmonary vasoconstrictor sensitivity by limiting NO-dependent pulmonary vasodilation.

Figure 2

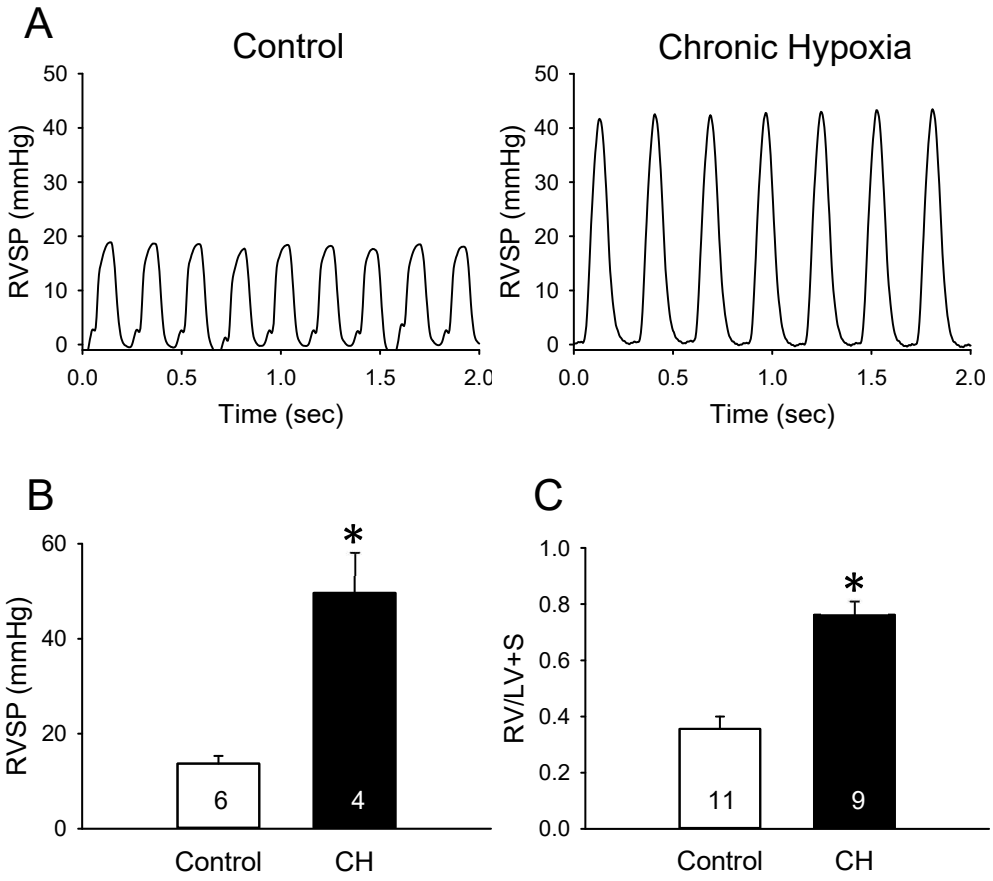

Figure 2. Chronic hypoxia (CH) increases peak right ventricular systolic pressure (RVSP) and induces RV hypertrophy in neonatal rats.
(A) Sample pressure traces and (B) Summary data for peak RVSP in control and CH neonates. (C) Ratio of right ventricular (RV) mass to left ventricular plus septal (LV+S) mass for each group. Values are means ± SEM; n = 4-11/group (indicated in bars); *p<0.05 vs. control, analyzed by unpaired t-test.

Table 1

	Control	CH
Final BW (g)	26.2 ± 0.5 (17)	20.0 ± 0.8 (9)*
RV/BW (mg/g)	1.12 ± 0.05 (11)	4.40 ± 0.39 (9)*
LV+S/BW (mg/g)	3.15 ± 0.07 (11)	5.85 ± 0.25 (9)*
RV/Total (mg/mg)	0.26 ± 0.01 (11)	0.43 ± 0.02 (9)*
Hematocrit (%)	31 ± 1 (11)	37 ± 1 (9)*
Heart Rate (beats/min)	255 ± 11 (6)	301 ± 26 (4)

Table 1. Body weight, heart weights, hematocrit, and heart rate from control and CH neonatal rats.
Values are means ± SEM; n = 4-11 animals/group (indicated in parentheses).
*p<0.05 vs. control; analyzed by unpaired t-test. RV, right ventricle; BW, body weight; LV+S, left ventricle plus the interventricular septum; Total, total heart weight.

Table 2

	Control	CH
pH	7.47 ± 0.04 (11)	7.49 ± 0.03 (22)
pCO_2 (mmHg)	18.93 ± 1.03 (11)	18.03 ± 0.78 (22)
pO_2 (mmHg)	106.64 ± 2.14 (11)	105 ± 2.84 (22)

Table 2. Saline gas values from recirculating perfusate of lungs from control and CH neonates.
Perfusate samples were taken following a 20 min equilibration period. Values are mean ± SEM with n in parenthesis; n = 11-22/group; analyzed by t-test, no significant differences between groups.

Endogenous NO Limits CH-Dependent Increases in Basal Pulmonary Vascular Resistance

In situ lungs from neonates exposed to CH displayed elevated total and arterial baseline vascular resistance compared to normoxic controls (**Figure 3**A, B). In contrast, venous resistance was unaltered by CH exposure (**Figure 3**C). L-NNA increased total, arterial and venous baseline PVR in lungs from CH neonates, while having no effect in control pups (**Figure 3**).

The contribution of basal tone to CH-dependent increases in PVR was assessed by evaluating changes in total and segmental resistances to the NO donor, spermine NONOate, in lungs from each group. CH increased basal tone (**Figure 4**A) in the absence of NOS inhibition. This effect of CH appeared to result from arterial constriction since changes in arterial resistance to spermine NONOate tended to be greater in lungs from CH rats compared to controls (**Figure 4**B), although this response did not reach statistical significance. NOS inhibition increased basal pulmonary vascular tone in CH rats (**Figure 4**A) by further augmenting arterial constriction (**Figure 4**B), while having no significant effect in control lungs. In contrast, venous tone was minimal and unaltered by either CH exposure or treatment with L-NNA (**Figure 4**C).

Endogenous NO Attenuates U-46619-Induced Pulmonary Vasoconstriction

In addition to effects of CH to increase basal tone (**Figure 4**), total, arterial and venous constrictor responses to U-46619 were greater in lungs from CH compared to normoxic neonates in the absence of NOS inhibition (**Figure 5**). L-NNA markedly augmented vasoconstrictor reactivity to U-46619 in lungs from CH rats, while having a more modest effect in control lungs. Enhanced vasoconstrictor sensitivity to U-46619 following CH was primarily a function of greater arterial constriction (**Figure 5**B), as venous responses to U-46619 were minimal (**Figure 5**C).

Figure 3

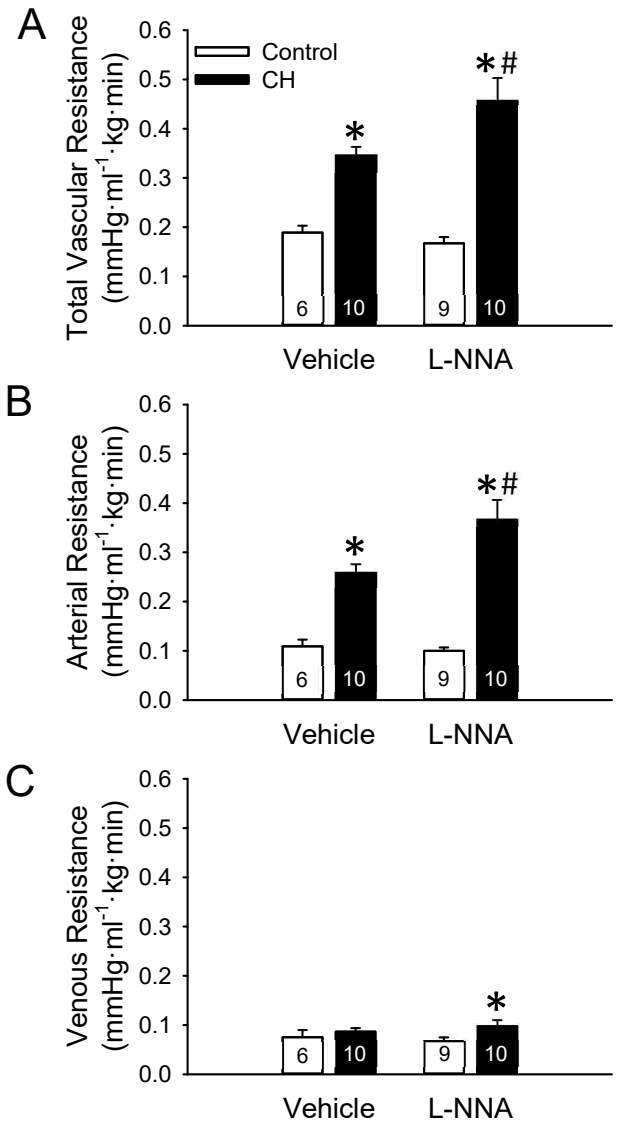

Figure 3. Endogenous NO limits CH-dependent increases in baseline pulmonary vascular resistance.
(A) total, (B) arterial, and (C) venous baseline vascular resistances in lungs (in situ) from control and CH neonatal rats in the presence or absence of the NOS inhibitor L-NNA (300 μM). Values are means ± SEM; n = 6-10/group (indicated in bars); *p<0.05 vs. control, #p<0.05 vs. vehicle, analyzed by two-way ANOVA followed by Student-Newman-Keuls post-hoc comparison.

Figure 4

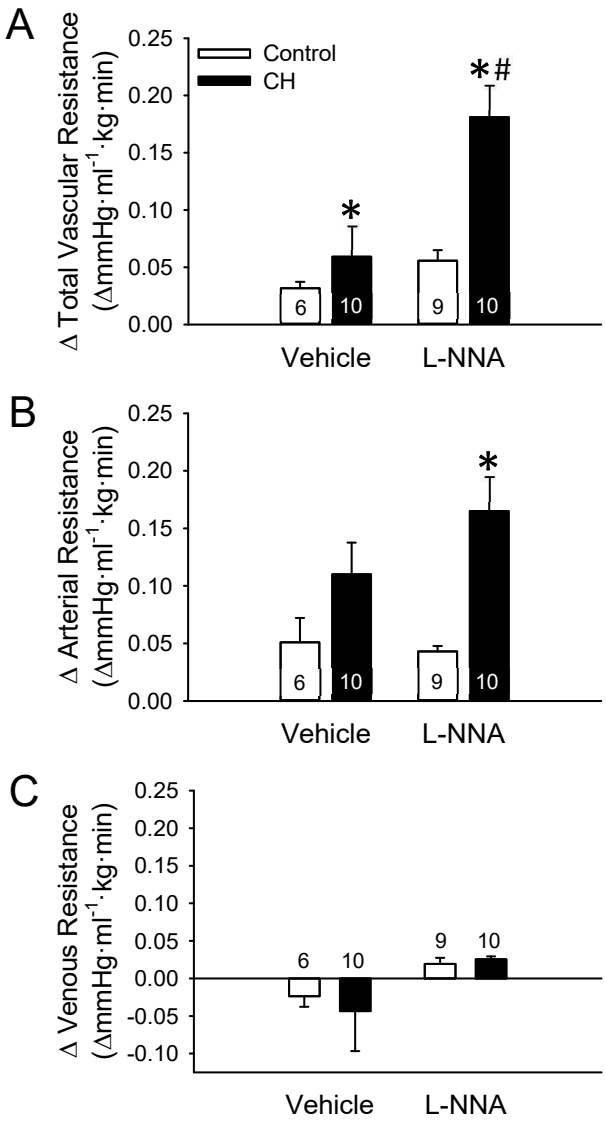

Figure 4. Endogenous NO limits CH-dependent increases in basal pulmonary arterial tone.
The contribution of basal tone to (A) total, (B) arterial and (C) venous resistance is expressed as the change in resistance to spermine NONOate (100 μM) in lungs (in situ) from control and CH neonates. Experiments were conducted in the presence or absence of L-NNA (300 μM). Values are means ± SEM; n = 6-10/group (indicated in or above bars); *p<0.05 vs. control, #p<0.05 vs. vehicle, analyzed by two-way ANOVA followed by Student-Newman-Keuls post-hoc comparison.

Figure 5

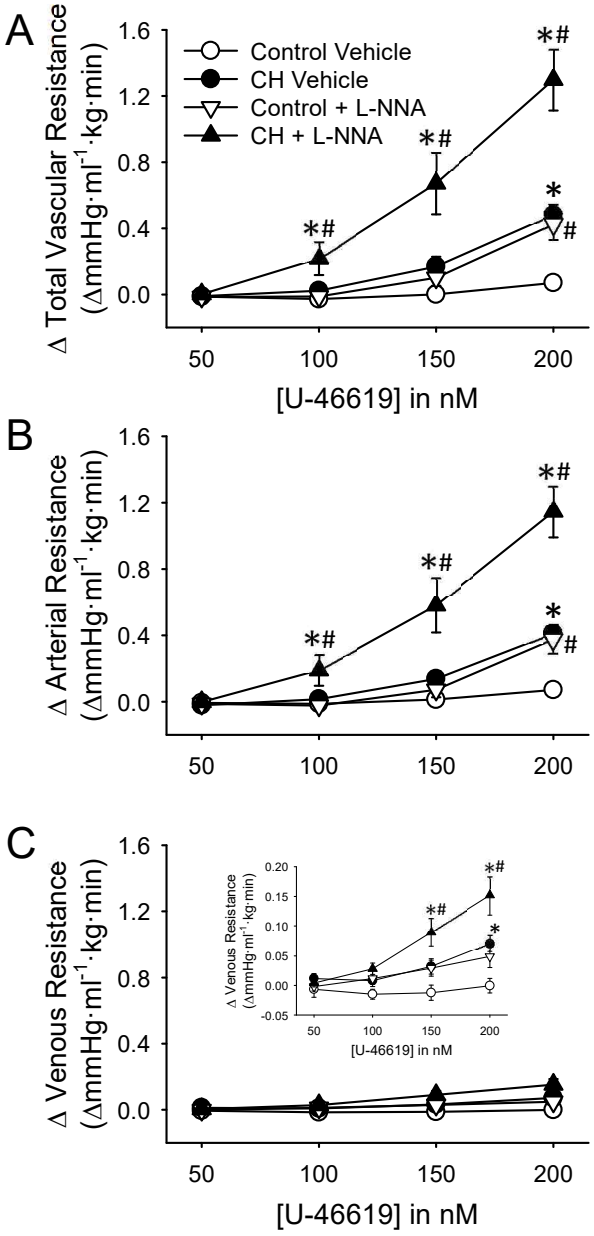

Figure 5. Endogenous NO limits CH-dependent increases in vasoconstrictor sensitivity to U-46619.
Changes in (A) total, (B) arterial, and (C) venous resistance to U-46619 in lungs (in situ) from control and CH neonates. Experiments were conducted in the presence or absence of L-NNA (300 μM). Values are means ± SEM; n = 8 for Control Vehicle, n = 10 for CH Vehicle, n = 9 for Control L-NNA, n = 9 for CH L-NNA; *p<0.05 vs. control, #p<0.05 vs. vehicle; analyzed by two way ANOVA at each concentration of U-46619 followed by Student-Newman-Keuls post-hoc comparison.

CH Augments EDNO-Dependent Pulmonary Vasodilation

Lungs from control and CH neonates were preconstricted with a concentration of U-46619 sufficient to achieve similar pressor responses between groups (**Table 3**) and then treated with AVP to dilate the pulmonary circulation. Vasodilatory responses to AVP were greatly augmented following exposure to CH (**Figure 6**A). L-NNA nearly abolished AVP-induced pulmonary vasodilation in lungs from each group demonstrating that this response depends on NOS-derived NO.

CH Does Not Alter Vasodilatory Responsiveness to Exogenous NO

In contrast to effects of CH to augment EDNO-dependent vasoreactivity (**Figure 6**A), vasodilatory responses to exogenous NO (spermine NONOate) in L-NNA pre-treated lungs were not different between lungs from control and CH neonatal rats (**Figure 6**B). Similar responses to spermine NONOate were observed whether U-46619 was added to achieve similar changes in PVR or total PVR between groups (**Table 4**).

CH Increases levels of Pulmonary eNOS as well as Serine-1177-Phosphorylated eNOS

Both total eNOS and the ratio of Ser-1177 phosphorylated eNOS to total eNOS were greater in lung samples from CH neonates compared to controls (**Figure 7**) as determined by western blotting. In contrast, CH had no significant effect on pulmonary nNOS or iNOS levels (**Figure 8**).

Table 3

	Control Vehicle	Control L-NNA	CH Vehicle	CH L-NNA
Baseline R	0.18 ± 0.01 (14)	0.22 ± 0.02 (6)	0.50 ± 0.03* (6)	0.70 ± 0.04*# (5)
Constricted R	0.75 ± 0.06 (14)	0.98 ± 0.13 (6)	1.35 ± 0.1* (6)	1.53 ± 0.16* (5)
ΔR to U-46619	0.57 ± 0.05 (14)	0.76 ± 0.13 (6)	0.84 ± 0.1 (6)	0.83 ± 0.16 (5)
ΔR to AVP	-0.17 ± 0.03 (14)	-0.05 ± 0.02 (6)#	-0.76 ± 0.08* (6)	-0.08 ± 0.01*# (5)

Table 3. Pulmonary vascular resistance values for lungs from control and CH neonates treated with AVP in the presence or absence of LNNA.
When indicated, 300 μM L-NNA present throughout experiment. Units of resistance (R) are mmHg ·ml^{-1}·kg·min. Values are means ± SEM with n in parenthesis; n = 5-14/group; *p<0.05 vs. control, #p<0.05 vs. vehicle; analyzed by two way ANOVA, individual groups were further evaluated using a Student-Newman-Keuls post-hoc comparison.

Figure 6

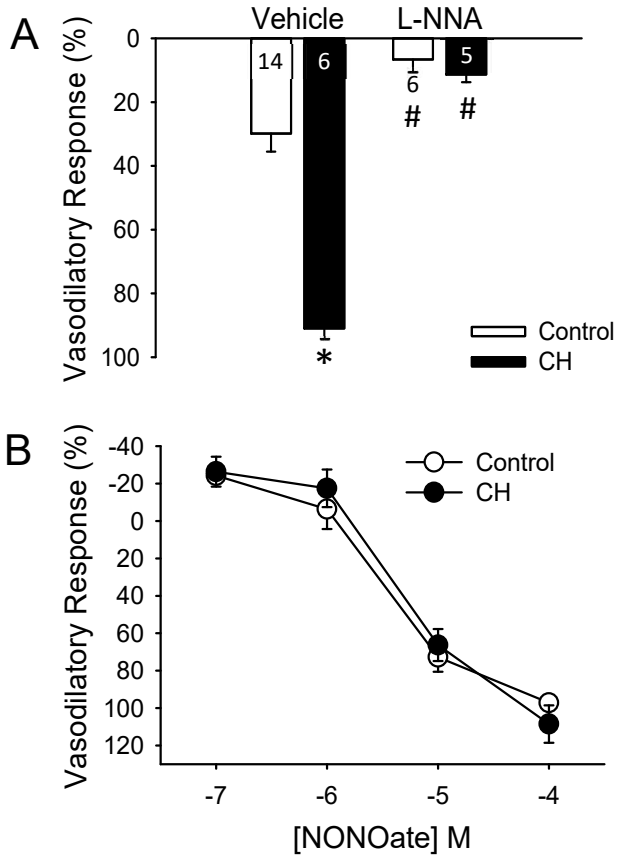

Figure 6. CH augments EDNO-dependent vasodilation to arginine vasopressin (AVP) without altering smooth muscle sensitivity to NO.
A. Total vasodilatory responses (percent reversal of U-46619-induced constriction) to AVP (25 nM) in lungs (in situ) from control and CH neonates. Experiments were conducted in the presence or absence of L-NNA (300 μM). Values are means ± SEM; n = 5-14/group (indicated in or below bars); *p<0.05 vs. control, #p<0.05 vs. vehicle, analyzed by two way ANOVA followed by Student-Newman-Keuls post-hoc comparison. **B.** Total vasodilatory responses (percent reversal of U-46619-induced constriction) to spermine NONOate. Experiments were conducted in the presence of L-NNA to limit the contribution of endogenous NO production. Values are means ± SEM; n = 5 for Control, n = 5 for CH; analyzed by two way ANOVA.

Table 4

	U-46619 added to achieve similar change in PVR between groups		U-46619 added to achieve similar total PVR between groups	
	Control	CH	Control	CH
Baseline R	0.20 ± 0.03 (5)	0.49 ± 0.04* (5)	0.2 ± 0.01 (4)	0.49 ± 0.05* (4)
Constricted R	0.87 ± 0.07 (5)	1.26 ± 0.09* (5)	1.13 ± 0.93 (4)	1.33 ± 0.08 (4)
ΔR to U-46619	0.67 ± 0.06 (5)	0.77 ± 0.10 (5)	0.93 ± 0.08 (4)	0.84 ± 0.09 (4)
ΔR to 10^{-7} M NONOate	0.16 ± 0.04 (5)	0.22 ± 0.09 (5)	0.25 ± 0.03 (4)	0.26 ± 0.01 (4)
ΔR to 10^{-6} M NONOate	0.04 ± 0.11 (5)	0.16 ± 0.09 (5)	0.22 ± 0.07 (4)	0.21 ± 0.10 (4)
ΔR to 10^{-5} M NONOate	-0.53 ± 0.03 (5)	-0.53 ± 0.11 (5)	-0.55 ± 0.06 (4)	-0.63 ± 0.06 (4)
ΔR to 10^{-4} M NONOate	-0.65 ± 0.05 (5)	-0.86 ± 0.14 (5)	-0.88 ± 0.07 (4)	0.98 ± 0.08 (4)

Table 4. Pulmonary vascular resistance values for lungs from control and CH neonates treated with NONOate.
300 μM L-NNA present throughout experiment. Left side of table shows data from lungs with [U-46619] sufficient to raise baseline pulmonary arterial pressure by 10 mmHg in both groups. Right side of table shows data from lungs with [U-46619] to equalize baseline pulmonary arterial pressure between groups. Units of resistance (R) are mmHg $\cdot ml^{-1} \cdot kg \cdot min$. Values are means ± SEM with n in parenthesis; n = 5-14/group; *$p<0.05$ vs. control; analyzed by unpaired t-test.

Figure 7

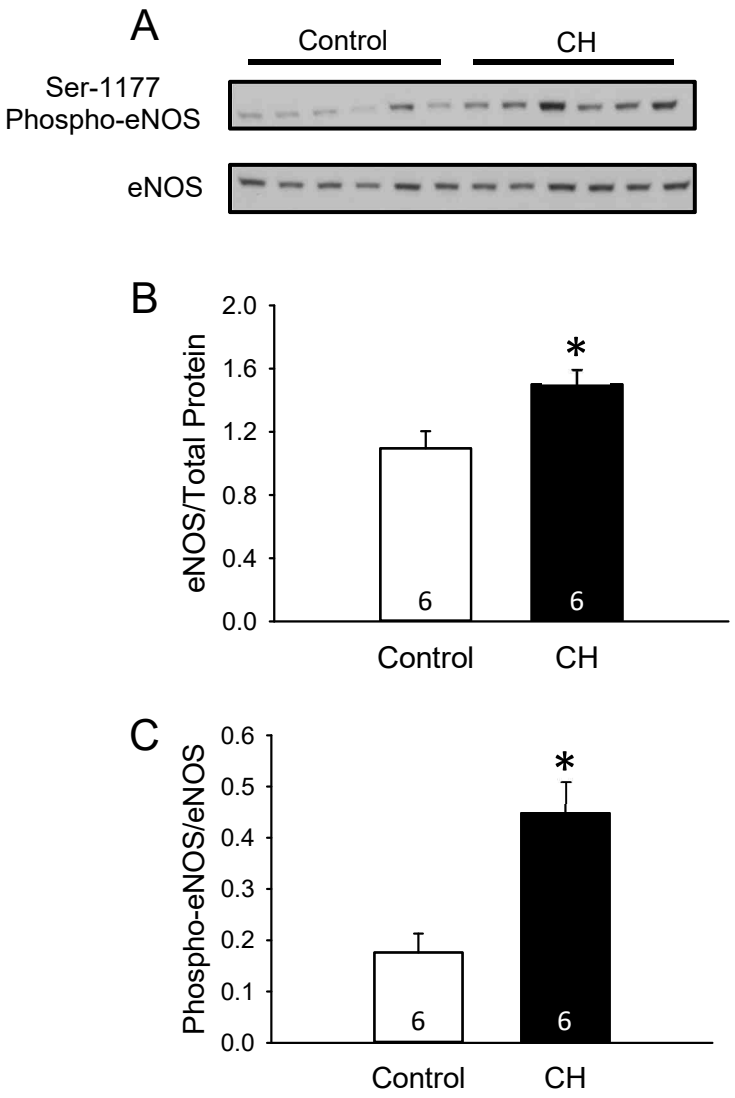

Figure 7. CH increases levels of eNOS and phosphorylated eNOS (Ser-1177) in neonatal rat lungs.
(A) Western blots for eNOS and phospho-eNOS, and (B, C) summary data for total eNOS and the ratio of phosphorylated eNOS to total eNOS in lungs from control and CH neonatal rats. Values are means ± SEM; n = 6/group (indicated in bars); *p<0.05 vs. control, analyzed by unpaired t-test.

Figure 8

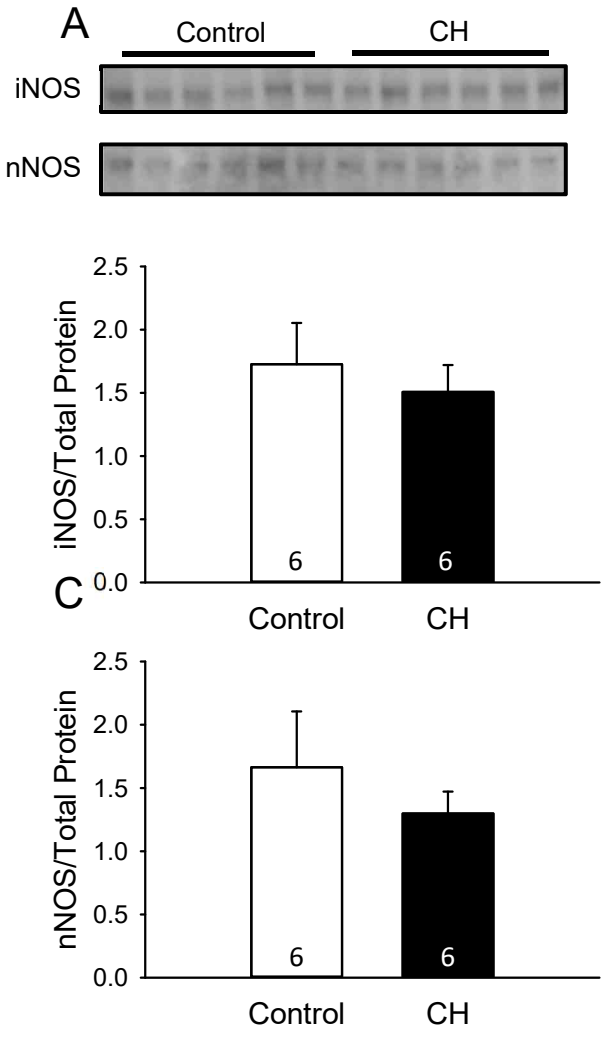

Figure 8. CH does not alter iNOS or nNOS protein expression in neonatal lungs. (A) Western blots and (B, C) summary data for total iNOS and nNOS in lungs from neonatal control and CH rats. n = 6/group (indicated in bars), analyzed by unpaired t-test.

Specific Aim 2

Establish the contribution of ROS to enhanced vasoconstriction in CH-induced neonatal pHTN.

Hypothesis:

We hypothesized that mitoROS contribute to enhanced basal and agonist-induced pulmonary arterial constriction in neonates with CH-induced pHTN.

ROS Facilitate Augmented Basal Pulmonary Arterial Tone Following CH

To eliminate the contribution of endogenous NO on observed pulmonary vascular tone, this study and all subsequent isolated (*in situ*) lung studies were done in the continued presence of L-NNA. CH-dependent increases in baseline PVR were fully relieved by TEMPOL (**Figure 9**A). Furthermore, TEMPOL normalized arterial resistance in lungs from both control and CH groups while neither CH nor TEMPOL altered venous resistance (**Figure 9**B, C). This result suggested that the CH-induced elevation in baseline PVR was due entirely to the effect of CH to increase arterial resistance.

To evaluate the contribution of basal tone to CH-dependent elevations in PVR, we assessed vasodilatory responses to the NO donor, spermine NONOate. Exposure of neonatal rats to CH lead to an elevation in basal tone, due to greater pulmonary arterial tone (**Figure 10**A, B). Pre-treatment with the SOD mimetic, TEMPOL prevented CH-dependent increases in basal tone and pulmonary vascular tone was normalized between control and CH neonates (**Figure 10**A). This finding suggested that augmented PVR observed following neonatal CH exposure was completely due to mechanisms of increased vasoconstriction.

Figure 9

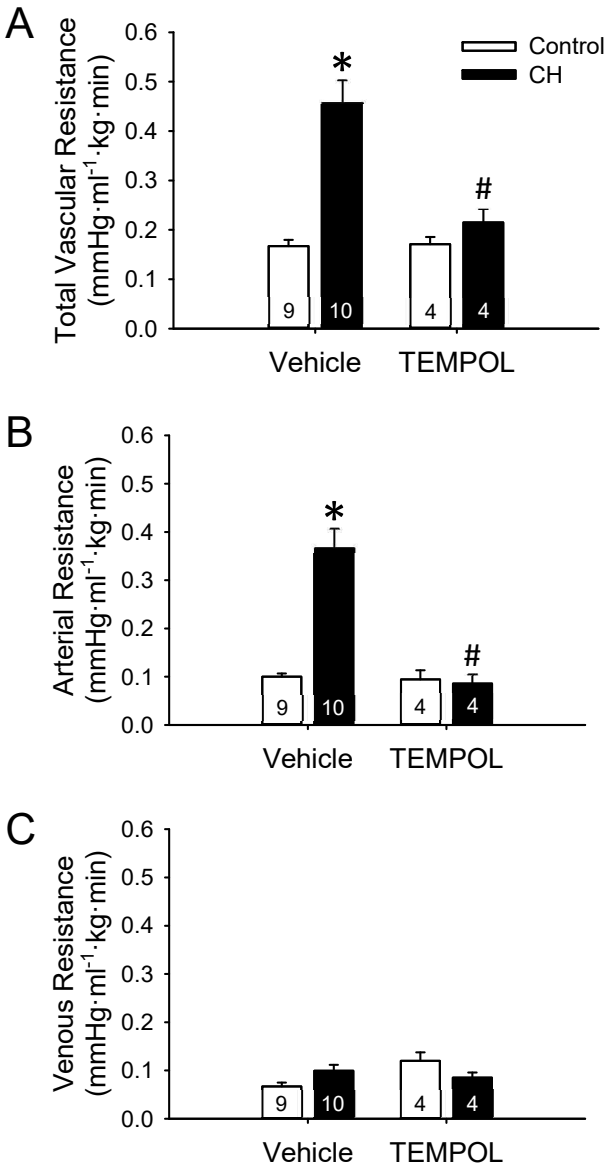

Figure 9. CH increases baseline pulmonary vascular resistance through ROS signaling.
(A) total, (B) arterial, and (C) venous baseline vascular resistances in lungs (*in situ*) from control and CH neonatal rats in the presence or absence of the SOD mimetic TEMPOL (1 mM). Experiments were conducted in the presence of L-NNA (300 μM). Values are means ± SEM; n = 4-10/group (indicated in bars); *p<0.05 vs. control, #p<0.05 vs. vehicle, analyzed by two-way ANOVA followed by Student-Newman-Keuls post-hoc comparison.

Figure 10

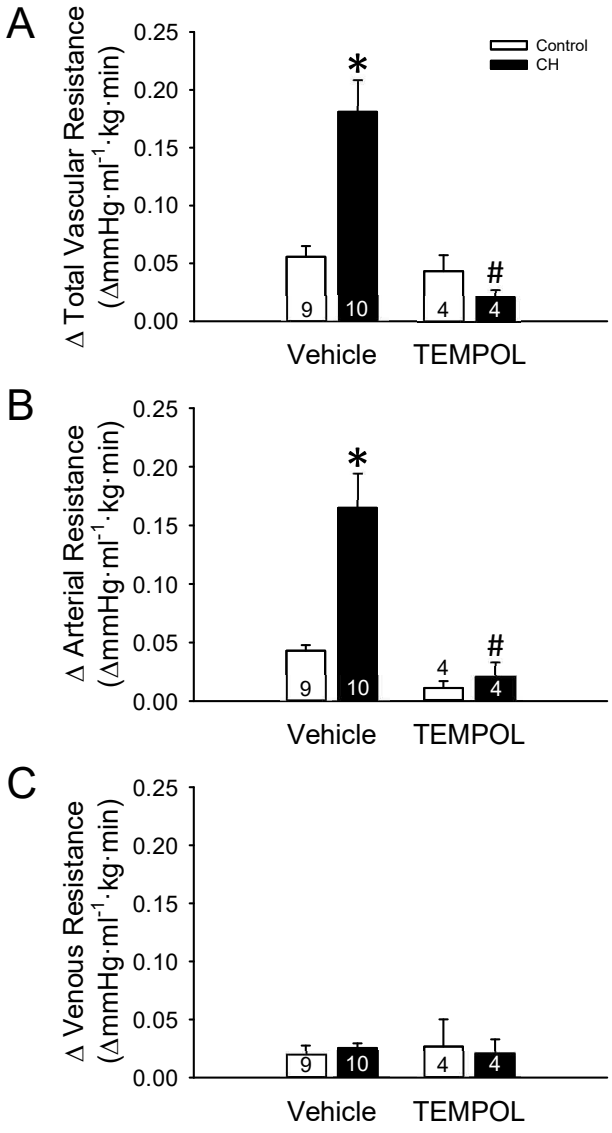

Figure 10. ROS contribute to augmented basal tone in lungs from neonatal rats exposed to CH.
The contribution of basal tone to (A) total, (B) arterial and (C) venous resistance is expressed as the change in resistance to spermine NONOate (100 μM) in lungs (in situ) from control and CH neonates. Experiments were conducted in the presence of L-NNA (300 μM) with or without the ROS scavenger, TEMPOL (1 mM). Values are means ± SEM; n = 4-10/group (indicated in or above bars); *p<0.05 vs. control, #p<0.05 vs. vehicle, analyzed by two way ANOVA with a Student-Newman-Keuls post-hoc test.

ROS Mediate Enhanced Vasoconstrictor Sensitivity to U-46619 Following CH Exposure

U-46619 produced concentration-dependent increases in total PVR in lungs from both control and CH neonates (**Figure 11**A). This effect of U-46619 was largely a result of arterial constriction (Figure 11B), as venous responses were relatively small in lungs from both groups of rats (Figure 11C).

Vasoconstrictor reactivity to U-46619 was significantly augmented by CH (Figure 11A) Neonatal pHTN induced by exposure to CH elevates vasoreactivity to U46619 (Figure 11A). This response to CH was primarily a function of increased arterial reactivity to U-46619 (Figure 11B), although venoconstriction to U-46619 was also augmented by CH exposure (Figure 11C). TEMPOL attenuated total, arterial and venous responses to U-46619 in lungs from CH rats (Figure 11A, B, C). Although TEMPOL also tended to reduce vascular reactivity to U46619 in control lungs, this effect did not achieve statistical significance (Figure 11). These findings suggest that O_2^- contributes to elevated pulmonary vasoconstrictor sensitivity to U46619 following neonatal CH.

MitoROS Contribute to Enhanced Pulmonary Arterial Tone Following CH

Exposure to CH lead to greater pulmonary arterial tone in isolated, pressurized pulmonary arteries collected from control and CH neonates (Figure 12, 13, and 14). Pretreatment with either the mitochondrial selective O_2^- scavenger MitoTEMPO or the inhibitor of mitoROS production, MitoQ, eliminated the CH-dependent increase in arterial tone. There was no significant effect of either MitoTEMPO of MitoQ to alter tone in vessels from control neonates (Figures 13 and 14). Ca^{2+}-free inner and outer diameters for pulmonary arteries included in this study are listed in Tables 5 and 6. Taken together, these results support a major contribution of mitoROS to mediate enhanced pulmonary arterial tone in neonatal rats exposed to CH.

Figure 11

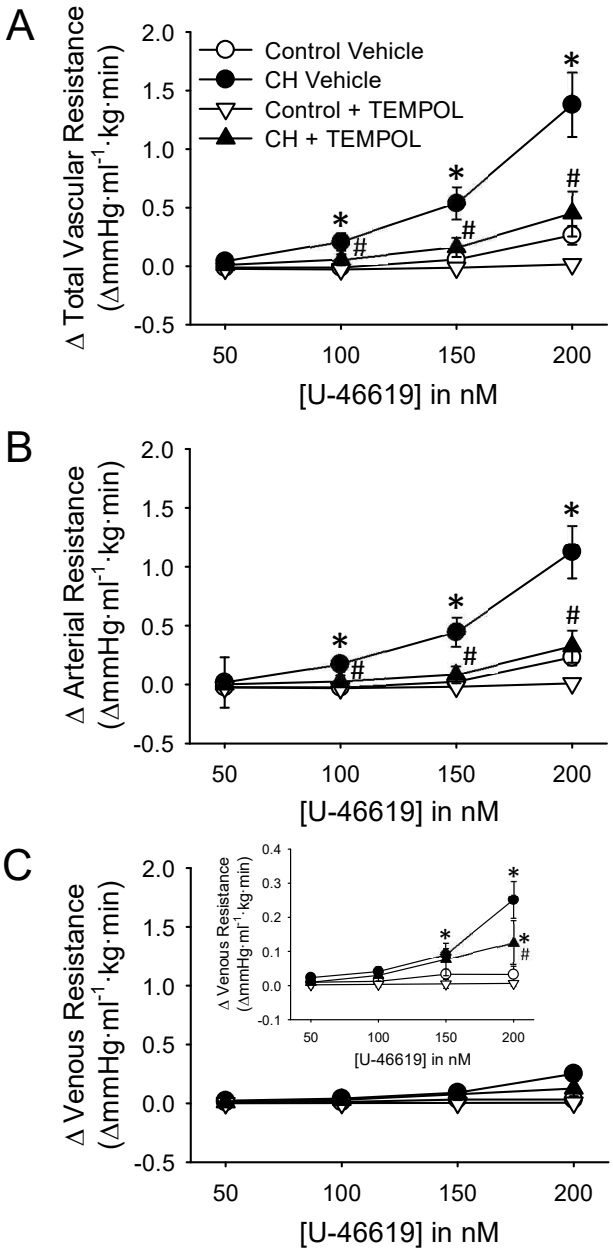

Figure 11. ROS facilitate enhanced vasoconstrictor sensitivity in lungs from CH neonates.
Changes in (A) total, (B) arterial, and (C) venous resistance to U-46619 in lungs from control and CH neonates. Experiments were conducted in the continued presence of L-NNA (300 μM) with or without the ROS scavenger, TEMPOL (1 mM). Values are means ± SEM; n = 6 for Control Vehicle, n = 5 for CH Vehicle, n = 6 for Control TEMPOL, n = 4 for CH TEMPOL; *p<0.05 vs. control, #p<0.05 vs. vehicle; analyzed by two way ANOVA at each [U-46619] with a Student-Newman-Keuls post-hoc comparison.

Figure 12

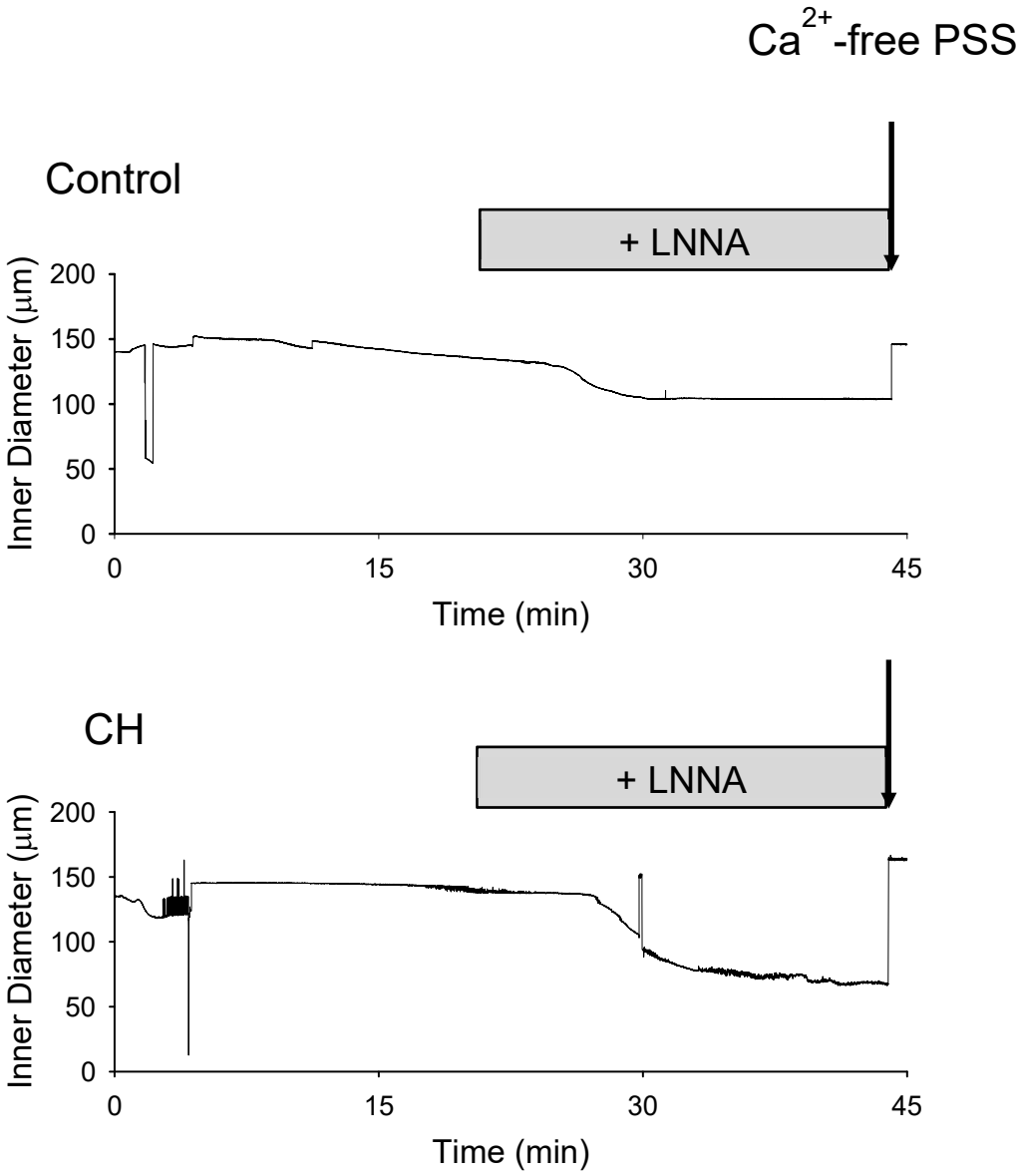

Figure 12. CH increases basal tone development in isolated, small pulmonary arteries from neonatal rats.
Representative pressure traces from control and CH groups showing arterial tone development in the presence of LNNA (300 µM) following 20 min equilibration period. Arrow indicates pausing of data acquisition to allow for 30 min Ca^{2+}-free PSS washout followed by 30 min in Ca^{2+}-free PSS + ionomycin (3 µM).

Figure 13

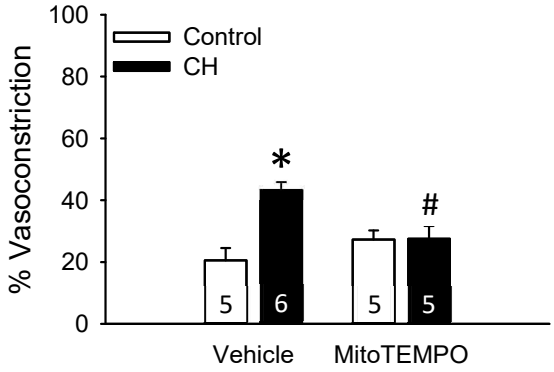

Figure 13. MitoROS contribute to increased basal tone isolated pulmonary arteries from CH neonates.
Vasoconstriction is % maximally dilated (Ca^{2+}-free) diameter, calculated using the formula: [(Ca^{2+}-free i.d. – Constricted i.d.)/Ca^{2+}-free i.d.]. Experiments were conducted in the continued presence of MitoTEMPO, (200 μM). The vessel was superfused with L-NNA (300 μM) following 20 min equilibration time. Values are means ± SEM; n = 5-6/group (indicated in bars); *p<0.05 vs. control, #p<0.05 vs. vehicle, analyzed by two way ANOVA followed by Student-Newman-Keuls post-hoc test.

Figure 14

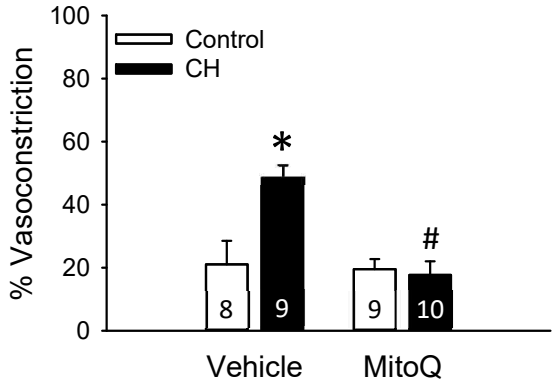

Figure 14. MitoROS contribute to increased basal tone in isolated pulmonary arteries from CH neonates.
Vasoconstriction is % maximally dilated (Ca^{2+}-free) Diameter, calculated using the formula: [(Ca^{2+}-free i.d. – Constricted i.d.)/Ca^{2+}-free i.d.]. Experiments were conducted in the continued presence of MitoQ, (1 μM, restores electron flux through the electron transport chain to lower oxidative stress). The vessel was superfused with L-NNA (300 μM) following 20 min equilibration time. Values are means ± SEM; n = 8-10/group (indicated in bars); *p<0.05 vs. control, #p<0.05 vs. vehicle, analyzed by two way ANOVA followed by Student-Newman-Keuls post-hoc test.

Table 5

	Ca^{2+}-Free Inner Diameter (μm)	Ca^{2+} Free Outer Diameter (μm)
Control Vehicle	191 ± 17 (5)	229 ± 15 (5)
CH Vehicle	180 ± 14 (6)	226 ± 15 (6)
Control MitoTEMPO	209 ± 12 (5)	262 ± 14 (5)
CH MitoTEMPO	181 ± 13 (5)	219 ± 8 (5)

Table 5. Ca^{2+}-free diameters for isolated pulmonary arteries from both control and CH neonates ± MitoTEMPO.
Values are mean ± SEM with n in parenthesis; n = 5-6/group; analyzed by two way ANOVA followed by Student-Newman-Keuls post-hoc test, no significant differences between groups.

Table 6

	Ca^{2+}-Free Inner Diameter (μm)	Ca^{2+} Free Outer Diameter (μm)
Control Vehicle	183 ± 10 (8)	222 ± 9 (8)
CH Vehicle	167 ± 6 (9)	191 ± 4* (9)
Control MitoQ	180 ± 12 (9)	217 ± 12 (9)
CH MitoQ	162 ± 6 (10)	199 ± 9 (10)

Table 6. Ca^{2+}-free diameters for isolated pulmonary arteries from both control and CH neonates ± MitoQ.
Values are mean ± SEM with n in parenthesis; n = 8-10/group; *p<0.05 vs. control; analyzed by two way ANOVA followed by Student-Newman-Keuls post-hoc test.

Specific Aim 3

Define the contribution of PKC_{β}-signaling to enhanced vascular reactivity following CH exposure in neonates.

Hypothesis:

PKC_{β}-dependent mitoROS generation in pulmonary vascular smooth muscle contributes to enhanced pulmonary arterial tone following neonatal CH.

PKC_{β} Contributes to Enhanced Pulmonary Arterial Vasoconstriction in Lungs from Neonates Exposed to CH

Pretreatment with PKC inhibitor Ro 31-8220 did not significantly reduce baseline PVR in lungs from CH neonates (Figure 15A), however PKC_{β} inhibition did significantly lower augmented baseline PVR (Figure 17A). CH-dependent increases in arterial resistance were significantly limited by either PKC or PKC_{β} inhibition (Figure 15B and 17B), suggesting that PKC and PKC_{β} signaling contribute to increased pulmonary arterial resistance following CH exposure. Neither CH nor PKC inhibitors altered venous resistance (Figure 15C and 17C) demonstrating that changes in arterial resistance following CH exposure are responsible for elevated baseline PVR in neonates exposed to CH.

The general PKC inhibitor, Ro 31-8220, attenuated CH-dependent increases in basal pulmonary arterial tone (Figure 16) as well as U-46619-induced vasoconstriction (Figure 19). Ro 31-8220 limited CH-dependent increases in both basal and U-46619-dependent changes in arterial tone (Figures 16 and 19). Pretreatment with LY-333,531 significantly reduced pulmonary arterial tone and agonist-induced vasoconstriction to U-46619 in lungs from CH neonates (Figure 18 and 20). Neither PKC nor PKC_{β} inhibition altered basal tone or pulmonary vasoreactivity to U-46619 in lungs from control neonates (Figure 16, 18, 19, and 20). Collectively, these findings suggest that PKC_{β}

Figure 15

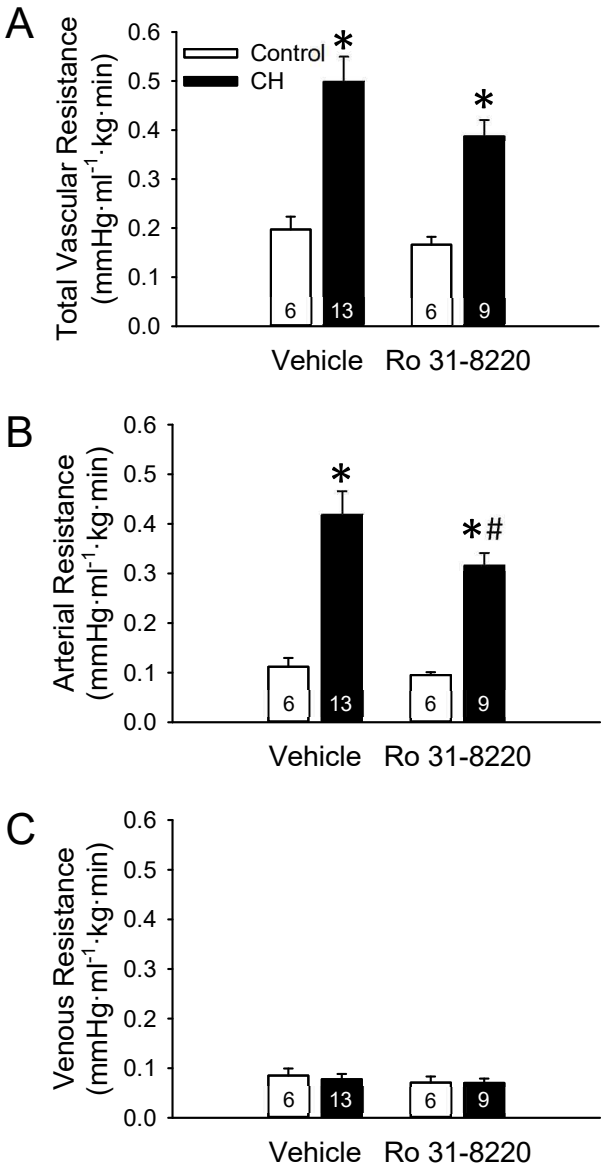

Figure 15. CH increases baseline pulmonary arterial resistance through PKC signaling.
(A) total, (B) arterial, and (C) venous baseline vascular resistances in lungs (*in situ*) from control and CH neonatal rats in the presence or absence of the PKC inhibitor Ro 31-8220 (10 μM). Experiments were conducted in the presence of L-NNA (300 μM). Values are means ± SEM; n = 6-13/group (indicated in bars); *p<0.05 vs. control, #p<0.05 vs. vehicle, analyzed by two-way ANOVA followed by Student-Newman-Keuls post-hoc comparison.

Figure 16

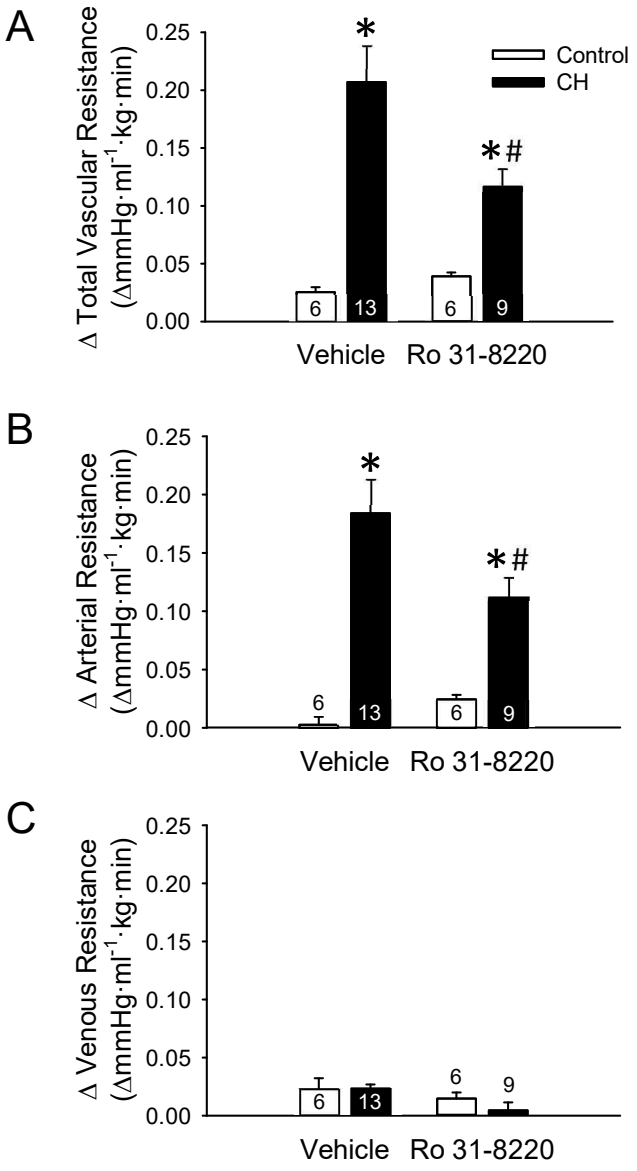

Figure 16. PKC contributes to augmented basal tone in lungs from neonatal rats exposed to CH.
The contribution of basal tone to (A) total, (B) arterial and (C) venous resistance is expressed as the change in resistance to spermine NONOate (100 μM) in lungs (in situ) from control and CH neonates. Experiments were conducted continued presence of L-NNA (300 μM) with or without the PKC inhibitor, Ro 31-8220 (10 μM). Values are means ± SEM; n = 6-13/group (indicated in or above bars); *p<0.05 vs. control, #p<0.05 vs. vehicle, analyzed by two way ANOVA with a Student-Newman-Keuls post-hoc test.

Figure 17

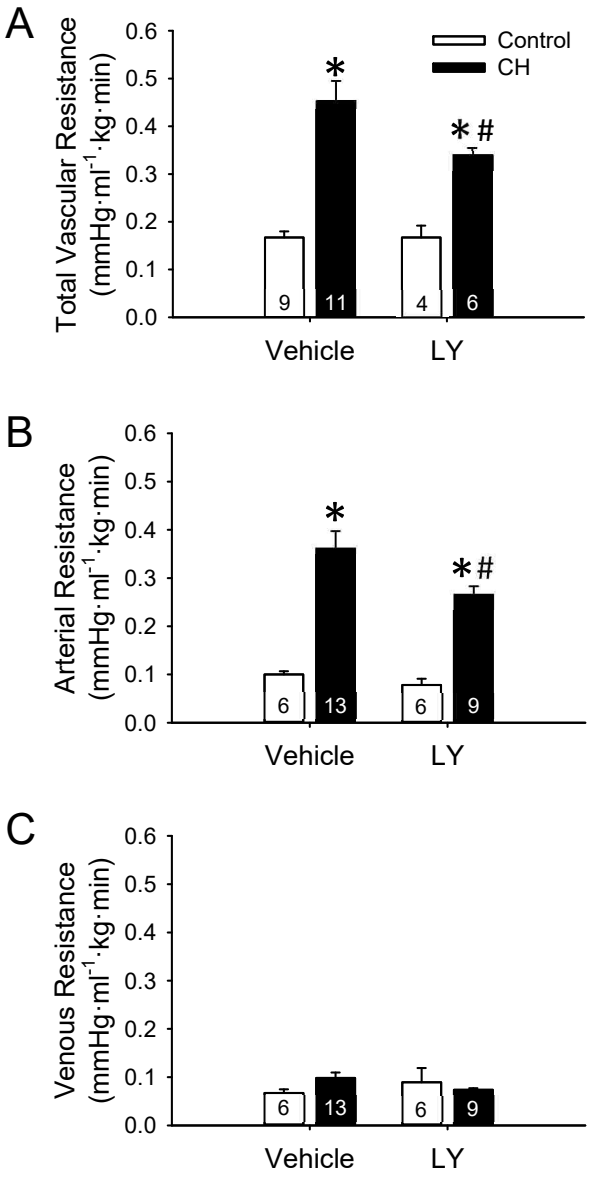

Figure 17. CH increases baseline pulmonary vascular resistance through PKC_{β} signaling.
(A) total, (B) arterial, and (C) venous baseline vascular resistances in lungs (*in situ*) from control and CH neonatal rats in the presence or absence of the PKC_{β} inhibitor LY-333,531 (10 nM). Experiments were conducted in the presence of L-NNA (300 μM). Values are means ± SEM; n = 6-13/group (indicated in bars); *p<0.05 vs. control, #p<0.05 vs. vehicle, analyzed by two-way ANOVA followed by Student-Newman-Keuls post-hoc comparison.

Figure 18

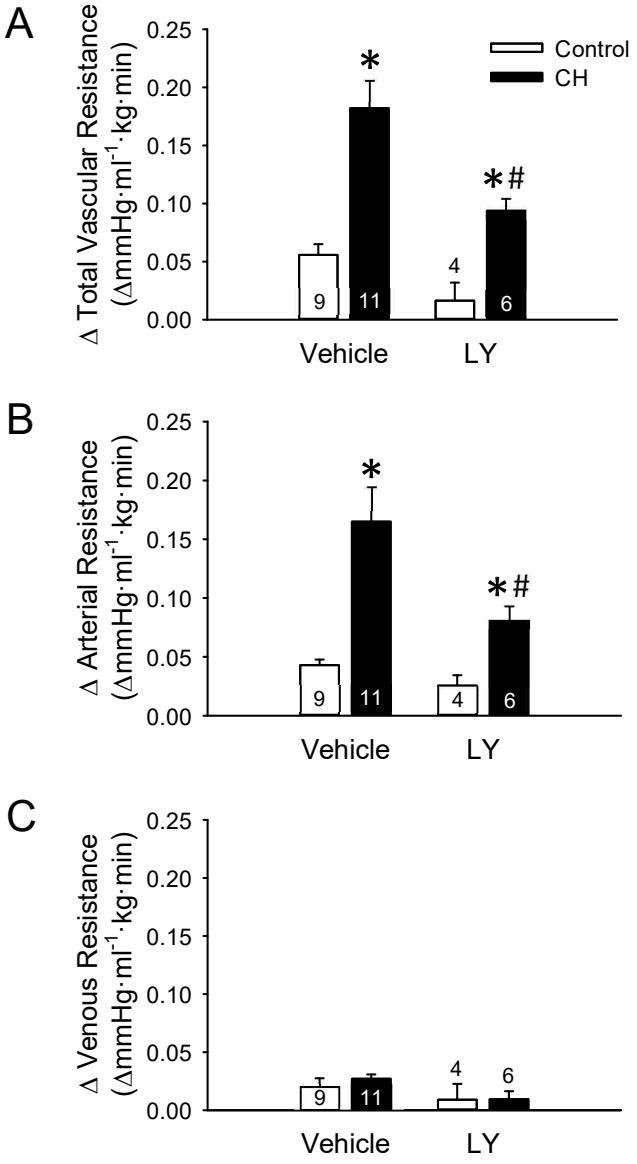

Figure 18. PKC_{β} inhibition limits CH-dependent increases in basal tone in lungs from neonatal rats.
The contribution of basal tone to (A) total, (B) arterial and (C) venous resistance is expressed as the change in resistance to spermine NONOate (100 μM) in lungs (in situ) from control and CH neonates. Experiments were conducted continued presence of L-NNA (300 μM) with or without the PKC_{β} inhibitor, LY-333,531 (10 nM). Values are means ± SEM; n = 4-11/group (indicated in or above bars); *p<0.05 vs. control, #p<0.05 vs. vehicle, analyzed by two way ANOVA with a Student-Newman-Keuls post-hoc test.

Figure 19

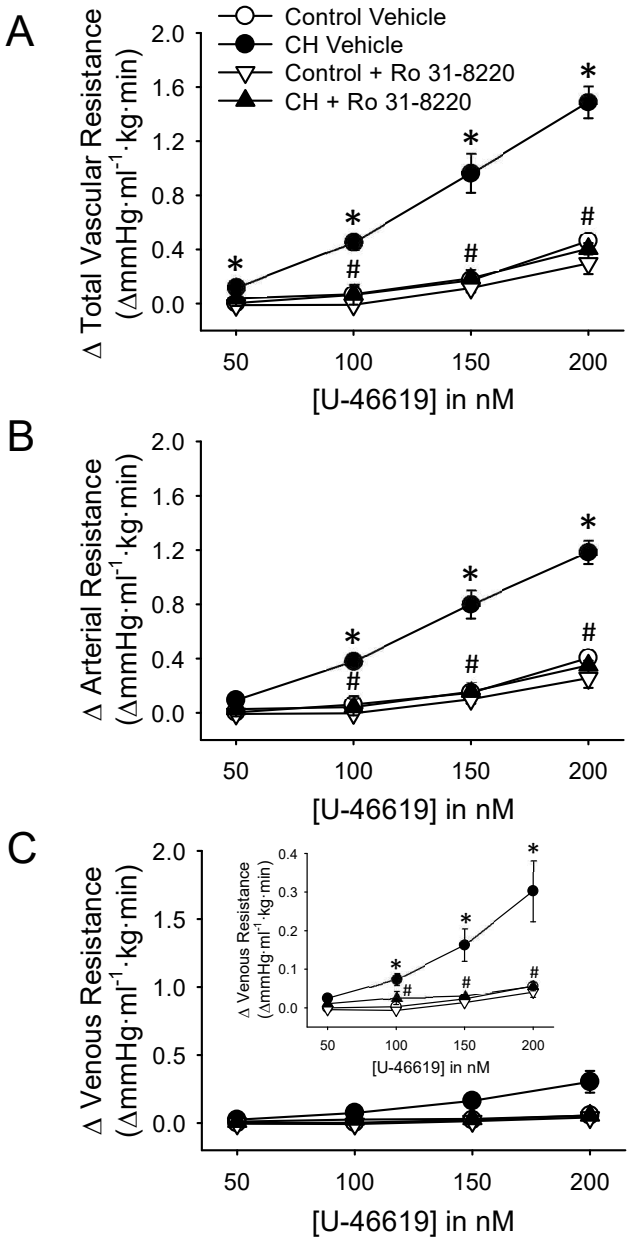

Figure 19. PKC facilitates enhanced vasoconstrictor sensitivity in lungs from CH neonates.
Changes in (A) total, (B) arterial, and (C) venous resistance to U-46619 in lungs from control and CH neonates. Experiments were conducted in the continued presence of L-NNA (300 μM) with or without the PKC inhibitor, Ro 31-8220 (10 μM). Values are means ± SEM; n = 5 for Control Vehicle, n = 6 for CH Vehicle, n = 5 for Control Ro 31-8220, n = 4 for CH Ro 31-8220; *p<0.05 vs. control, #p<0.05 vs. vehicle, analyzed by two way ANOVA at each [U-46619] with a Student-Newman-Keuls post-hoc test.

Figure 20

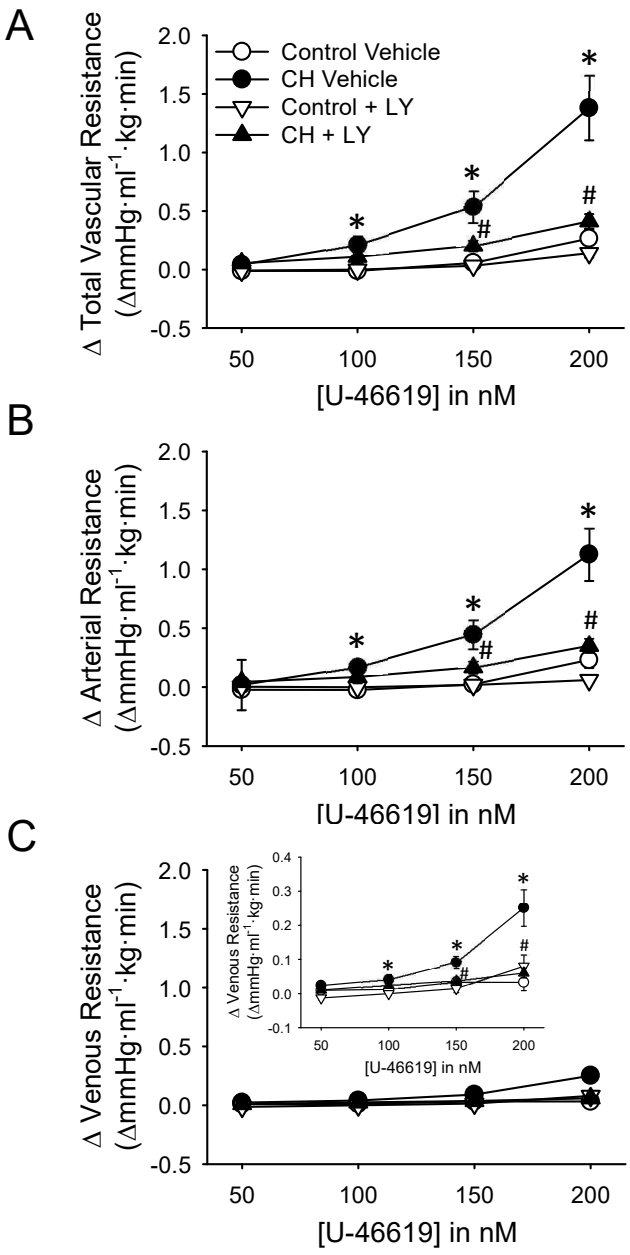

Figure 20. PKC_{β} facilitates enhanced vasoconstrictor sensitivity in lungs from CH neonates.
Changes in (A) total, (B) arterial, and (C) venous resistance to U-46619 in lungs from control and CH neonates. Experiments were conducted in the continued presence of L-NNA (300 μM) with or without the PKC_{β} inhibitor, LY-333,531 (10 nM). Values are means ± SEM; n = 6 for Control Vehicle, n = 5 for CH Vehicle, n = 5 for Control LY-333,531, n = 5 for CH LY-333,531; *p<0.05 vs. control, #p<0.05 vs. vehicle, analyzed by two way ANOVA at each [U-46619] with a Student-Newman-Keuls post-hoc test.

contributes to enhanced pulmonary arterial tone and pulmonary arterial vasoconstrictor sensitivity to U-46619 in neonates with CH-induced pHTN.

PKC$_\beta$ Mediates CH-induced Basal Tone in Isolated Pulmonary Arteries

Consistent with effects of LY-333,531 to reduce CH-dependent increases in basal tone in the *in situ* lung preparation, PKC$_\beta$ inhibition reduced basal tone development in isolated, pressurized pulmonary arteries from CH rats (Figure 21). We also observed no effect of PKC$_\beta$ inhibition on basal tone in arteries from normoxic control neonates (Figure 21). Inner and outer Ca^{2+}-free diameters of vessels included in this study are listed in Table 7.

PMA Stimulates mitoROS Production in a PKC$_\beta$-Dependent Manner in Isolated PASMCs from Control Neonates

In transiently cultured PASMCs collected from pulmonary arteries of control neonatal rats, we evaluated PKC$_\beta$-dependent mitoROS production using the PKC activator, PMA to simulate an increase in mitochondrial O_2^- production assessed by fluorescence of the mitochondrial selective O_2^- indicator, MitoSOX. Upon stimulation with PMA, we observed that MitoSOX fluorescence increased in a manner sensitive to either PKC$_\beta$ inhibition with LY-333,531 or O_2^- scavenging via either TEMPOL or tiron (Figure 22). MitoTEMPO similarly prevented PMA-mediated increases in mitoROS generation (Figure 22). These inhibitors were without effect on MitoSOX fluorescence in the absence of PMA treatment (Figure 22).

PKC$_\beta$ Protein Expression in lungs from neonatal control and CH rats

Western blot analysis revealed protein expression of both PKC βI or PKC βII isoforms in lungs from each group of rats (Figure 23). Although levels of each isoform

Figure 21

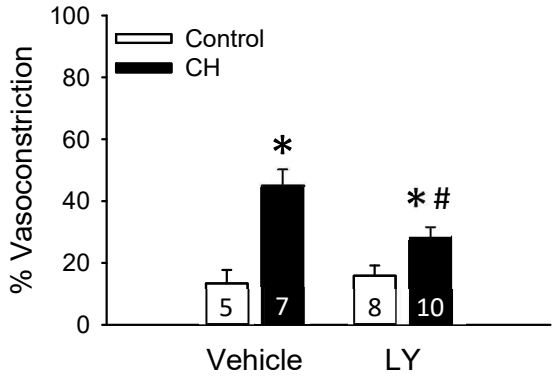

Figure 21. PKC_{β} contributes to increased basal tone in isolated pulmonary arteries from CH neonates.
Vasoconstriction is % maximally dilated (Ca^{2+}-free) diameter, calculated using the formula: [(Ca^{2+}-free i.d. – Constricted i.d.)/Ca^{2+}-free i.d.]. Experiments were conducted in the continued presence of PKC_{β} inhibitor, LY-333,531 (10 nM). The vessel was superfused with L-NNA (300 μM) following 20 min equilibration time. Values are means ± SEM; n = 5-10/ group (indicated in bars); *p<0.05 vs. control, #p<0.05 vs. vehicle, analyzed by two way ANOVA followed by Student-Newman-Keuls post-hoc test.

Table 7

	Ca^{2+}-Free Inner Diameter (μm)	Ca^{2+} Free Outer Diameter (μm)
Control Vehicle	191 ± 14 (5)	233 ± 12 (5)
CH Vehicle	183 ± 10 (7)	225 ± 12 (7)
Control LY	185 ± 8 (8)	214 ± 12 (8)
CH LY	152 ± 7*# (10)	187 ± 8*# (10)

Table 7. Ca^{2+}-free diameters for isolated pulmonary arteries from both control and CH neonates ± LY-333,531.
Values are mean ± SEM with n in parenthesis; n = 5-10/group; *p<0.05 vs. control, #p<0.05 vs. vehicle; analyzed by two way ANOVA followed by Student-Newman-Keuls post-hoc test.

Figure 22

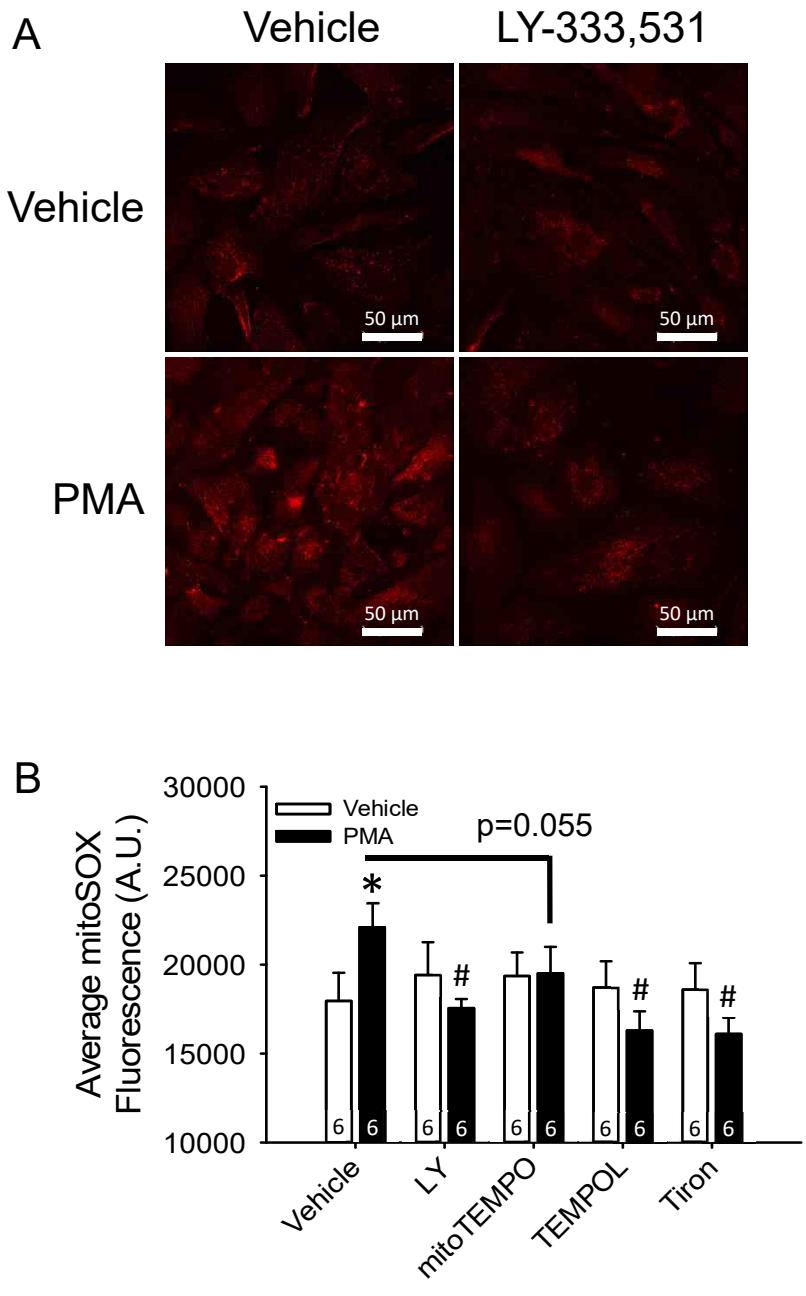

Figure 22. PKC$_\beta$ signaling leads to mitoROS production in PASMCs from control neonates.
(A) Representative photomicrographs of mitoSOX fluorescence from transiently cultured PASMCs collected from pulmonary arteries of control neonates. (B) Summary data for 6 biological replicates for each treatment condition. Values are means ± SEM; n = 6/group (indicated in bars), analyzed by two way ANOVA followed by Student-Newman-Keuls post-hoc test.

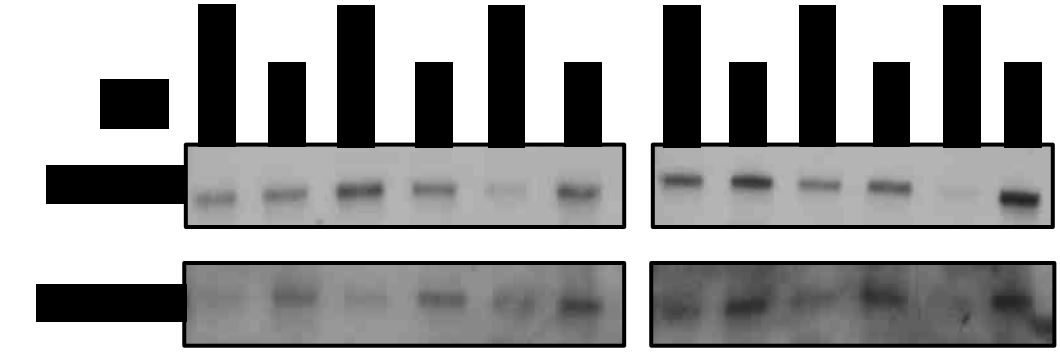

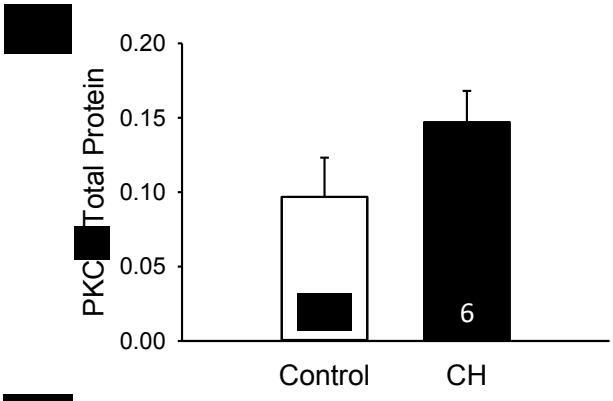

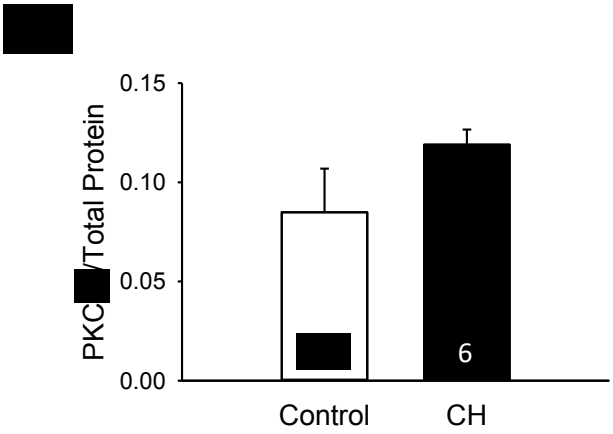

tended to be greater in lungs from CH compared to control neonates, this effect did not achieve statistical significance.

CHAPTER 4 - DISCUSSION

<u>Specific Aim 1</u>: Determine the contribution of endothelial dysfunction to enhanced basal tone and agonist-induced vasoconstriction in neonatal pHTN.

Vasoconstrictor mechanisms play an important role in the development of CH-induced neonatal pHTN (15, 40, 91, 129). However, whether vasoconstriction in this setting is a consequence of diminished endothelium-dependent vasodilatory capacity, enhanced production of a contractile factor, or an inherent increase in VSM contractility is poorly understood. Considering that endothelial dysfunction is implicated in the development of neonatal pHTN (89, 129), the present aim *examined the hypothesis that neonatal CH enhances basal tone and pulmonary vasoconstrictor sensitivity by limiting NO-dependent pulmonary vasodilation.* The major findings from this aim are that 1) neonatal CH enhances both basal pulmonary arterial tone and agonist-induced vasoconstrictor sensitivity; 2) endogenous NO limits these responses to CH, while having little to no effect in lungs from normoxic control animals; 3) CH augments receptor-mediated, EDNO-dependent pulmonary arterial dilation, but is without effect on vasoreactivity to exogenous NO; and 4) CH increases pulmonary expression of eNOS as well as eNOS phosphorylation at Ser-1177, a post-translational modification associated with enhanced NO generation (75). Collectively, these data demonstrate an effect of CH to enhance both basal pulmonary arterial tone and receptor-mediated vasoconstrictor sensitivity despite a compensatory increase in eNOS expression and activity.

Exposure to CH leads to neonatal pHTN in a variety of animals models (40, 87, 148) by elevating PVR through increased basal arterial tone and augmented reactivity to endogenous vasoconstrictor agonists (15, 40, 233). Direct evidence supporting an

important contribution of vasoconstriction to this response includes findings that ROK inhibition (180) or inhaled NO (81) acutely reverse PVR in neonatal CH rats. Furthermore, pulmonary vasoconstrictor sensitivity to serotonin is enhanced in newborn lambs housed at high altitude (3801 meters) relative to low altitude (335 meters) lambs in a manner sensitive to ROK inhibition (40). Following exposure to chronic normobaric hypoxia in neonatal piglets, endothelium-derived thromboxane products lead to pulmonary arterial vasoconstriction that is absent in normoxic controls (91). In a neonatal lamb model of pHTN that involves banding of the ductus arteriosus acute increases in pulmonary blood flow lead to vasoconstriction in a manner consistent with a myogenic response (250). Although enhanced pulmonary vasoconstriction in the setting of neonatal pHTN may be due to enhanced production of and sensitivity to endogenous vasoconstrictor agonists, there is also evidence for diminished production of endothelium-derived relaxing factors as well (87, 238). However, the relative contributions of diminished endothelium-dependent vasodilation and increased VSM contractile responsiveness to the vasoconstrictor component of neonatal pHTN is not well defined.

One potential mechanism by which neonatal pHTN may occur is through limitation of the normal NO-dependent fall in PVR. During gestation, the fetal pulmonary circulation is marked by high resistance to pulmonary blood flow that is maintained by hypoxic pulmonary vasoconstriction (246). At birth, the increase in O_2 tension stimulates pulmonary arterial eNOS-dependent vasodilation that relieves fetal pulmonary arterial tone (4, 102). However, even after delivery, the pulmonary circulation retains residual arterial tone that can be uncovered by eNOS inhibition. For example, in studies using isolated, perfused lungs from neonatal rats, acute administration of L-NNA increased baseline PVR by three fold, with the majority of the response in the pulmonary arterial circulation (53). Furthermore, occlusion of the ductus arteriosus in neonatal lambs

following NOS inhibition leads to an increase in PVR in a manner consistent with a myogenic response (251). NO-dependent pulmonary vasodilation is an important mediator of the transition from high resistance fetal to low resistance antenatal pulmonary circulation. Therefore, enhanced vasoconstriction may occur in neonatal pHTN though reduction in NO-dependent vasodilatory capacity.

As mentioned above, neonatal pHTN is often associated with reduced NO-dependent vasodilatory responsiveness, which has been attributed to both endothelial dysfunction and impaired VSM sensitivity to NO. In neonatal lambs with pHTN, pulmonary eNOS levels are reduced (238) and expression of PDE5 in the pulmonary circulation is elevated (37). Increased protein expression of PDE5 can limit the vasodilatory effect of NO in the setting of neonatal pHTN due to disruption of the signaling cascade of NO (37). In animal models of CH-induced neonatal pHTN, NO and eNOS levels are also diminished (52, 87, 129). Given evidence for endothelial dysfunction in the setting of neonatal pHTN, the purpose of the present study was to address whether neonatal CH elevates PVR through a similar mechanism related to diminished NO-dependent pulmonary vasodilation.

Our present findings demonstrate that, in contrast to the evidence in the literature of diminished NO-dependent pulmonary vasodilation, CH exposure enhanced EDNO-dependent vasodilation in the pulmonary circulation of newborn rats. In this aim, we observed increased basal tone and vasoconstrictor sensitivity to U-46619 in lungs from neonatal CH rats that was greatly enhanced following inhibition of NOS, supporting an effect of endogenous NO to limit CH-dependent vasoconstriction. In addition, the majority of the CH-dependent increases in PVR resulted from arterial constriction as determined by double occlusion technique. These results suggest that neonatal CH preferentially impacts arterial function, perhaps by increasing arterial smooth muscle

contractility due to enhanced Ca^{2+}-dependent mechanisms (250) and/or by enhancing Ca^{2+} sensitivity via ROK-dependent signaling (180, 262).

Consistent with effects of NOS inhibition to markedly augment basal tone and agonist-induced arterial constriction following neonatal CH, we found that CH also augments endogenous NO-dependent pulmonary vasodilation to AVP while having no effect on reactivity to the NO donor, spermine NONOate. These findings suggest that CH augments EDNO-dependent pulmonary vasodilation without altering responsiveness to exogenous NO, and are consistent with previous observations in adult rats from our group and others that CH selectively increases pulmonary arterial eNOS expression and enhances NO-dependent pulmonary vasodilation (62, 224, 226, 237).

Our study further suggests a potential mechanism by which CH elevates endogenous NO production through CH-dependent increases in protein expression of eNOS as well as levels of phosphorylated eNOS at Ser-1177, while having no detectable effect on levels of nNOS or iNOS. The lack of CH-dependent changes in iNOS protein expression is interesting considering that iNOS is a hypoxia-inducible gene (200) and increased in lungs from adult rats exposed to CH (63, 225). However, in isolated, pressurized pulmonary arteries from neonatal piglets exposed to either CH or normoxia, selective iNOS inhibition with aminoguanidine had no effect on baseline arterial diameter in arteries from either group suggesting that iNOS does not play a role in regulation of baseline tone in the neonatal pulmonary circulation (87).

The mechanism by which CH increases pulmonary eNOS expression and Ser-1177 phosphorylation is not clear, but may result from increased arterial shear stress associated with CH exposure (253). Ser-1177 phosphorylation of eNOS occurs mainly due to activity of the serine/threonine kinase, Akt (75). Akt-dependent Ser-1177 phosphorylation of eNOS is increased by shear stress on endothelial cells *in vitro* (220) and shear stress increases eNOS mRNA and protein expression in fetal lambs (35).

Our findings of enhanced endothelium-dependent pulmonary vasodilation and associated increases in eNOS protein expression/Ser-1177 phosphorylation differ from previous reports of diminished NO-dependent pulmonary vasodilation in neonatal pHTN (37, 87). Some of this difference could be attributable to study design as well as species difference. Whereas the present study employed a CH model of pHTN involving chronic exposure to hypobaric hypoxia, others have studied effects chronic exposure to normobaric hypoxia (19, 148) or occlusion of the ductus arteriosus (9, 181). Other reports describe pulmonary endothelial dysfunction in response to chronic hypobaric hypoxia in alternate species, including piglets (87) or lambs (40), suggesting a possible species difference in the neonatal response to hypobaric CH.

Effects of neonatal CH to augment basal and agonist-induced vasoconstriction following NOS blockade may be explained by an increase in intrinsic VSM contractility or possibly greater sensitivity to endogenous contractile factors. In neonatal piglets exposed to CH, endothelium-derived thromboxane products contribute to pulmonary vasoconstriction (91). Additionally, in neonatal lambs with pHTN, Ca^{2+} influx through voltage-gated Ca^{2+} channels facilitates a myogenic response (250). Furthermore, enhanced Ca^{2+} entry via a store-operated mechanism contributes to vasoconstriction In adult mice with CH-induced pHTN (166, 195, 271). In addition to Ca^{2+}-dependent mechanisms of enhancing pulmonary VSM contractility, ROK-induced myofilament Ca^{2+} sensitization has been implicated in both the fetal pulmonary myogenic response (262) and in mediating enhanced vasoconstrictor reactivity in neonatal pHTN (40, 180, 287). Similar effects of ROK-dependent Ca^{2+} sensitization contribute to enhanced VSM contractility and pressure-dependent tone in lungs from adult CH rats (44, 145).

The literature also points to a potential role for ROS in enhanced pulmonary vasoconstrictor sensitivity in neonatal pHTN. Levels of ROS resulting from NADPH oxidase (73), xanthine oxidase (142), uncoupled eNOS (159), and mitochondria (9) are

elevated in models of neonatal pHTN. ROS-signaling has additionally been linked to increases in ROK-dependent Ca^{2+} sensitization (145). Although not directly tested, ROS-induced ROK-dependent Ca^{2+} sensitization may play a role in mediating enhanced VSM contractility and subsequent augmentation of pulmonary arterial vasoconstrictor sensitivity in the setting of neonatal pHTN.

In conclusion, this aim demonstrates a previously undescribed effect of neonatal CH to augment both basal pulmonary arterial tone and receptor-mediated vasoconstrictor sensitivity despite a compensatory increase in NO-mediated pulmonary vasodilation, eNOS expression and activity. These results advance our understanding of protective mechanisms that may limit the severity of neonatal pHTN, and are consistent with an effect of CH to increase basal VSM tone and contractile responsiveness rather than to impair endothelium-dependent vasodilation.

<u>Specific Aim 2:</u> Establish the role of ROS in enhanced vasoconstriction in the setting of pHTN in neonates exposed to CH.

Studies in Aim 1 argue against a role for impaired EDNO-dependent pulmonary vasodilation in mediating augmented vasoconstrictor sensitivity following CH in neonatal rats. Considering that lung levels of cellular and mitochondrial-derived ROS are elevated in neonates with pHTN (10, 43, 142) and that ROS contribute to enhanced arterial vasoconstriction in the hypertensive neonatal pulmonary circulation (43, 145, 197), the present aim *examined the hypothesis that mitoROS contribute to enhanced pulmonary arterial vasoconstriction in neonates with CH-induced pHTN.* The major findings from this aim are that 1) CH-dependent increases in basal and agonist-induced vasoconstrictor reactivity rely on ROS and 2) mitochondrial O_2^- augments pulmonary arterial tone following neonatal CH exposure. Taken together, these data demonstrate

an effect of CH to enhance both basal pulmonary arterial tone and receptor-mediated vasoconstrictor sensitivity in a mitoROS dependent manner. Additionally, the normalization of baseline total vascular and arterial resistance between lungs from control and CH neonates after TEMPOL pretreatment suggests that CH-dependent increases in PVR are due entirely to mechanisms of pulmonary arterial vasoconstriction, independent of remodeling effects.

Our data suggest that a specific ROS species, O_2^-, is responsible for mediating enhanced pulmonary vasoconstriction in neonates with pHTN. In this aim, we used both TEMPOL and MitoTEMPO to scavenge pulmonary ROS. Both TEMPOL and MitoTEMPO are SOD mimetics meaning that they convert O_2^- to H_2O_2 (74, 161). Lowering lung levels of O_2^- correlating with reductions in elevated pulmonary vasoconstrictor sensitivity in neonates with pHTN has been demonstrated in the literature (43, 73, 82, 142), however those studies focused on the restoration of NO-dependent pulmonary vasodilation. Elevated vascular levels of O_2^- can scavenge and therefore limit the bioavailability of NO (43, 82). In this aim, all experiments were done in the presence of L-NNA to inhibit endogenous NO production. We observed that pre-treatment of lungs with TEMPOL abolishes CH-dependent increases in pulmonary arterial tone. This finding is consistent with an interpretation that O_2^- potentiates pulmonary vasoconstriction at the level of the VSM, perhaps by increasing contractility. Indeed, in adult rodents with CH-induced pHTN, increased levels of pulmonary arterial O_2^- activates RhoA/ROK-dependent myofilament Ca^{2+} sensitization and promotes pulmonary arterial pressure-dependent tone and enhanced vasoconstrictor sensitivity (44, 145, 197). This signaling mechanism may contribute to enhanced VSM contractility in neonates with CH-induced pHTN. We cannot however eliminate the possibility that the observed effect of TEMPOL and MitoTEMPO (both SOD mimetics which dismute O_2^- to H_2O_2) to reduce vasoconstrictor reactivity could be due to the pulmonary vasodilatory

effect of H_2O_2 (45, 163, 174). Additionally, TEMPOL has been shown to promote vasodilation through direct activation of K^+-channels in the membranes of vascular smooth muscle cells (288, 289). However, the finding that MitoQ, a molecule that is not an SOD mimetic, but instead an inhibitor of mitochondrial O_2^- production, similarly abolishes CH-dependent enhancement of pulmonary arterial tone argues against this possibility.

There are several sources of ROS that may contribute to enhanced lung levels of ROS observed in the setting of neonatal pHTN. ROS generation by NOX, xanthine oxidase, and uncoupled eNOS contribute to ROS production in the pulmonary circulation of neonates with pHTN (92, 142, 254). The mitochondria are also a potent source of cellular O_2^- in the pulmonary vasculature (12). In the setting of neonatal pHTN, there are several potential mechanisms whereby lung mitoROS levels might be enhanced. In transiently cultured PASMCs from newborn lambs, cyclic stretch stimulates mitochondrial O_2^- production (278). This finding suggests that stretch on the VSM, as might be expected in neonates with elevated pulmonary arterial pressure, stimulates mitochondrial O_2^- production. Moreover, recent studies in lambs with pHTN, demonstrate that basal mitochondrial-derived O_2^- levels are increased in endothelial cells from pulmonary hypertensive lambs due to lower SOD2 (the SOD isoform present in mitochondria that scavenges O_2^-) protein expression and activity relative to cells from healthy controls (9). Mitochondrial-derived O_2^- limits NO bioavailability and therefore potentiates pulmonary vasoconstrictor sensitivity (9, 10). Restoration of SOD2 expression in pulmonary arterial endothelial cells from lambs with pHTN using adenoviral transfection not only limits mitochondrial O_2^- levels, but also improves NO-dependent pulmonary vasodilation and increases eNOS mRNA and protein expression to levels observed in cells from control lambs (9). These findings from the literature suggest that increased basal mitochondrial O_2^- generation in neonates with pHTN

potentiates pulmonary vasoconstriction not only by limiting NO-dependent pulmonary vasodilation through scavenging NO, but also by reducing mechanisms for NO production. Findings from Aim 1 of this dissertation however suggest that neonatal CH exposure potentiates NO-dependent pulmonary dilation in animals with pHTN. Furthermore, findings from Aim 2 indicate that mitoROS are important mediators of augmented vasoconstriction, perhaps through a direct effect to promote enhanced VSM contractility.

Findings from this aim suggest that mitochondrial-derived O_2^- contributes to enhanced pulmonary arterial tone following neonatal CH exposure. Our studies in isolated pulmonary arteries from both control and CH neonates used MitoTEMPO and MitoQ, both mitochondrial-targeted strategies for reducing levels of mitochondrial-derived O_2^-. In the presence of either compound, CH-dependent increases in pulmonary arterial tone were eliminated suggesting a pivotal role of mitochondrial O_2^- following CH exposure to augment arterial tone in the pulmonary circulation. Furthermore, the effect of both MitoTEMPO and MitoQ to remove enhanced arterial tone in the presence of L-NNA suggests that mitochondrial O_2^- enhance tone by promoting mechanisms of vasoconstriction such as increased production of an endothelium-derived contractile factor and/or by enhancing VSM contractility, not by reducing NO-dependent pulmonary arterial vasodilation. Although we identify a potential subcellular source of O_2^- production, we do not examine the cell-type responsible for mitochondrial O_2^- production. Future studies in endothelium denuded (removed), isolated pulmonary arteries are important to determine whether enhanced pulmonary arterial tone observed in CH exposed neonates is a consequence of mitochondrial O_2^- production in the endothelium or in VSM of the medial layer/fibroblasts in the adventitia.

Furthermore, findings related to mitochondrial-derived O_2^- relied on studies in isolated, endothelium-intact, pulmonary arteries which also presents some limitations.

The lung is a multicellular tissue with a variety of cell types such as endothelial cells (46) and adventitial fibroblasts (189) that may contribute to regulation of pulmonary vascular tone in the setting of pHTN. There are also factors such as NO, AVP, ET-1, and 5-HT, released from the lung and other endocrine organs that can alter the level of tone within the pulmonary circulation *in vivo*. Additionally, our studies focus on only a segment of one branch in the arterial tree, making it difficult to extend our findings to the entire pulmonary circulation. However, our finding that TEMPOL eliminates CH-dependent increases in pulmonary vascular resistance in the isolated (*in situ*) lung, were the entire pulmonary circulation is present, by limiting pulmonary arterial tone bolster a role for our findings related to mitochondrial O_2^- in the intact pulmonary circulation.

MitoROS generation in the endothelium may lead to increased production of an endothelium-derived contractile factor such as ET-1 (144). Enhanced mitochondrial O_2^- levels in endothelial cells from lambs with pHTN limit eNOS mRNA and protein expression and limit vasodilation to endogenous NO (9). NO can limit ET-1 production and secretion by pulmonary arterial endothelial cells through downregulating expression of preproET-1 mRNA (151). In the setting of neonatal pHTN, reduced pulmonary vascular NO may contribute to elevations in ET-1 levels observed in neonates with pHTN (144, 228). Findings from Aim 1 of this dissertation however, make this interpretation unlikely in our model due to the observed effect of CH to increase NO-dependent pulmonary vasodilation in neonates with pHTN. The literature also supports a role for O_2^- to lead to lipid peroxidation-dependent increases in ET-1 lung levels in neonates with pHTN (144). It is possible that in our model, mitochondrial O_2^- may increase ET-1 production through other means, such as promotion of lipid peroxidation.

In addition to the possible role of mitoROS to promote activity of ET-1, mitochondrial O_2^- is also important for 5-HT-induced pulmonary arterial vasoconstriction as well. In intrapulmonary arteries from adult rats, mitochondrial O_2^- is important for 5-

HT-induced vasoconstriction (34, 103). In isolated PASMCs from these animals, 5-HT treatment leads to mitochondrial O_2^- production that is sensitive to 5-HT receptor antagonists (103). 5-HT binds 5-HT_{2A} receptors on rat PASMCs and stimulates influx of extracellular Ca^{2+} which then leads increased mitochondrial Ca^{2+} uptake, mitochondrial depolarization, and subsequent mitochondrial O_2^- generation from complex I (103). Moreover, mitoROS (9, 83), 5-HT-induced pulmonary vasoconstriction (40, 49, 72), VSM $[Ca^{2+}]_i$ (124), and vascular tone (180, 250, 251) are known to be increased in the setting of neonatal pHTN, suggesting that 5-HT-induced mitochondrial O_2^- may be an important mediator of neonatal pHTN.

Mitochondrial O_2^- may increase VSM contractility in pulmonary arteries of neonates with CH-induced pHTN by altering Ca^{2+} signaling and/or by increasing myofilament Ca^{2+} sensitivity. In addition to their energy-generating capacity, mitochondria also participate in regulation of $[Ca^{2+}]_i$ (176). Studies of transiently cultured PASMCs from adult mice have demonstrated that mitoROS contribute to acute-hypoxia dependent increases in $[Ca^{2+}]_i$ and subsequent VSM contraction (272). It is also possible that in addition to a potential role to alter $[Ca^{2+}]_i$ signaling, mitoROS may contribute to enhanced myofilament Ca^{2+}-sensitization. As mentioned earlier, cellular ROS contribute to RhoA/ROK-dependent Ca^{2+} sensitization in adult rodents with CH-induced pHTN (145). ROK has been shown to activate actin polymerization (18). Actin polymerization is thought to promote myofilament Ca^{2+} sensitization by enhancing transmission force to the extracellular matrix (258, 293) and by increasing the assembly of contractile units between actin and myosin (38). In cultured mouse and human fibroblasts, treatment with rotenone, an electron transport chain complex 1 inhibitor, reduces mitoROS production and limits cellular attachment and membrane spreading (292), processes driven by actin polymerization (291). These findings suggest that mitoROS promote actin polymerization, a mechanism that increases myofilament Ca^{2+}

sensitization.

Several intracellular signaling pathways can promote mitoROS generation. In primary cultures of mouse microvascular endothelial cells, extracellular O_2^- generated by NOX can stimulate increased $[Ca^{2+}]_i$ which in turn results in mitochondrial O_2^- production (94). In disease models such as cardiac ischemic preconditioning and angiotensin II-induced systemic hypertension, mitoROS production in cardiac myocytes (175) and bovine aortic endothelial cells (76) is a downstream event in several signaling pathways such those impacted by Akt, MAP kinases, PKA, and PKC (76, 175). In disease states such as diabetes, ischemia-reperfusion injury, multiple sclerosis, obesity, and osteoporosis the β isoform of PKC contributes to mitoROS production and cellular oxidant stress that may facilitate disease pathogenesis (16, 182, 244, 270). The effect of mitochondrial O_2^- to mediate enhanced pulmonary arterial vasoconstriction may be a downstream consequence of kinase signaling, perhaps PKC_β considering its role to mediate cellular dysfunction in several disease states.

In conclusion, this aim demonstrates that augmented pulmonary arterial tone and pulmonary vasoconstrictor sensitivity rely on mitochondrial O_2^- signaling. Considering the link between PKC_β, mitoROS, and cellular dysfunction, studies in Aim 3 were designed to pursue the contribution of PKC_β to enhanced pulmonary vasoconstriction occurring in neonates with CH-induced pHTN.

<u>Specific Aim 3:</u> Define the contribution of PKC_β-signaling to enhanced vascular reactivity following CH exposure in neonates.

Findings from Aim 2 of this dissertation demonstrate that mitochondrial O_2^- contributes to enhanced pulmonary arterial vasoconstriction in neonates with CH-induced pHTN. The upstream signaling mechanism for mitochondrial O_2^- generation

however was still unknown. Considering previous evidence linking PKC_β signaling with mitoROS production in several disease states, the present aim *examined the hypothesis that PKC_β-dependent mitoROS generation in pulmonary vascular smooth muscle contributes to enhanced pulmonary arterial tone following neonatal CH.* The major findings from this aim are that 1) PKC_β signaling leads to increases in mitoROS production in transiently cultured PASMCs from control neonates; 2) PKC_β signaling contributes to enhanced pulmonary arterial tone and vasoconstrictor sensitivity following CH; and 3) PKC βI and PKC βII are both expressed in pulmonary arteries from both control and CH neonates, but they were not significantly altered by CH. Taken together, these data demonstrate that PKC_β signaling leads to mitoROS generation in PASMCs from neonatal rats and that PKC_β and mitoROS are important mediators of enhanced pulmonary arterial vasoconstriction occurring in the setting of neonatal pHTN.

PKC is an important regulatory kinase in the pulmonary vasculature where it contributes to VSM contractility and proliferation (28, 41). In the setting of neonatal pHTN, PKC signaling is an important mediator of enhanced basal pulmonary vascular tone (31). Additionally, studies in isolated pulmonary arteries from adult rats with intermittent hypoxia-induced pHTN demonstrate that enhanced vasoconstrictor sensitivity of ET-1 is sensitive to myrPKC (a myristoylated PKCα/β psudosubstrate inhibitor) and LY-333,531 (a selective PKC_β inhibitor), but not rottlerin (a PKCδ inhibitor) (242). These results demonstrate that enhanced pulmonary arterial vasoconstrictor reactivity occurring in the setting of pHTN rely on PKC isoform signaling, likely PKC_β.

PKC_β is a classical PKC isoform which is regulated by both changes in $[Ca^{2+}]_i$ and diacylglycerol (268). Findings from aim 3 of this dissertation demonstrate that both splice variants of PKC_β, PKC βI and PKC βII, are expressed pulmonary arteries of both control and CH neonates. As protein expression of PKC_β splice variants was unaltered by CH, mechanisms other than changes in protein content account for the PKC_β-

dependency of tone development and agonist-induced pulmonary vasoconstriction observed only in neonates exposed to CH. Subcellular localization of PKC isoforms is an important regulator of their activity (193) with increased cell membrane association correlated with enhanced activity of PKC isoforms (193, 211, 265). In adult rats with intermittent hypoxia-induced pHTN, PKC_{β} protein expression was unaltered by intermittent hypoxia exposure, but the basal cell membrane association of PKC_{β} is increased as is ET-1-dependent translocation away from the plasma membrane in pulmonary arteries from animals exposed to intermittent hypoxia compared to normoxic controls (242). This finding suggests that although neonatal CH does not increase protein expression of PKC_{β}, it may alter the subcellular localization of PKC_{β} to be more membrane associated and therefore more active.

Considering the role of Ca^{2+} in promoting activation of classical PKC isoforms such as PKC_{β}, it is also possible that following CH exposure in neonatal rats, increased PASMC $[Ca^{2+}]_i$ activates PKC_{β}-dependent pulmonary arterial vasoconstriction. In PASMCs collected from both control and CH-exposed piglets, basal Ca^{2+} is elevated in cells from piglets exposed to CH (124). Additionally, exposure of PASMCs from either control or CH piglets to 3 days of hypoxia *in vitro* increased $[Ca^{2+}]_i$ (124). Finally, stimulation of cultured PASMCs with U-46619 was associated with greater changes in $[Ca^{2+}]_i$ in cells from CH exposed piglets (124). In transiently cultured PASMCs from both healthy control lambs and those with pHTN, Ca^{2+} release from intracellular stores as well as SOCE was enhanced in cells from neonates with pHTN (223). However, this group did not report whether there was a difference in basal Ca^{2+} between PASMCs collected from control lambs and those with pHTN (223). Findings in pulmonary VSM from neonatal piglets and lambs suggest that intracellular Ca^{2+} levels may be elevated in neonates with pHTN which may then contribute to PKC_{β} activation.

In addition to $[Ca^{2+}]_i$ contributing to PKC_{β} activation in pulmonary VSM of

neonatal rats exposed to CH, PKC_β is also regulated by cellular redox state. Oxidative stress associated with certain diseases such as multiple sclerosis, obesity, and osteoporosis is thought to activate PKC_β signaling (16, 182, 252, 295). The enzymatic structure of PKC_β contains an auto-inhibitory zone with cysteine thiols vulnerable to reversible oxidation to form a sulfenylated (-SOH) side group (106). Protein sulfenylation of the auto-inhibitory zone it thought to produce an increase in the catalytic activity as well as potentiate agonist-dependent activation of PKC_β (107, 155).

An important downstream consequence of PKC_β activation and signaling is mitoROS generation (16, 252). In this aim, we observe that PKC_β signaling promotes mitoROS generation in isolated PASMCs from neonatal rats. PKC_β-induced mitoROS generation occurring in disorders such as aging, multiple sclerosis, obesity, and osteoporosis involves PKC_β-dependent translocation of the redox enzyme p66shc to the mitochondria (16, 182, 252, 295). Normally the factor p66shc resides in the cytoplasm, but under conditions of oxidative stress, such as that observed in neonatal pHTN, PKC_β-dependent phosphorylation of p66shc stimulates its translocation to the mitochondrial inner membrane. Once there, p66shc oxidizes cytochrome c and then reduces molecular oxygen into O_2^- (207, 252).

An additional potential mechanism whereby PKC_β may promote the generation of mitoROS involves the $mitoK_{ATP}$ channel. The $mitoK_{ATP}$ channel is expressed on the mitochondria and appears to be distinct from K_{ATP} channels located in the plasma membrane in terms of its regulation and composition (135). In cardiomyocytes collected from adult rabbits, $mitoK_{ATP}$ channel opening was associated with increased mitoROS generation (199). Opening of the $mitoK_{ATP}$ channel permits K^+ influx into the mitochondrial matrix and matrix alkalization as incoming K^+ ions replace H^+ pumped out by the respiratory chain (59, 85). Matrix alkalization uncouples the electron transport chain and leads to mitoROS production (59, 85). The opening of $mitoK_{ATP}$ channels is

promoted by PKC signaling. In isolated mitochondria collected from homogenates of adult rat hearts, inhibition of PKC prevented PMA-induced mitoK$_{ATP}$ channel opening. Although this group went further and demonstrated that PKC$_{\varepsilon}$ contributed to mitoK$_{ATP}$ opening in isolated cardiac mitochondria (58), they did not test a role for PKC$_{\beta}$. Findings from this aim evaluating PMA-dependent increases in mitochondrial O_2^- production assessed using mitoSOX fluorescence in transient cultures of neonatal PASMCs, demonstrate that PKC$_{\beta}$ signals to induce mitoROS generation. There may be a difference in which PKC isoform modifies mitoK$_{ATP}$ channel kinetics depending on a given cell type with VSM and cardiac muscle regulated in different ways.

We observe in this aim that PKC$_{\beta}$ is upstream of mitochondrial O_2^- production and findings from Aim 2 of this dissertation indicate that mitochondrial O_2^- are important mediators of elevated pulmonary arterial tone following neonatal CH exposure. Therefore, it is possible that PKC$_{\beta}$-dependent mitochondrial O_2^- contributes to enhanced pulmonary arterial tone in neonates with CH-induced pHTN. Of interest, whereas inhibition of mitochondrial O_2^- signaling fully alleviated elevated tone in pulmonary arteries from CH neonates, PKC$_{\beta}$ inhibition was only partially effective. This finding is also true in results from the isolated (*in situ*) lung preparation where TEMPOL eliminated CH-dependent enhancement of both basal tone and agonist-induced vasoconstrictor sensitivity, whereas PKC$_{\beta}$ inhibition only partially relieved those responses. These findings together suggest that perhaps PKC$_{\beta}$ is not fully inhibited by the concentration of LY-333,531 used in these studies or that there are other mechanisms for mitochondrial O_2^- production. Additionally, it is possible that there may be sources of ROS in the whole lung that are not mitochondrial. In the discussion section for Aim 2, it was suggested that mechanisms such as increased $[Ca^{2+}]_i$ (103) and/or elevated cytoplasmic or extracellular levels of O_2^- (94) may stimulate mitoROS generation, independent of PKC$_{\beta}$ signaling.

PKC_{β} may also facilitate enhanced pulmonary vasoconstriction independent of downstream mitoROS signaling. Classical PKC signaling leads to the inhibition of myosin light-chain phosphatase via phosphorylation by the peptide CPI-17. CPI-17-dependent phosphorylation of the myosin light chain leads to greater Ca^{2+}-sensitization and subsequent increases in vasoconstrictor sensitivity (154). Considering that PKC_{β} contributes to enhanced pulmonary arterial tone and pulmonary vasoconstrictor sensitivity in neonatal rats with CH-induced pHTN, CPI-17-dependent increases in myofilament Ca^{2+}-sensitivity may be involved in this response.

However, in adult rats with pHTN induced by exposure to intermittent hypoxia, PKC_{β} contributed to enhanced ET-1 vasoconstrictor sensitivity and Ca^{2+}-sensitization without altering levels of phosphorylated myosin light-chain (242). Additionally, activation of PKC in uterine arteries of pregnant sheep increased arterial tone without altering levels of phosphorylated myosin light-chain (286). These findings suggest PKC signaling, even involving PKC_{β}, may use pathways independent of CPI-17 to promote Ca^{2+} sensitization and enhanced pulmonary vasoconstriction. As mentioned above, actin polymerization may also contribute to enhanced vasoconstrictor reactivity independent of changes in $[Ca^{2+}]_i$. CH exposure of pregnant sheep increased PKC-dependent uterine artery constriction in a manner dependent on actin polymerization (285). This finding suggested that PKC-induced actin polymerization is important for uterine artery constriction following CH exposure during pregnancy. We observe that antenatal CH exposure of neonatal rats increases pulmonary arterial tone and vasoconstrictor sensitivity in a PKC_{β}-dependent manner, perhaps dependent on actin polymerization.

Actin polymerization can also be promoted by mitochondrial-derived O_2^- (291, 292). Findings from Aims 2 and 3, demonstrate that PKC_{β} signaling in transiently cultured PASMCs from neonatal rats increases mitochondrial O_2^- generation and that

PKC_β and mitoROS contribute to enhanced pulmonary arterial tone following CH exposure. It is possible that PKC_β-dependent mitoROS generation in PASMCs of neonatal rats contributes to mitoROS-dependent actin polymerization and subsequent promotion of myofilament Ca^{2+} sensitivity.

In conclusion, this aim demonstrates that augmented pulmonary arterial tone and pulmonary vasoconstrictor sensitivity rely on PKC_β and that PKC_β signaling in neonatal PASMCs is upstream of mitochondrial O_2^- generation in PASMCs from control neonates. We know from aim 2 that mitoROS are important mediators of enhanced pulmonary arterial tone following neonatal CH exposure. Future investigation into the link between PKC_β and mitoROS occurring in pulmonary VSM of neonates with CH-induced pHTN is important to understand how this pathway is activated and contributes to enhanced pulmonary arterial vasoconstriction.

Conclusions

The aim of this dissertation was to examine mechanisms of enhanced pulmonary vasoconstriction occurring in CH-induced neonatal pHTN. We first investigated the contribution of diminished endothelium-dependent pulmonary vasodilation to enhanced pulmonary vasoconstriction. In contrast to our hypothesis, we found that following CH, vasodilatory responses to endogenous NO were enhanced in a manner dependent on increased eNOS protein expression and Ser1177 phosphorylation. We additionally observed that CH did not alter VSM sensitivity to exogenous NO. We concluded that neonatal CH exposure promotes endogenous NO-dependent pulmonary vasodilation by upregulation of protein expression and Ser1177 phosphorylation of eNOS. Despite this potentially adaptive response, neonates exposed to CH still demonstrated increased baseline PVR, enhanced pulmonary vasoconstrictor sensitivity, and pHTN.

We next evaluated the role of enhanced VSM contraction involving PKC_{β}/mitoROS signaling to mediate enhanced pulmonary arterial vasoconstriction. We found that PKC_{β} activation in neonatal pulmonary VSM leads to mitoROS generation. We additionally observed that PKC_{β} contributes to enhanced basal pulmonary arterial tone and vasoconstrictor reactivity following neonatal CH exposure. ROS signaling similarly contributes to enhanced pulmonary arterial basal tone and agonist-induced vasoconstriction in CH-exposed neonates with mitoROS contributing to enhanced arterial tone development in isolated pulmonary arteries from CH neonates. In conclusion, these data suggest that CH augments pulmonary arterial vasoconstriction in a manner dependent on PKC_{β}/mitoROS and that this response occurs despite a CH-dependent increase in NO-dependent pulmonary vasodilation.

Clinical Significance

Neonatal pHTN is a significant source of morbidity and mortality in infants (5, 246). Research into underlying mechanisms contributing to neonatal pHTN have identified vasoconstriction as an important mediator of the disease (180, 246). Investigation into factors that contribute to enhanced pulmonary vasoconstriction has focused on the role of diminished pulmonary vasodilation to limit vasoconstriction (43, 83, 87). Studying mechanisms of reduced pulmonary vasodilation has yielded clinical interventions for infants with pHTN focused on improving mechanisms of pulmonary vasodilation (5, 246). Evaluation of the effectiveness of current vasodilator therapies demonstrates that these strategies are met with limited success and do not improve mortality or length/cost of hospital stay (160, 273). Therefore, investigation into mechanisms that contribute to enhanced pulmonary vasoconstriction through promotion of enhanced VSM tone and pulmonary vasoconstrictor sensitivity are important to help generate new therapeutics for neonates with pHTN. Through these studies, we have demonstrated that enhanced pulmonary arterial vasoconstriction occurring in neonates with pHTN depends on PKC_{β}, a PKC isoform not previously linked to vasoconstriction in the neonatal pulmonary circulation, and mitoROS signaling. Further, we demonstrated that PKC_{β} can signal to promote mitoROS generation in neonatal PASMCs. The ability to understand these cellular pathways involving PKC_{β} and mitoROS may provide a new means of treating neonatal pHTN. Considering the need for improved understanding of mechanisms responsible for enhanced pulmonary VSM contractility and the subsequent contribution of those factors to enhanced pulmonary vasoconstriction, the findings from this investigation represent a novel step toward improved therapeutic intervention for infants with pHTN.

Future Directions

Although our present findings support a role of PKC_{β}/mitoROS signaling to mediate enhanced pulmonary arterial vasoconstriction in neonates with CH-induced pHTN, several questions remain unanswered by the current study. Future studies are necessary to establish the link between CH and PKC_{β} activation, PKC_{β} and mitoROS generation, and finally the mechanism by which PKC_{β}/mitoROS may enhance pulmonary arterial vasoconstriction. In addition, it is important to determine whether the PKC_{β}/mitoROS signaling axis contributes to the progression and maintenance of CH-induced pHTN in neonates.

As indicated above, future studies will evaluate the upstream initiator of this pathway following exposure to CH. Considering that ROS are important in the development of neonatal PH (40, 142), our data suggesting that PKC_{β} stimulates mitoROS production, and the known role of oxidation to activate PKC_{β} (106, 155, 206), we suspect that CH stimulates PKC_{β} activity through oxidation of the enzyme in a feed-forward fashion. However, investigation into the impact of neonatal CH exposure on $[Ca^{2+}]_i$ in VSM is also important considering that PKC_{β} is also sensitive to changes in $[Ca^{2+}]_i$ (268).

More investigation is important to better understand how PKC_{β} promotes mitoROS generation in PASMCs from neonatal rats. The literature suggests that signaling involving PKC_{β}-dependent activation of p66shc and/or mitoK_{ATP} channel opening may contribute to mitoROS generation (16, 58, 252). Additionally, more work is needed to better understand if neonatal CH exposure leads to PKC_{β}-dependent mitoROS generation and, if so, how CH may activate this signaling pathway. CH does not appear to impact protein expression of PKC_{β} splice variants, but some PKC isoforms translocate from the cell membrane to mitochondria to stimulate mitochondrial O_2^- production (54, 175). It is possible that subcellular localization of PKC_{β} may account for

CH-dependent activation of PKC_{β}/mitoROS signaling.

We are also interested in the downstream mechanism of PKC_{β}/mitoROS-dependent vasoconstriction. Dynamic actin cytoskeletal reorganization in VSM is vital to tension generation (258, 259) and early studies from our laboratory in adult rats suggest PKC_{β}/mitoROS signaling contribute to enhanced vasoconstriction in a manner dependent on myofilament Ca^{2+} sensitization reliant on actin polymerization. Classical signaling of PKC to promote Ca^{2+}-sensitization in arterial smooth muscle relies on CPI-17-dependent inhibition of myosin light-chain phosphatase (245). Evaluation of the contribution of CPI-17-induced Ca^{2+} sensitization and the contribution of PKC_{β} in this response is important to better understand potential mechanisms by which PKC_{β} leads to enhanced pulmonary arterial vasoconstriction.

Investigation into the potential mechanism by which PKC_{β}/mitoROS leads to enhanced pulmonary arterial vasoconstriction also needs to address which cell type is responsible for observed responses. Our current findings in transiently cultured PASMCs suggest that PKC_{β}/mitoROS signaling is observed in pulmonary VSM. However, studies in endothelium-disrupted, isolated pulmonary arteries are important to determine whether enhanced pulmonary arterial tone observed in CH exposed neonates is a consequence of PKC_{β}/mitoROS acting as endothelium-derived contractile factors.

Finally, increased PKC_{β} and mitoROS signaling may represent early onset responses that initiate the development of pHTN in response to neonatal CH. Furthermore, this mechanism may contribute to the maintenance of pHTN through vasoconstrictor actions. Future studies are necessary to evaluate the contribution of both PKC_{β} and mitoROS to the development of CH-induced neonatal pHTN, and the regression of established pHTN in this model.

In closing, the results from this dissertation as well as potential follow up investigation could identify therapeutic targets for neonatal pHTN. The potential of this

goal is enhanced by the recent use of the PKC_{β} inhibitor, LY-333-351 (13, 239) and the mitochondrial selective ROS scavenger, MitoQ (241, 257) in clinical trials to treat disease in adult humans.

APPENDIX A – ABBREVIATIONS AND ACRONYMS

ACh = acetylcholine
ANOVA = analysis of variance
AVP = arginine vasopressin
BK_{Ca} = Big conductance potassium channel
BSA = bovine serum albumin
$[Ca^{2+}]_i$ = intracellular calcium concentration
Ca^{2+} = calcium
CH = chronic hypoxia
DHE = dihydroethidium
eNOS = endothelial nitric oxide synthase
EGTA = ethylene glycol-bis(β-aminoethyl ether)-N,N,N'N'-tetraacetic acid
ET-1 = endothelin-1
FBS = fetal bovine serum
HBSS = Hank's buffered saline solution
5-HT = serotonin
20-hydroxyeicosatetraenoic acid = 20 HETE
i.d. = inner diameter
i.p. = intraperitoneal
iNOS = inducible nitric oxide synthase
L-NNA = N^{ω}-nitro-L-arginine
LV+S = left ventricle plus the interventricular septum
mitoROS = mitochondrial-derived reactive oxygen species
mitoTEMPO = 2-(2,2,6,6-tetramethylpiperidin-1-oxyl-4-ylamino)-2-oxoethyl)triphenylphosphonium chloride
mRNA = messenger ribonucleic acid
N_2 = nitrogen
NADPH = nicotinamide adenine dinucleotide phosphate
nNOS = neuronal nitric oxide synthase
NO = nitric oxide
NOS = nitric oxide synthase
NOX = nicotinamide adenine dinucleotide phosphate oxidase
O_2 = oxygen
O_2^- = superoxide anion
P14 = post-natal day 14
P_a = pulmonary arterial pressure
PAF = platelet activating factor
PASMC = pulmonary arterial smooth muscle cell
Pc = microvascular capillary pressure in the lung
PE-20 = polyethylene tubing 20
PE-90 = polyethylene tubing 90
PE-160 = polyethylene tubing 160
pHTN = pulmonary hypertension

PKC = protein kinase C
PMA = phorbol 12-myristate 13-acetate
P_v = pulmonary venous pressure
PVR = pulmonary vascular resistance
Q = perfusion rate
RNA = ribonucleic acid
ROK = Rho kinase
ROS = reactive oxygen species
RT-PCR = real-time polymerase chain reaction
RV = right ventricle
RVH = right ventricular hypertrophy
RVSP = right ventricular systolic pressure
SEM = standard error of the mean
shRNA = short hairpin ribonucleic acid
SOCE = store operated calcium entry
SOD = super oxide dismutase
SR = sarcoplasmic reticulum
SSRI = selective serotonin reuptake inhibitor
TBS = tris-buffered saline
TEMPOL = 1-oxyl-2,2,6,6-tetramethyl-4-hydroxypiperdine
Tiron = dihydroxy-1,3-benzenedisulfonic acid disodium salt
TTBS = tween-20 plus tris-buffered saline
VEGF = vascular endothelial growth factor
VSM = vascular smooth muscle

REFERENCES

1. **Aaronson PI**, **Robertson TP**, **Knock GA**, **Becker S**, **Lewis TH**, **Snetkov V**, **Ward JPT**. Hypoxic pulmonary vasoconstriction: mechanisms and controversies. *J Physiol* 570: 53–58, 2006.

2. **Aaronson PI**, **Robertson TP**, **Ward JPT**. Endothelium-derived mediators and hypoxic pulmonary vasoconstriction. *Respir Physiol Neurobiol* 132: 107–120, 2002.

3. **Abman SH**, **Accurso FJ**. Acute effects of partial compression of ductus arteriosus on fetal pulmonary circulation. *Am J Physiol Hear Circ Physiol* 257: H626–H634, 1989.

4. **Abman SH**, **Chatfield BA**, **Hall SL**, **McMurtry IF**. Role of endothelium-derived relaxing factor during transition of pulmonary circulation at birth. *Am J Physiol Hear Circ Physiol* 259: H1921–H1927, 1990.

5. **Abman SH**, **Hansmann G**, **Archer SL**, **Ivy DD**, **Adatia IT**, **Chung WK**, **Hanna BD**, **Rosenzweig EB**, **Raj JU**, **Cornfield D**, **Stenmark KR**, **Steinhorn RH**, **Thébaud B**, **Fineman JR**, **Kuehne T**, **Feinstein JA**, **Friedberg MK**, **Earing M**, **Barst RJ**, **Keller RL**, **Kinsella JP**, **Mullen M**, **Deterding R**, **Kulik T**, **Mallory G**, **Humpl T**, **Wessel DL**. Pediatric Pulmonary Hypertension. *Circulation* 132: 2037–2099, 2015.

6. **Abman SH**, **Shanley PF**, **Accurso FJ**. Failure of postnatal adaptation of the pulmonary circulation after chronic intrauterine pulmonary hypertension in fetal lambs. *J Clin Invest* 83: 1849–58, 1989.

7. **Adatia IT**, **Barrow SE**, **Stratton PD**, **Miall-Allen VM**, **Ritter JM**, **Haworth SG**. Thromboxane A2 and prostacyclin biosynthesis in children and adolescents with pulmonary vascular disease. *Circulation* 88: 2117–2122, 1993.

8. **Adatia IT**, **Barrow SE**, **Stratton PD**, **Ritter JM**, **Haworth SG**. Effect of intracardiac repair on biosynthesis of thromboxane A2 and prostacyclin in children with a left to right shunt. *Br Heart J* 72: 452–456, 1994.

9. **Afolayan AJ**, **Eis A**, **Teng R-J**, **Bakhutashvili I**, **Kaul S**, **Davis JM**, **Konduri GG**.

Decreases in manganese superoxide dismutase expression and activity contribute to oxidative stress in persistent pulmonary hypertension of the newborn. *Am J Physiol Lung Cell Mol Physiol* 303: L870-879, 2012.

10. **Afolayan AJ**, **Teng R-J**, **Eis A**, **Rana U**, **Broniowska KA**, **Corbett JA**, **Pritchard K**, **Konduri GG**. Inducible HSP70 regulates superoxide dismutase-2 and mitochondrial oxidative stress in the endothelial cells from developing lungs. *Am J Physiol Lung Cell Mol Physiol* 306: L351-60, 2014.

11. **Afshar S**, **Gibson LL**, **Yuhanna IS**, **Sherman TS**, **Kerecman JD**, **Grubb PH**, **Yoder BA**, **McCurnin DC**, **Shaul PW**. Pulmonary NO synthase expression is attenuated in a fetal baboon model of chronic lung disease. *Am J Physiol Lung Cell Mol Physiol* 284: L749–L758, 2003.

12. **Aggarwal S**, **Gross CM**, **Sharma S**, **Fineman JR**, **Black SM**. Reactive Oxygen Species in Pulmonary Vascular Remodeling. *Compr Physiol* 3: 1011–34, 2013.

13. **Aiello LP**, **Vignati L**, **Sheetz MJ**, **Zhi X**, **Girach A**, **Davis MD**, **Wolka AM**, **Shahri N**, **Milton RC**. Oral protein kinase c β inhibition using ruboxistaurin: efficacy, safety, and causes of vision loss among 813 patients (1,392 eyes) with diabetic retinopathy in the Protein Kinase C β Inhibitor-Diabetic Retinopathy Study and the Protein Kinase C β Inhibit. *Retina* 31: 2084–94, 2011.

14. **Allen J**, **Zwerdling R**, **Ehrenkranz RA**, **Gaultier C**, **Geggel R**, **Greenough A**, **Kleinman R**, **Klijanowicz A**, **Martinez F**, **Ozdemir A**, **Panitch HB**, **Phelps D**, **Nickerson BG**, **Stein MT**, **Tomezsko J**, **Van den Anker J**. Statement on the care of the child with chronic lung disease of infancy and childhood. *Am J Respir Crit Care Med* 168: 356–396, 2003.

15. **Allen SW**, **Chatfield BA**, **Koppenhafer SA**, **Schaffer MS**, **Wolfe RR**, **Abman SH**. Circulating immunoreactive endothelin-1 in children with pulmonary hypertension. Association with acute hypoxic pulmonary vasoreactivity. *Am Rev Respir Dis* 148: 519–522, 1993.

16. **Almeida M**, **Han L**, **Ambrogini E**, **Bartell SM**, **Manolagas SC**. Oxidative stress stimulates apoptosis and activates NF-kappaB in osteoblastic cells via a PKCbeta/p66shc signaling cascade: counter regulation by estrogens or

androgens. *Mol Endocrinol* 24: 2030–2037, 2010.

17. **Althoff TF**, **Offermanns S**. G-protein-mediated signaling in vascular smooth muscle cells - implications for vascular disease. *J Mol Med* 93: 973–81, 2015.

18. **Amano M**, **Chihara K**, **Kimura K**, **Fukata Y**, **Nakamura N**, **Matsuura Y**, **Kaibuchi K**. Formation of Actin Stress Fibers and Focal Adhesions Enhanced by Rho-Kinase Formation of Actin Stress Fibers and Focal Adhesions Enhanced by Rho-Kinase. *Science (80-)* 275: 1308–1311, 1997.

19. **Ambalavanan N**, **Bulger A**, **Murphy-Ullrich J**, **Oparil S**, **Chen Y-F**. Endothelin-A receptor blockade prevents and partially reverses neonatal hypoxic pulmonary vascular remodeling. *Pediatr Res* 57: 631–636, 2005.

20. **Ambalavanan N**, **Li P**, **Bulger A**, **Murphy-Ullrich J**, **Oparil S**, **Chen Y-F**. Endothelin-1 mediates hypoxia-induced increases in vascular collagen in the newborn mouse lung. *Pediatr Res* 61: 559–564, 2007.

21. **Ambalavanan N**, **Nicola T**, **Hagood J**, **Bulger A**, **Serra R**, **Murphy-Ullrich J**, **Oparil S**, **Chen Y-F**. Transforming growth factor-β signaling mediates hypoxia-induced pulmonary arterial remodeling and inhibition of alveolar development in newborn mouse lung. *Am J Physiol Lung Cell Mol Physiol* 295: 86–95, 2008.

22. **Archer SL**, **Gomberg-Maitland M**, **Maitland ML**, **Rich S**, **Garcia JGN**, **Weir EK**. Mitochondrial metabolism, redox signaling, and fusion: a mitochondria-ROS-HIF-1alpha-Kv1.5 O2-sensing pathway at the intersection of pulmonary hypertension and cancer. *Am J Physiol Hear Circ Physiol* 294: H570-8, 2008.

23. **Arrigoni FI**, **Vallance P**, **Haworth SG**, **Leiper JM**. Metabolism of asymmetric dimethylarginines is regulated in the lung developmentally and with pulmonary hypertension induced by hypobaric hypoxia. *Circulation* 107: 1195–1201, 2003.

24. **Assali NS**, **Kirschbaum TH**, **Dilts P V.** Effects of Hyperbaric Oxygen on Uteroplacental and Fetal Circulation. *Circ Res* 22: 573–588, 1968.

25. **Balasubramaniam V**, **le Cras TD**, **Ivy DD**, **Grover TR**, **Kinsella JP**, **Abman SH**. Role of platelet-derived growth factor in vascular remodeling during pulmonary

hypertension in the ovine fetus. *Am J Physiol Lung Cell Mol Physiol* 284: 826–833, 2003.

26. **Banerjee A**, **Roman C**, **Heymann MA**. Bradykinin receptor blockade does not affect oxygen-mediated pulmonary vasodilation in fetal lambs. *Pediatr Res* 36: 474–480, 1994.

27. **Baraldi E**, **Filippone M**. Chronic lung disease after premature birth. *N Engl J Med* 357: 1946–55, 2007.

28. **Barman SA**. Vasoconstrictor Effect of Endothelin-1 on Hypertensive Pulmonary Arterial Smooth Muscle Involves Rho Kinase and Protein Kinase C. *Am. J. Physiol. Lung Cell. Mol. Physiol.* (2007). doi: 10.1152/ajplung.00101.2006.

29. **Benveniste J**. Platelet-activating factor, a new mediator of anaphylaxis and immune complex deposition from rabbit and human basophils. *Nature* 249: 581–582, 1974.

30. **Berger RMF**, **Beghetti M**, **Humpl T**, **Raskob GE**, **Ivy DD**, **Jing Z-C**, **Bonnet D**, **Schulze-Neick I**, **Barst RJ**. Clinical features of paediatric pulmonary hypertension: a registry study. *Lancet* 379: 537–46, 2012.

31. **Berkenbosch JW**, **Baribeau J**, **Ferretti E**, **Perreault T**. Role of protein kinase C and phosphatases in the pulmonary vasculature of neonatal piglets [Online]. *Crit Care Med* 29: 1229–1233, 2001. http://www.ncbi.nlm.nih.gov/entrez/query.fcgi?cmd=Retrieve&db=PubMed&dopt=Citation&list_uids=11395610.

32. **Bhatt AJ**, **Pryhuber GS**, **Huyck H**, **Watkins RH**, **Metlay LA**, **Maniscalco WM**. Disrupted pulmonary vasculature and decreased vascular endothelial growth factor, Flt-1, and TIE-2 in human infants dying with bronchopulmonary dysplasia. *Am J Respir Crit Care Med* 164: 1971–1980, 2001.

33. **Bierer R**, **Nitta CH**, **Friedman J**, **Codianni S**, **de Frutos S**, **Dominguez-Bautista JA**, **Howard TA**, **Resta TC**, **Gonzalez Bosc L V.** NFATc3 is required for chronic hypoxia-induced pulmonary hypertension in adult and neonatal mice. *Am J Physiol Lung Cell Mol Physiol* 301: L872–L880, 2011.

34. **Billaud M**, **Marthan R**, **Savineau JP**, **Guibert C**. Vascular smooth muscle modulates endothelial control of vasoreactivity via reactive oxygen species production through myoendothelial communications. *PLoS One* 4: 1–11, 2009.

35. **Black SM**, **Johengen MJ**, **Ma Z-D**, **Bristow J**, **Soifer SJ**. Ventilation and oxygenation induce endothelial nitric oxide synthase gene expression in the lungs of fetal lambs. *J Clin Invest* 100: 1448–1458, 1997.

36. **Black SM**, **Johengen MJ**, **Soifer SJ**. Coordinated regulation of genes of the nitric oxide and endothelin pathways during the development of pulmonary hypertension in fetal lambs. *Pediatr Res* 44: 821–30, 1998.

37. **Black SM**, **Sanchez LS**, **Mata-Greenwood E**, **Bekker JM**, **Steinhorn RH**, **Fineman JR**. sGC and PDE5 are elevated in lambs with increased pulmonary blood flow and pulmonary hypertension. *Am J Physiol Lung Cell Mol Physiol* 281: L1051–L1057, 2001.

38. **Blanchoin L**, **Boujemaa-Paterski R**, **Sykes C**, **Plastino J**. Actin dynamics, architecture, and mechanics in cell motility. *Physiol Rev* 94: 235–63, 2014.

39. **Bland RD**, **Nielson DW**. Developmental Changes in Lung Epithelial Ion Transport and Liquid Movement. *Annu Rev Pharmacol Toxicol* 54: 373–394, 1992.

40. **Blood AB**, **Terry MH**, **Merritt TA**, **Papamatheakis DG**, **Blood Q**, **Ross JM**, **Power GG**, **Longo LD**, **Wilson SM**. Effect of chronic perinatal hypoxia on the role of rho-kinase in pulmonary artery contraction in newborn lambs. *Am J Physiol Regul Integr Comp Physiol* 304: R136–R146, 2013.

41. **Bobik A**, **Grooms A**, **Millar JA**, **Mitchell A**, **Grinpukel S**. Growth factor activity of endothelin on vascular smooth muscle [Online]. *Am J Physiol Cell Physiol* 258: C408–C415, 1990. http://ajpcell.physiology.org/content/258/3/C408.

42. **Brannon TS**, **North AJ**, **Wells LB**, **Shaul PW**. Prostacyclin synthesis in ovine pulmonary artery is developmentally regulated by changes in cyclooxygenase-1 gene expression. *J Clin Invest* 93: 2230–2235, 1994.

43. **Brennan LA**, **Steinhorn RH**, **Wedgwood S**, **Mata-Greenwood E**, **Roark EA**,

Russell JA, **Black SM**. Increased superoxide generation is associated with pulmonary hypertension in fetal lambs: a role for NADPH oxidase. *Circ Res* 92: 683–91, 2003.

44. **Broughton BRS**, **Walker BR**, **Resta TC**. Chronic hypoxia induces Rho kinase-dependent myogenic tone in small pulmonary arteries. *Am J Physiol Lung Cell Mol Physiol* 294: L797–L806, 2008.

45. **Burke TM**, **Wolin MS**. Hydrogen peroxide elicits pulmonary arterial relaxation and guanylate cyclase activation. *Am J Physiol* 252: H721–H732, 1987.

46. **Busse R**, **Trogisch G**, **Bassenge E**. The role of endothelium in the control of vascular tone [Online]. *Basic Res Cardiol* 80: 475–90, 1985. http://www.ncbi.nlm.nih.gov/pubmed/3000343 [3 Mar. 2017].

47. **Cassin S**, **Dawes GS**, **Mott JC**, **Rosst BB**, **Strang LB**. The vascular resistance of the foetal and newly ventilated lung of the lamb. *J Physiol* 171: 61–79, 1964.

48. **Cassin S**, **Kristova V**, **Davis T**, **Kadowitz PJ**, **Gause G**. Tone-dependent responses to endothelin in the isolated perfused fetal sheep pulmonary circulation in situ [Online]. *J Appl Physiol* 70: 1228–1234, 1991. http://www.ncbi.nlm.nih.gov/pubmed/2032988.

49. **Chambers CD**, **Hernandez-Diaz S**, **Van Marter LJ**, **Werler MM**, **Louik C**, **Jones KL**, **Mitchell A a**. Selective serotonin-reuptake inhibitors and risk of persistent pulmonary hypertension of the newborn. *N Engl J Med* 354: 579–87, 2006.

50. **Chatfield BA**, **McMurtry IF**, **Hall SL**, **Abman SH**. Hemodynamic effects of endothelin-1 on ovine fetal pulmonary circulation [Online]. *Am J Physiol Regul Integr Comp Physiol* 261: R182–R187, 1991. http://www.ncbi.nlm.nih.gov/entrez/query.fcgi?cmd=Retrieve&db=PubMed&dopt=Citation&list_uids=1858946.

51. **Chi AY**, **Waypa GB**, **Mungai PT**, **Schumacker PT**. Prolonged hypoxia increases ROS signaling and RhoA activation in pulmonary artery smooth muscle and endothelial cells. *Antioxid Redox Signal* 12: 603–610, 2010.

52. **Chicoine LG**, **Avitia JW**, **Deen C**, **Nelin LD**, **Earley S**, **Walker BR**. Developmental differences in pulmonary eNOS expression in response to chronic hypoxia in the rat. *J Appl Physiol* 93: 311–318, 2002.

53. **Chicoine LG**, **Paffett ML**, **Girton MR**, **Metropoulus MJ**, **Joshi MS**, **Bauer JA**, **Nelin LD**, **Resta TC**, **Walker BR**. Maturational changes in the regulation of pulmonary vascular tone by nitric oxide in neonatal rats. *Am J Physiol Lung Cell Mol Physiol* 293: L1261–L1270, 2007.

54. **Churchill EN**, **Szweda LI**. Translocation of deltaPKC to mitochondria during cardiac reperfusion enhances superoxide anion production and induces loss in mitochondrial function. *Arch Biochem Biophys* 439: 194–199, 2005.

55. **Clempus RE**, **Griendling KK**. Reactive oxygen species signaling in vascular smooth muscle cells. *Cardiovasc Res* 71: 216–225, 2006.

56. **Cogolludo A**, **Moreno L**, **Lodi F**, **Tamargo J**, **Perez-Vizcaino F**. Postnatal maturational shift from PKCζ and voltage-gated K+ channels to RhoA/Rho kinase in pulmonary vasoconstriction. *Cardiovasc Res* 66: 84–93, 2005.

57. **Cornfield DN**, **Chatfield BA**, **McQueston JA**, **McMurtry IF**, **Abman SH**. Effects of birth-related stimuli on L-arginine-dependent pulmonary vasodilation in ovine fetus. *Am J Physiol Hear Circ Physiol* 262: H1474–H1481, 1992.

58. **Costa ADT**, **Garlid KD**, **West IC**, **Lincoln TM**, **Downey JM**, **Cohen M V.**, **Critz SD**. Protein kinase G transmits the cardioprotective signal from cytosol to mitochondria. *Circ Res* 97: 329–336, 2005.

59. **Costa ADT**, **Quinlan CL**, **Andrukhiv A**, **West IC**, **Jabůrek M**, **Garlid KD**. The direct physiological effects of mitoK(ATP) opening on heart mitochondria. *Am J Physiol Hear Circ Physiol* 290: H406–H415, 2006.

60. **Le Cras TD**, **Kim D-H**, **Markham NE**, **Abman SH**. Early abnormalities of pulmonary vascular development in the Fawn-Hooded rat raised at Denver's altitude. *Am J Physiol Lung Cell Mol Physiol* 279: L283–L291, 2000.

61. **Le Cras TD**, **Markham NE**, **Tuder RM**, **Voelkel NF**, **Abman SH**. Treatment of

newborn rats with a VEGF receptor inhibitor causes pulmonary hypertension and abnormal lung structure. *Am J Physiol Lung Cell Mol Physiol* 283: L555-62, 2002.

62. **Le Cras TD**, **Tyler RC**, **Horan MP**, **Morris KG**, **Tuder RM**, **Mcmurtry IF**, **Johns RA**, **Abman SH**. Effects of Chronic Hypoxia and Altered Hemodynamics on Endothelial Nitric Oxide Synthase Expression in the Adult Rat Lung. *J Clin Invest* 101: 795–801, 1998.

63. **Le Cras TD**, **Xue C**, **Rengasamy A**, **Johns RA**. Chronic hypoxia upregulates endothelial and inducible NO synthase gene and protein expression in rat lung [Online]. *Am J Physiol Lung Cell Mol Physiol* 270: L164–L170, 1996. http://ajplung.physiology.org/content/270/1/L164.abstract.

64. **Crnich R**, **Amberg GC**, **Leo MD**, **Gonzales AL**, **Tamkun MM**, **Jaggar JH**, **Earley S**. Vasoconstriction resulting from dynamic membrane trafficking of TRPM4 in vascular smooth muscle cells. *Am J Physiol Cell Physiol* 299: C682-94, 2010.

65. **D'Angelo G**, **Davis MJ**, **Meninger GA**. Calcium and mechanotransduction of the myogenic response [Online]. *Am J Physiol Hear Circ Physiol* 273: H175–H182, 1997. http://ajpheart.physiology.org/content/273/1/H175.short [13 Mar. 2014].

66. **Dakshinamurti S**. Pathophysiologic mechanisms of persistent pulmonary hypertension of the newborn. *Pediatr Pulmonol* 39: 492–503, 2005.

67. **Dashdorj A**, **Jyothi KR**, **Lim S**, **Jo A**, **Nguyen MN**, **Ha J**, **Yoon K-S**, **Kim HJ**, **Park J-H**, **Murphy MP**, **Kim SS**. Mitochondria-targeted antioxidant MitoQ ameliorates experimental mouse colitis by suppressing NLRP3 inflammasome-mediated inflammatory cytokines. *BMC Med* 11: 178, 2013.

68. **Davidson D**. Pulmonary hemodynamics at birth: effect of acute cyclooxygenase inhibition in lambs. *J Appl Physiol* 64: 1676–1682, 1988.

69. **Davis MJ**, **Hill MA**. Signaling mechanisms underlying the vascular myogenic response. *Physiol Rev* 79: 387–423, 1999.

70. **Davis MJ**, **Sikes PJ**. Myogenic responses of isolated arterioles: test for a rate-sensitive mechanism [Online]. *Am J Physiol Lung Cell Mol Physiol* 259: H1890-

900, 1990. http://ajpheart.physiology.org/content/259/6/H1890.long%5Cnpapers://35bd2bc7-b5b1-49ed-bd73-ff0858dd5ce0/Paper/p3648.

71. **Delaney C**, **Gien J**, **Grover TR**, **Roe G**, **Abman SH**. Pulmonary vascular effects of serotonin and selective serotonin reuptake inhibitors in the late-gestation ovine fetus. *Am J Physiol Lung Cell Mol Physiol* 301: L937–L944, 2011.

72. **Delaney C**, **Gien J**, **Roe G**, **Isenberg N**, **Kailey J**, **Abman SH**. Serotonin contributes to high pulmonary vascular tone in a sheep model of persistent pulmonary hypertension of the newborn. *Am J Physiol Lung Cell Mol Physiol* 304: L894-901, 2013.

73. **Dennis KE**, **Aschner JL**, **Milatovic D**, **Schmidt JW**, **Aschner M**, **Kaplowitz MR**, **Zhang Y**, **Fike CD**. NADPH oxidases and reactive oxygen species at different stages of chronic hypoxia-induced pulmonary hypertension in newborn piglets. *Am J Physiol Lung Cell Mol Physiol* 297: L596–L607, 2009.

74. **Dikalova AE**, **Bikineyeva AT**, **Budzyn K**, **Nazarewicz RR**, **McCann L**, **Lewis W**, **Harrison DG**, **Dikalov SI**. Therapeutic targeting of mitochondrial superoxide in hypertension. *Circ Res* 107: 106–116, 2010.

75. **Dimmeler S**, **Fleming I**, **Fisslthaler B**, **Hermann C**, **Busse R**, **Zeiher AM**. Activation of nitric oxide synthase in endothelial cells by Akt-dependent phosphorylation. *Nature* 399: 601–605, 1999.

76. **Doughan AK**, **Harrison DG**, **Dikalov SI**. Molecular mechanisms of angiotensin II-mediated mitochondrial dysfunction: Linking mitochondrial oxidative damage and vascular endothelial dysfunction. *Circ Res* 102: 488–496, 2008.

77. **Dunham-Snary KJ**, **Danchen Wu**, **Sykes EA**, **Thakrar A**, **Parlow LRG**, **Mewburn JD**, **Parlow JL**, **Archer SL**. Hypoxic pulmonary vasoconstriction: from molecular mechanisms to medicine. *Chest* 151: 181–192, 2017.

78. **Dunham-Snary KJ**, **Hong ZG**, **Xiong PY**, **Del Paggio JC**, **Herr JE**, **Johri AM**, **Archer SL**. A mitochondrial redox oxygen sensor in the pulmonary vasculature and ductus arteriosus. *Pflugers Arch Eur J Physiol* 468: 43–58, 2016.

79. **Durmowicz AG**, **Orton EC**, **Stenmark KR**. Progressive Loss of Vasodilator Responsive Component of Pulmonary-Hypertension in Neonatal Calves Exposed to 4,570 m. *Am J Physiol Hear Circ Physiol* 265: H2175–H2183, 1993.

80. **Eichinger MR**, **Walker BR**. Enhanced pulmonary arterial dilation to arginine vasopressin in chronically hypoxic rats [Online]. *Am J Physiol Hear Circ Physiol* 267: H2413–H2419, 1994. http://www.ncbi.nlm.nih.gov/pubmed/7528996.

81. **Enomoto M**, **Jain A**, **Pan J**, **Shifrin Y**, **Van Vliet T**, **McNamara PJ**, **Jankov RP**, **Belik J**. Newborn rat response to single vs. combined cGMP-dependent pulmonary vasodilators. *Am J Physiol Lung Cell Mol Physiol* 306: L207–L215, 2014.

82. **Farrow KN**, **Lakshminrusimha S**, **Reda WJ**, **Wedgwood S**, **Czech L**, **Gugino SF**, **Davis JM**, **Russell JA**, **Steinhorn RH**. Superoxide dismutase restores eNOS expression and function in resistance pulmonary arteries from neonatal lambs with persistent pulmonary hypertension. *Am J Physiol Lung Cell Mol Physiol* 295: L979–L987, 2008.

83. **Farrow KN**, **Wedgwood S**, **Lee KJ**, **Czech L**, **Gugino SF**, **Lakshminrusimha S**, **Schumacker PT**, **Steinhorn RH**. Mitochondrial oxidant stress increases PDE5 activity in persistent pulmonary hypertension of the newborn. *Respir Physiol Neurobiol* 174: 272–281, 2010.

84. **Fasano A**, **Fiorentini C**, **Donelli G**, **Uzzau S**, **Kaper JB**, **Margaretten K**, **Ding X**, **Guandalini S**, **Comstock L**, **Goldblum SE**. Zonula occludens toxin modulates tight junctions through protein kinase C-dependent actin reorganization, in vitro. *J Clin Invest* 96: 710–720, 1995.

85. **Feissner RF**, **Skalska J**, **Gaum WE**, **Sheu S-S**. Crosstalk signaling between mitochondrial Ca2+ and ROS. *Front Biosci* 14: 1197–1218, 2009.

86. **Fike CD**, **Aschner JL**, **Kaplowitz MR**, **Zhang Y**, **Madden JA**. Reactive oxygen species scavengers improve voltage-gated K + channel function in pulmonary arteries of newborn pigs with progressive hypoxia-induced pulmonary hypertension. *Pulm Circ* 3: 551–563, 2013.

87. **Fike CD**, **Aschner JL**, **Zhang Y**, **Kaplowitz MR**. Impaired NO signaling in small pulmonary arteries of chronically hypoxic newborn piglets. *Am J Physiol Lung Cell Mol Physiol* 286: L1244–L1254, 2004.

88. **Fike CD**, **Kaplowitz MR**. Effect of chronic hypoxia on pulmonary vascular pressures in isolated lungs of newborn pigs. *J Appl Physiol* 77: 2853–2862, 1994.

89. **Fike CD**, **Kaplowitz MR**, **Thomas CJ**, **Nelin LD**. Chronic hypoxia decreases nitric oxide production and endothelial nitric oxide synthase in newborn pig lungs. *Am J Physiol Lung Cell Mol Physiol* 274: L517–L526, 1998.

90. **Fike CD**, **Kaplowitz MR**, **Zhang Y**, **Pfister SL**. Cyclooxygenase-2 and an early stage of chronic hypoxia-induced pulmonary hypertension in newborn pigs. *J Appl Physiol* 98: 1111–8; discussion 1091, 2005.

91. **Fike CD**, **Pfister SL**, **Kaplowitz MR**, **Madden JA**. Cyclooxygenase contracting factors and altered pulmonary vascular responses in chronically hypoxic newborn pigs [Online]. *J Appl Physiol* 92: 67–74, 2002. http://jap.physiology.org/content/92/1/67.short [25 Sep. 2014].

92. **Fike CD**, **Slaughter JC**, **Kaplowitz MR**, **Zhang Y**, **Aschner JL**. Reactive oxygen species from NADPH oxidase contribute to altered pulmonary vascular responses in piglets with chronic hypoxia-induced pulmonary hypertension. *Am J Physiol Lung Cell Mol Physiol* 295: L881–L888, 2008.

93. **Fike CD**, **Zhang Y**, **Kaplowitz MR**. Thromboxane inhibition reduces an early stage of chronic hypoxia-induced pulmonary hypertension in piglets. *J Appl Physiol* 99: 670–676, 2005.

94. **Fisher AB**. Redox signaling across cell membranes. *Antioxid Redox Signal* 11: 1349–1356, 2009.

95. **Fleming I**, **Busse R**. Endothelial Dysfunction : a Novel Therapeutic Target NO : the Primary EDRF The Endothelial Nitric Oxide Synthase : 14: 5–14, 1999.

96. **Fleming I**, **Busse R**. Molecular mechanisms involved in the regulation of the endothelial nitric oxide synthase. *Am J Physiol Regul Integr Comp Physiol* 284:

R1–R12, 2003.

97. **Forestier F**, **Daffos F**, **Catherine N**, **Renard M**, **Andreux J-P**. Developmental hematopoiesis in normal human fetal blood [Online]. *Blood* 77: 2360–3, 1991. http://www.bloodjournal.org/content/77/11/2360.abstract.

98. **Förstermann U**, **Sessa WC**. Nitric oxide synthases: Regulation and function. *Eur Heart J* 33: 829–837, 2012.

99. **de Frutos S**, **Diaz JMR**, **Nitta CH**, **Sherpa ML**, **Gonzalez Bosc L V.** Endothelin-1 contributes to increased NFATc3 activation by chronic hypoxia in pulmonary arteries. *Am J Physiol Cell Physiol* 301: C441–C450, 2011.

100. **Furchgott RF**, **Zawadzki J V.** The obligatory role of endothelial cells in the relaxation of arterial smooth muscle by acetylcholine. *Nature* 288: 373–376, 1980.

101. **Gao Y**, **Portugal AD**, **Negash S**, **Zhou W**, **Longo LD**, **Raj JU**. Role of Rho kinases in PKG-mediated relaxation of pulmonary arteries of fetal lambs exposed to chronic high altitude hypoxia. *Am J Physiol Lung Cell Mol Physiol* 292: L678–L684, 2007.

102. **Gao Y**, **Raj JU**. Regulation of the Pulmonary Circulation in the Fetus and Newborn. *Physiol Rev* 90: 1291–1335, 2010.

103. **Genet N**, **Billaud M**, **Rossignol R**, **Dubois M**, **Gillibert-Duplantier J**, **Isakson BE**, **Marthan R**, **Savineau J-P**, **Guibert C**. Signaling Pathways Linked to Serotonin-Induced Superoxide Anion Production: A Physiological Role for Mitochondria in Pulmonary Arteries. *Front Physiol* 8: 1–12, 2017.

104. **Ghanayem NS**, **Gordon JB**. Modulation of pulmonary vasomotor tone in the fetus and neonate. *Respir Res* 2: 139–144, 2001.

105. **Gien J**, **Seedorf GJ**, **Balasubramaniam V**, **Tseng N**, **Markham N**, **Abman SH**. Chronic intrauterine pulmonary hypertension increases endothelial cell Rho kinase activity and impairs angiogenesis in vitro. *Am J Physiol Lung Cell Mol Physiol* 295: L680–L687, 2008.

106. **Giorgi C**, **Agnoletto C**, **Baldini C**, **Bononi A**, **Bonora M**, **Marchi S**, **Missiroli S**,

Patergnani S, **Poletti F**, **Rimessi A**, **Zavan B**, **Pinton P**. Redox Control of Protein Kinase C: Cell- and Disease-Specific Aspects. *Antioxid Redox Signal* 13: 1051–1085, 2010.

107. **Gopalakrishna R**, **Jaken S**. Protein kinase C signaling and oxidative stress. *Free Radic Biol Med* 28: 1349–1361, 2000.

108. **Goyal R**, **Papamatheakis DG**, **Loftin M**, **Vrancken K**, **Dawson AS**, **Osman NJ**, **Blood AB**, **Pearce WJ**, **Longo LD**, **Wilson SM**. Long-term maternal hypoxia: the role of extracellular Ca2+ entry during serotonin-mediated contractility in fetal ovine pulmonary arteries. *Reprod Sci* 18: 948–62, 2011.

109. **Graham D**, **Huynh NN**, **Hamilton CA**, **Beattie E**, **Smith RAJ**, **Cochemé HM**, **Murphy MP**, **Dominiczak AF**. Mitochondria-targeted antioxidant mitoq10 improves endothelial function and attenuates cardiac hypertrophy. *Hypertension* 54: 322–328, 2009.

110. **Greene EL**, **Houghton O**, **Collinsworth G**, **Garnovskaya MN**, **Nagai T**, **Sajjad T**, **Bheemanathini V**, **Grewal JS**, **Paul R V.**, **Raymond JR**. 5-HT(2A) receptors stimulate mitogen-activated protein kinase via H(2)O(2) generation in rat renal mesangial cells. [Online]. *Am J Physiol Ren Physiol* 278: F650–F658, 2000. http://www.ncbi.nlm.nih.gov/pubmed/10751227.

111. **Grobe AC**, **Wells SM**, **Benavidez E**, **Oishi P**, **Azakie A**, **Fineman JR**, **Black SM**. Increased oxidative stress in lambs with increased pulmonary blood flow and pulmonary hypertension : role of NADPH oxidase and endothelial NO synthase. *Am J Physiol Lung Cell Mol Physiol* 290: 1069–1077, 2006.

112. **Hajjar KA**, **Marcus AJ**, **Muller W**. Vascular Function in Hemostasis. In: *Williams Hematology*, edited by Kaushansky K, Lichtman MA, Prchal JT, Levi MM, Press OW, Burns LJ, Caligiuri M. New York, NY: McGraw-Hill, 2016.

113. **Hakim TS**, **Pedoto A**, **Mangar D**, **Camporesi EM**. Nitric oxide plays a minimal role in hypoxic pulmonary vasoconstriction in isolated rat lungs. *Respir Physiol Neurobiol* 189: 93–98, 2013.

114. **Hall SM**, **Gorenflo M**, **Reader J**, **Lawson D**, **Haworth SG**. Neonatal pulmonary

hypertension prevents reorganisation of the pulmonary arterial smooth muscle cytoskeleton after birth. *J Anat* 196: 391–403, 2000.

115. **Hall SM**, **Haworth SG**. Onset and evolution of pulmonary vascular disease in young children: abnormal postnatal remodelling studied in lung biopsies. *J Pathol* 166: 183–93, 1992.

116. **Hanson KA**, **Ziegler JW**, **Rybalkin SD**, **Miller JW**, **Abman SH**, **Clarke WR**. Chronic pulmonary hypertension increases fetal lung cGMP phosphodiesterase activity. [Online]. *Am J Physiol Lung Cell Mol Physiol* 275: L931–L941, 1998. http://www.ncbi.nlm.nih.gov/pubmed/9815111.

117. **Harrison RE**, **Berger R**, **Haworth SG**, **Tulloh R**, **Mache CJ**, **Morrell NW**, **Aldred MA**, **Trembath RC**. Transforming growth factor-beta receptor mutations and pulmonary arterial hypertension in childhood. *Circulation* 111: 435–441, 2005.

118. **Haworth SG**. Development of the normal and hypertensive pulmonary vasculature. *Exp Physiol* 80: 843–853, 1995.

119. **Haworth SG**. Pathobiology of pulmonary hypertension in infants and children. *Prog Pediatr Cardiol* 12: 249–269, 2001.

120. **Haworth SG**, **Hislop AA**. Lung development-the effects of chronic hypoxia. *Semin Neonatol* 8: 1–8, 2003.

121. **Heymann MA**, **Rudolph AM**. Control of the ductus arteriosus [Online]. *Physiol Rev* 55: 62–78, 1975. http://www.ncbi.nlm.nih.gov/pubmed/1088992.

122. **Heymann MA**, **Rudolph AM**, **Nies AS**, **Melmon KL**. Bradykinin production associated with oxygenation of the fetal lamb. *Circ Res* 25: 521–534, 1969.

123. **Hill MA**, **Meininger GA**, **Davis MJ**, **Laher I**. Therapeutic potential of pharmacologically targeting arteriolar myogenic tone. *Trends Pharmacol Sci* 30: 363–374, 2009.

124. **Hinton M**, **Mellow L**, **Halayko AJ**, **Gutsol A**, **Dakshinamurti S**. Hypoxia induces hypersensitivity and hyperreactivity to thromboxane receptor agonist in neonatal pulmonary arterial myocytes. *Am J Physiol Lung Cell Mol Physiol* 290: L375–

L384, 2006.

125. **Hirenallur-S DK**, **Haworth ST**, **Leming JT**, **Chang J**, **Hernandez G**, **Gordon JB**, **Rusch NJ**. Upregulation of vascular calcium channels in neonatal piglets with hypoxia-induced pulmonary hypertension. *Am J Physiol Lung Cell Mol Physiol* 295: L915–L924, 2008.

126. **Hislop AA**. Developmental biology of the pulmonary circulation. *Paediatr Respir Rev* 6: 35–43, 2005.

127. **Hislop AA**, **Reid LM**. Intra-pulmonary arterial development during fetal life-branching pattern and structure [Online]. *J Anat* 113: 35–48, 1972. http://www.pubmedcentral.nih.gov/articlerender.fcgi?artid=1271365&tool=pmcentrez&rendertype=abstract.

128. **Hislop AA**, **Reid LM**. Pulmonary arterial development during childhood: branching pattern and structure. *Thorax* 28: 313–9, 1973.

129. **Hislop AA**, **Springall DR**, **Oliveira H**, **Pollock JS**, **Polak JM**, **Haworth SG**. Endothelial nitric oxide synthase in hypoxic newborn porcine pulmonary vessels. *Arch Dis Child Fetal Neonatal Ed* 77: F16–F22, 1997.

130. **Hooper CW**, **Delaney C**, **Streeter T**, **Yarboro MT**, **Poole SD**, **Brown N**, **Slaughter JC**, **Cotton RB**, **Reese J**, **Shelton EL**. Selective serotonin reuptake inhibitor (SSRI) exposure constricts the mouse ductus arteriosus in utero. *Am. J. Physiol. Hear. Circ. Physiol.* (2016). doi: 10.1152/ajpheart.00822.2015.

131. **Hooper SB**. Role of luminal volume changes in the increase in pulmonary blood flow at birth in sheep. *Exp Physiol* 83: 833–842, 1998.

132. **Ibe BO**, **Hibler S**, **Raj JU**. Platelet-activating factor modulates pulmonary vasomotor tone in the perinatal lamb. *J Appl Physiol* 85: 1079–1085, 1998.

133. **Ibe BO**, **Portugal AM**, **Chaturvedi S**, **Raj JU**. Oxygen-dependent PAF receptor binding and intracellular signaling in ovine fetal pulmonary vascular smooth muscle. *Am J Physiol Lung Cell Mol Physiol* 288: L879–L886, 2005.

134. **Ibe BO**, **Portugal AM**, **Usha Raj J**. Metabolism of platelet activating factor by

intrapulmonary vascular smooth muscle cells. Effect of oxygen on phospholipase A2 protein expression and activities of acetyl-CoA acetyltransferase and cholinephosphotransferase. *Mol Genet Metab* 77: 237–248, 2002.

135. **Inoue I**, **Nagase H**, **Kishi K**, **Higuti T**. ATP-sensitive K+ channel in the mitochondrial inner membrane. *Nature* 352: 244–247, 1991.

136. **Ivy DD**, **Kinsella JP**, **Abman SH**. Physiologic characterization of endothelin A and B receptor activity in the ovine fetal pulmonary circulation. *J Clin Invest* 93: 2141–2148, 1994.

137. **Ivy DD**, **Kinsella JP**, **Abman SH**. Endothelin blockade augments pulmonary vasodilation in the ovine fetus. *J Appl Physiol* 81: 2481–2487, 1996.

138. **Jain A**, **McNamara PJ**. Persistent pulmonary hypertension of the newborn: Advances in diagnosis and treatment. *Semin Fetal Neonatal Med* 20: 262–271, 2015.

139. **Jain R**, **Shaul PW**, **Borok Z**, **Willis BC**. Endothelin-1 induces alveolar epithelial-mesenchymal transition through endothelin type A receptor-mediated production of TGF-beta1. *Am J Respir Cell Mol Biol* 37: 38–47, 2007.

140. **Jankov RP**, **Kantores C**, **Belcastro R**, **Yi M**, **Tanswell AK**. Endothelin-1 inhibits apoptosis of pulmonary arterial smooth muscle in the neonatal rat. *Pediatr Res* 60: 245–251, 2006.

141. **Jankov RP**, **Kantores C**, **Belcastro R**, **Yi S**, **Ridsdale RA**, **Post M**, **Tanswell AK**. A role for platelet-derived growth factor beta-receptor in a newborn rat model of endothelin-mediated pulmonary vascular remodeling. *Am J Physiol Lung Cell Mol Physiol* 288: L1162–L1170, 2005.

142. **Jankov RP**, **Kantores C**, **Pan J**, **Belik J**. Contribution of xanthine oxidase-derived superoxide to chronic hypoxic pulmonary hypertension in neonatal rats. *Am J Physiol Lung Cell Mol Physiol* 294: L233–L245, 2008.

143. **Jankov RP**, **Luo X**, **Belcastro R**, **Copland I**, **Frndova H**, **Lye SJ**, **Hoidal JR**, **Post M**, **Tanswell AK**. Gadolinium chloride inhibits pulmonary macrophage influx

and prevents O(2)-induced pulmonary hypertension in the neonatal rat. *Pediatr Res* 50: 172–183, 2001.

144. **Jankov RP**, **Luo X**, **Cabacungan J**, **Belcastro R**, **Frndova H**, **Lye SJ**, **Tanswell AK**. Endothelin-1 and O2-mediated pulmonary hypertension in neonatal rats: a role for products of lipid peroxidation. *Pediatr Res* 48: 289–298, 2000.

145. **Jernigan NL**, **Walker BR**, **Resta TC**. Reactive oxygen species mediate RhoA/Rho kinase-induced Ca2+ sensitization in pulmonary vascular smooth muscle following chronic hypoxia. *Am J Physiol Lung Cell Mol Physiol* 295: L515–L529, 2008.

146. **Jirousek MR**, **Gillig JR**, **Gonzalez CM**, **Heath WF**, **Iii JHM**, **Neel DA**, **Rito CJ**, **Singh U**, **Stramm LE**, **Melikian-badalian A**, **Baevsky M**, **Ballas LM**, **Hall SE**, **Winneroski LL**, **Faul MM**. (S)-13-[(dimethylamino)methyl]-10,11,14,15-tetrahydro-4,9:16, 21-dimetheno-1H, 13H-dibenzo[e,k]pyrrolo[3,4-h][1,4,13]oxadiazacyclohexadecene-1,3(2H)-d ione (LY333531) and related analogues: isozyme selective inhibitors of protein kinase C beta. *J Med Chem* 3: 2664–2671, 1996.

147. **Kalyanaraman B**, **Dranka BP**, **Hardy M**, **Michalski R**, **Zielonka J**. HPLC-based monitoring of products formed from hydroethidine-based fluorogenic probes - The ultimate approach for intra- and extracellular superoxide detection. *Biochim Biophys Acta - Gen Subj* 1840: 739–44, 2014.

148. **Kantores C**, **McNamara PJ**, **Teixeira L**, **Engelberts D**, **Murthy P**, **Kavanagh BP**, **Jankov RP**. Therapeutic hypercapnia prevents chronic hypoxia-induced pulmonary hypertension in the newborn rat. *Am J Physiol Lung Cell Mol Physiol* 291: L912–L922, 2006.

149. **Katzung BG**. Vasodilators & The Treatment of Angina Pectoris. In: *Basic & Clinical Pharmacology*, edited by Katzung BG, Trevor AJ. New York, NY: McGraw-Hill, 2015.

150. **Kawai N**, **Bloch DB**, **Filippov G**, **Rabkina D**, **Suen H-C**, **Losty PD**, **Janssens SP**, **Zapol WM**, **De La Monte SM**, **Bloch KD**. Constitutive endothelial nitric oxide synthase gene expression is regulated during lung development. *Am J Physiol*

Lung Cell Mol Physiol 268: L589-95, 1995.

151. **Kelly LK**, **Wedgwood S**, **Steinhorn RH**, **Black SM**. Nitric oxide decreases endothelin-1 secretion through the activation of soluble guanylate cyclase. *Am J Physiol Lung Cell Mol Physiol* 286: L984–L991, 2004.

152. **Kinsella JP**, **Abman SH**. Recent developments in the pathophysiology and treatment of persistent pulmonary hypertension of the newborn [Online]. *J Pediatr* 126: 853–864, 1995. http://www.ncbi.nlm.nih.gov/pubmed/7776084%5Cnhttp://ac.els-cdn.com/S0022347695701974/1-s2.0-S0022347695701974-main.pdf?_tid=55a05a56-ff00-11e4-8546-00000aacb35d&acdnat=1432133943_1da9bb089d7970f99b680fbc5ba4a6b4.

153. **Kiserud T**. Physiology of the fetal circulation. *Semin Fetal Neonatal Med* 10: 493–503, 2005.

154. **Kitazawa T**, **Takizawa N**, **Ikebe M**, **Eto M**. Reconstitution of protein kinase C-induced contractile Ca2+ sensitization in Triton X-100-demembranated rabbit arterial smooth muscle. *J Physiol* 520: 139–152, 1999.

155. **Knapp LT**, **Klann E**. Superoxide-induced Stimulation of Protein Kinase C via Thiol Modification and Modulation of Zinc Content. *J Biol Chem* 275: 24136–24145, 2000.

156. **Knock GA**, **Snetkov VA**, **Shaifta Y**, **Connolly M**, **Drndarski S**, **Noah A**, **Pourmahram GE**, **Becker S**, **Aaronson PI**, **Ward JPT**. Superoxide constricts rat pulmonary arteries via Rho-kinase-mediated Ca2+ sensitization. *Free Radic Biol Med* 46: 633–642, 2009.

157. **Komai H**, **Adatia IT**, **Elliott MJ**, **de Leval MR**, **Haworth SG**. Increased plasma levels of endothelin-1 after cardiopulmonary bypass in patients with pulmonary hypertension and congenital heart disease [Online]. *J Thorac Cardiovasc Surg* 106: 473–8, 1993. http://www.ncbi.nlm.nih.gov/pubmed/8361190 [9 Mar. 2017].

158. **Konduri GG**, **Bakhutashvili I**, **Eis A**, **Gauthier KM**. Impaired voltage gated potassium channel responses in a fetal lamb model of persistent pulmonary

hypertension of the newborn. *Pediatr Res* 66: 289–294, 2009.

159. **Konduri GG**, **Ou J**, **Shi Y**, **Pritchard KA**. Decreased association of HSP90 impairs endothelial nitric oxide synthase in fetal lambs with persistent pulmonary hypertension. *Am J Physiol Hear Circ Physiol* 285: H204–H211, 2003.

160. **Konduri GG**, **Solimano A**, **Sokol GM**, **Singer J**, **Ehrenkranz RA**, **Singhal N**, **Wright LL**, **Van Meurs K**, **Stork E**, **Kirpalani H**, **Peliowski A**. A randomized trial of early versus standard inhaled nitric oxide therapy in term and near-term newborn infants with hypoxic respiratory failure. *Pediatrics* 113: 559–564, 2004.

161. **Krishna MC**, **Russo A**, **Mitchell JB**, **Goldstein S**, **Dafni H**, **Samuni A**. Do nitroxide antioxidants act as scavengers of O2/-· or as SOD mimics? *J Biol Chem* 271: 26026–26031, 1996.

162. **Kuo IY**, **Ehrlich BE**. Signaling in muscle contraction. *Cold Spring Harb Perspect Biol* 7: 1–15, 2015.

163. **Lakshminrusimha S**, **Wiseman D**, **Black SM**, **Russell JA**, **Gugino SF**, **Oishi P**, **Steinhorn RH**, **Fineman JR**. The role of nitric oxide synthase-derived reactive oxygen species in the altered relaxation of pulmonary arteries from lambs with increased pulmonary blood flow. *Am J Physiol Hear Circ Physiol* 293: H1491–H1497, 2007.

164. **Leffler CW**, **Hessler JR**, **Green RS**. The onset of breathing at birth stimulates pulmonary vascular prostacyclin synthesis [Online]. *Pediatr Res* 18: 938–42, 1984. http://www.ncbi.nlm.nih.gov/pubmed/6387607.

165. **Leffler CW**, **Tyler TL**, **Cassin S**. Effect of indomethacin on pulmonary vascular response to ventilation of fetal goats [Online]. *Am J Physiol Hear Circ Physiol* 234: H346–H351, 1978. http://ajpheart.physiology.org/content/234/4/H346.full-text.pdf+html.

166. **Lin MJ**, **Leung GPH**, **Zhang WM**, **Yang XR**, **Yip KP**, **Tse CM**, **Sham JSK**. Chronic hypoxia-induced upregulation of store-operated and receptor-operated Ca2+ channels in pulmonary arterial smooth muscle cells: A novel mechanism of hypoxic pulmonary hypertension. *Circ Res* 95: 496–505, 2004.

167. **Liu Y**, **Suzuki YJ**, **Day RM**, **Fanburg BL**. Rho kinase-induced nuclear translocation of ERK1/ERK2 in smooth muscle cell mitogenesis caused by serotonin. *Circ Res* 95: 579–586, 2004.

168. **Madden JA**, **Ahlf SB**, **Dantuma MW**, **Olson KR**, **Roerig DL**. Precursors and inhibitors of hydrogen sulfide synthesis affect acute hypoxic pulmonary vasoconstriction in the intact lung. *J Appl Physiol* 112: 411–8, 2012.

169. **Madden JA**, **Vadula MS**, **Kurup VP**. Effects of hypoxia and other vasoactive agents on pulmonary and cerebral artery smooth muscle cells [Online]. *Am J Physiol* 263: L384–L393, 1992. http://www.ncbi.nlm.nih.gov/pubmed/1415563.

170. **Maniscalco WM**, **Watkins RH**, **Pryhuber GS**, **Bhatt A**, **Shea C**, **Huyck H**. Angiogenic factors and alveolar vasculature: development and alterations by injury in very premature baboons. *Am J Physiol Lung Cell Mol Physiol* 282: L811–L823, 2002.

171. **Van Marter LJ**, **Hernandez-Diaz S**, **Werler MM**, **Louik C**, **Mitchell AA**. Nonsteroidal antiinflammatory drugs in late pregnancy and persistent pulmonary hypertension of the newborn. *Pediatrics* 131: 79–87, 2013.

172. **Martínez MC**, **Randriamboavonjy V**, **Ohlmann P**, **Komas N**, **Duarte J**, **Schneider F**, **Stoclet J-C**, **Andriantsitohaina R**. Involvement of protein kinase C, tyrosine kinases, and Rho kinase in Ca(2+) handling of human small arteries. *Am J Physiol Hear Circ Physiol* 279: H1228–H1238, 2000.

173. **Masood A**, **Yi M**, **Lau M**, **Belcastro R**, **Shek S**, **Pan J**, **Kantores C**, **McNamara PJ**, **Kavanagh BP**, **Belik J**, **Jankov RP**, **Tanswell AK**. Therapeutic effects of hypercapnia on chronic lung injury and vascular remodeling in neonatal rats. *Am J Physiol Lung Cell Mol Physiol* 297: L920-30, 2009.

174. **Mata-Greenwood E**, **Jenkins C**, **Farrow KN**, **Konduri GG**, **Russell JA**, **Lakshminrusimha S**, **Black SM**, **Steinhorn RH**. eNOS function is developmentally regulated: uncoupling of eNOS occurs postnatally. *Am J Physiol Lung Cell Mol Physiol* 290: L232–L241, 2005.

175. **Matsuzaki S**, **Szweda PA**, **Szweda LI**, **Humphries KM**. Regulated production of

free radicals by the mitochondrial electron transport chain: Cardiac ischemic preconditioning. *Adv Drug Deliv Rev* 61: 1324–1331, 2009.

176. **McCarron JG**, **Olson ML**, **Wilson C**, **Sandison ME**, **Chalmers S**. Examining the role of mitochondria in Ca^{2+} signaling in native vascular smooth muscle. *Microcirculation* 20: 317–29, 2013.

177. **McCarron JG**, **Wilson C**, **Sandison ME**, **Olson ML**, **Girkin JM**, **Saunter C**, **Chalmers S**. From structure to function: Mitochondrial morphology, motion and shaping in vascular smooth muscle. *J Vasc Res* 50: 357–371, 2013.

178. **McCray PB**, **Bettencourt JD**, **Bastacky J**. Developing bronchopulmonary epithelium of the human fetus secretes fluid [Online]. *Am J Physiol Lung Cell Mol Physiol* 262: L270-9, 1992. http://www.ncbi.nlm.nih.gov/pubmed/1372486.

179. **McMurtry IF**, **Davidson AB**, **Reeves JT**, **Grover RF**. Inhibition of hypoxic pulmonary vasoconstriction by calcium antagonists in isolated rat lungs [Online]. *Circ Res* 38: 99–104, 1976. http://www.ncbi.nlm.nih.gov/pubmed/1245025.

180. **McNamara PJ**, **Murthy P**, **Kantores C**, **Teixeira L**, **Engelberts D**, **van Vliet T**, **Kavanagh BP**, **Jankov RP**. Acute vasodilator effects of Rho-kinase inhibitors in neonatal rats with pulmonary hypertension unresponsive to nitric oxide. *Am J Physiol Lung Cell Mol Physiol* 294: L205–L213, 2008.

181. **McQueston JA**, **Kinsella JP**, **Ivy DD**, **McMurtry IF**, **Abman SH**. Chronic pulmonary hypertension in utero impairs endothelium-dependent vasodilation [Online]. *Am J Physiol Hear Circ Physiol* 268: H288–H294, 1995. http://www.ncbi.nlm.nih.gov/entrez/query.fcgi?cmd=Retrieve&db=PubMed&dopt=Citation&list_uids=7840274.

182. **Mehta NK**, **Mehta KD**. Protein kinase C-beta: an emerging connection between nutrient excess and obesity. *Biochim Biophys Acta - Mol Cell Biol Lipids* 1841: 1491–1497, 2014.

183. **Meyrick B**, **Reid LM**. Hypoxia and incorporation of 3H-thymidine by cells of the rat pulmonary arteries and alveolar wall [Online]. *Am J Pathol* 96: 51–70, 1979. http://www.pubmedcentral.nih.gov/articlerender.fcgi?artid=2042349&tool=pmcentr

ez&rendertype=abstract.

184. **Meyrick B**, **Reid LM**. Ultrastructural findings in lung biopsy material from children with congenital heart defects. *Am J Pathol* 101: 527–537, 1980.

185. **Moore PK**, **Al-Swayeh OA**, **Chong NW**, **Evans RA**, **Gibson A**. L-NG-nitro arginine (L-NOARG), a novel, L-arginine-reversible inhibitor of endothelium-dependent vasodilatation in vitro. [Online]. *Br J Pharmacol* 99: 408–12, 1990. http://www.pubmedcentral.nih.gov/articlerender.fcgi?artid=1917379&tool=pmcentrez&rendertype=abstract.

186. **Moreno-Domínguez A**, **Colinas O**, **El-Yazbi A**, **Walsh EJ**, **Hill MA**, **Walsh MP**, **Cole WC**. Ca2+ sensitization due to myosin light chain phosphatase inhibition and cytoskeletal reorganization in the myogenic response of skeletal muscle resistance arteries. *J Physiol* 591: 1235–1250, 2013.

187. **Morin, Frederick C. 3rd**, **Egan EA**. Pulmonary hemodynamics in fetal lambs during development at normal and increased oxygen tension. *J Appl Physiol* 73: 213–218, 1992.

188. **Morin, Frederick C. 3rd**, **Egan EA**, **Ferguson W**, **Lundgren CEG**. Development of pulmonary vascular response to oxygen [Online]. *Am J Physiol Hear Circ Physiol* 254: H542-6, 1988. http://www.ncbi.nlm.nih.gov/pubmed/3348432.

189. **Morrell NW**, **Adnot S**, **Archer SL**, **Dupuis J**, **Jones PL**, **MacLean MR**, **McMurtry IF**, **Stenmark KR**, **Thistlethwaite PA**, **Weissmann N**, **Yuan JX-J**, **Weir EK**. Cellular and molecular basis of pulmonary arterial hypertension. *J Am Coll Cardiol* 54: S20-31, 2009.

190. **Moss AJ**, **Emmanouilides G**, **Duffie ERJ**. Closure of the ductus arteriosus in the newborn infant. *Pediatrics* 32: 25–30, 1963.

191. **Nair J**, **Lakshminrusimha S**. Update on PPHN: Mechanisms and treatment. *Semin Perinatol* 38: 78–91, 2014.

192. **Narayanan D**, **Bulley S**, **Leo MD**, **Burris SK**, **Gabrick KS**, **Boop FA**, **Jaggar JH**. Smooth muscle cell transient receptor potential polycystin-2 (TRPP2) channels

contribute to the myogenic response in cerebral arteries. *J Physiol* 591: 5031–46, 2013.

193. **Nelson CP**, **Willets JM**, **Davies NW**, **Challiss RAJ**, **Standen NB**. Visualizing the temporal effects of vasoconstrictors on PKC translocation and Ca2+ signaling in single resistance arterial smooth muscle cells. *Am J Physiol Cell Physiol* 295: C1590–C1601, 2008.

194. **Niiro N**, **Koga Y**, **Ikebe M**. Agonist-induced changes in the phosphorylation of the myosin- binding subunit of myosin light chain phosphatase and CPI17, two regulatory factors of myosin light chain phosphatase, in smooth muscle. *Biochem J* 369: 117–128, 2003.

195. **Nitta CH**, **Osmond DA**, **Herbert LM**, **Beasley BF**, **Resta TC**, **Walker BR**, **Jernigan NL**. Role of ASIC1 in the development of chronic hypoxia-induced pulmonary hypertension. *Am J Physiol Hear Circ Physiol* 306: H41-52, 2014.

196. **North AJ**, **Star RA**, **Brannon TS**, **Ujiie K**, **Wells LB**, **Lowenstein CJ**, **Snyder SH**, **Shaul PW**. Nitric oxide synthase type I and type III gene expression are developmentally regulated in rat lung. *Am J Physiol Lung Cell Mol Physiol* 266: L635–L641, 1994.

197. **Norton CE**, **Broughton BRS**, **Jernigan NL**, **Walker BR**, **Resta TC**. Enhanced Depolarization-Induced Pulmonary Vasoconstriction Following Chronic Hypoxia Requires EGFR-Dependent Activation of NAD(P)H Oxidase 2. *Antioxid Redox Signal* 18: 1777–1788, 2012.

198. **Norton CE**, **Jernigan NL**, **Kanagy NL**, **Walker BR**, **Resta TC**. Intermittent hypoxia augments pulmonary vascular smooth muscle reactivity to NO: regulation by reactive oxygen species. *J Appl Physiol* 111: 980–988, 2011.

199. **Oldenburg O**, **Qin Q**, **Krieg T**, **Yang X-M**, **Philipp S**, **Critz SD**, **Cohen M V.**, **Downey JM**. Bradykinin induces mitochondrial ROS generation via NO, cGMP, PKG, and mitoKATP channel opening and leads to cardioprotection. *Am J Physiol Hear Circ Physiol* 286: H468–H476, 2004.

200. **Palmer LA**, **Semenza GL**, **Stoler MH**, **Johns RA**. Hypoxia induces type II NOS

gene expression in pulmonary artery endothelial cells via HIF-1 [Online]. *Am J Physiol Lung Cell Mol Physiol* 274: L212–L219, 1998. http://www.ncbi.nlm.nih.gov/pubmed/9486205.

201. **Parera MC**, **van Dooren M**, **van Kempen M**, **de Krijger R**, **Grosveld F**, **Tibboel D**, **Rottier R**. Distal angiogenesis: a new concept for lung vascular morphogenesis. *Am J Physiol Lung Cell Mol Physiol* 288: L141–L149, 2005.

202. **Parker TA**, **Roe G**, **Grover TR**, **Abman SH**. Rho kinase activation maintains high pulmonary vascular resistance in the ovine fetal lung. *Am J Physiol Lung Cell Mol Physiol* 291: L976–L982, 2006.

203. **Parrau D**, **Ebensperger G**, **Herrera EA**, **Moraga F**, **Riquelme RA**, **Ulloa CE**, **Rojas RT**, **Silva P**, **Hernandez I**, **Ferrada J**, **Diaz M**, **Parer JT**, **Cabello G**, **Llanos AJ**, **Reyes R V.** Store-operated channels in the pulmonary circulation of high- and low-altitude neonatal lambs. *Am J Physiol Lung Cell Mol Physiol* 304: L540-8, 2013.

204. **Peliowski A**, **Society CP**, **Committee N**. Inhaled nitric oxide use in newborns. 17: 95–97, 2012.

205. **Pierce CM**, **Krywawych S**, **Petros AJ**. Elevated levels of asymmetric di-methylarginine in neonates with congenital diaphragmatic hernia. *Eur J Pediatr* 164: 248–249, 2005.

206. **Pinton P**, **Rimessi A**, **Marchi S**, **Orsini F**, **Migliaccio E**, **Giorgio M**, **Contursi C**, **Minucci S**, **Mantovani F**, **Wieckowski MR**, **Del Sal G**, **Pelicci PG**, **Rizzuto R**. Protein kinase C beta and prolyl isomerase 1 regulate mitochondrial effects of the life-span determinant p66Shc. *Science* 315: 659–663, 2007.

207. **Pinton P**, **Rimessi A**, **Marchi S**, **Orsini F**, **Migliaccio E**, **Giorgio M**, **Contursi C**, **Minucci S**, **Mantovani F**, **Wieckowski MR**, **Del Sal G**, **Pelicci PG**, **Rizzuto R**. Protein kinase C beta and prolyl isomerase 1 regulate mitochondrial effects of the life-span determinant p66Shc. *Science (80-)* 315: 659–63, 2007.

208. **Plomaritas DR**, **Herbert LM**, **Yellowhair TR**, **Resta TC**, **Gonzalez Bosc L V.**, **Walker BR**, **Jernigan NL**. Chronic hypoxia limits H2O2-induced inhibition of

ASIC1-dependent store-operated calcium entry in pulmonary arterial smooth muscle. *Am J Physiol Lung Cell Mol Physiol* 307: L419–L430, 2014.

209. **Popp RL**, **Velasquez O**, **Bland J**, **Hughes P**. Characterization of protein kinase C isoforms in primary cultured cerebellar granule cells. *Brain Res* 1083: 70–84, 2006.

210. **Quagliaro L**, **Piconi L**, **Assaloni R**, **Da Ros R**, **Maier A**, **Zuodar G**, **Ceriello A**. Intermittent high glucose enhances ICAM-1, VCAM-1 and E-selectin expression in human umbilical vein endothelial cells in culture: The distinct role of protein kinase C and mitochondrial superoxide production. *Atherosclerosis* 183: 259–267, 2005.

211. **Quittau-Prevostel C**, **Delaunay N**, **Collazos A**, **Vallentin A**, **Joubert D**. Targeting of PKCalpha and epsilon in the pituitary: a highly regulated mechanism involving a GD(E)E motif of the V3 region. *J Cell Sci* 117: 63–72, 2004.

212. **Rabinovitch M**. Developmental Biology of the Pulmonary Vasculature. In: *Fetal and Neonatal Physiology*, edited by Polin RA, Fox WW, Abman SH. Philadelphia, PA: Elsevier Saunders, 2011, p. 757–772.

213. **Rabinovitch M**, **Haworth SG**, **Castaneda AR**, **Nadas AS**, **Reid LM**. Lung biopsy in congenital heart disease: a morphometric approach to pulmonary vascular disease. *Circulation* 58: 1107–1122, 1978.

214. **Rabinovitch M**, **Keane JF**, **Norwood WI**, **Castaneda AR**, **Reid LM**. Vascular structure in lung tissue obtained at biopsy correlated with pulmonary hemodynamic findings after repair of congenital heart defects. *Circulation* 69: 655–667, 1984.

215. **Rairigh RL**, **Parker TA**, **Ivy DD**, **Kinsella JP**, **Fan I-D**, **Abman SH**. Role of inducible nitric oxide synthase in the pulmonary vascular response to birth-related stimuli in the ovine fetus. *Circ Res* 88: 721–726, 2001.

216. **Rairigh RL**, **Storme L**, **Parker TA**, **le Cras TD**, **Kinsella JP**, **Jakkula M**, **Abman SH**. Inducible NO synthase inhibition attenuates shear stress-induced pulmonary vasodilation in the ovine fetus [Online]. *Am J Physiol Lung Cell Mol Physiol* 276: L513–L521, 1999. http://ajplung.physiology.org/cgi/content/full/276/3/L513.

217. **Rairigh RL**, **Storme L**, **Parker TA**, **Le Cras TD**, **Markham N**, **Jakkula M**, **Abman SH**. Role of neuronal nitric oxide synthase in regulation of vascular and ductus arteriosus tone in the ovine fetus. *Am J Physiol Lung Cell Mol Physiol* 278: L105-10, 2000.

218. **Ramiro-Diaz JM**, **Nitta CH**, **Maston LD**, **Codianni S**, **Giermakowska W**, **Resta TC**, **Gonzalez Bosc L V.** NFAT is required for spontaneous pulmonary hypertension in superoxide dismutase 1 knockout mice. *Am J Physiol Lung Cell Mol Physiol* 304: L613-25, 2013.

219. **Rampono J**, **Proud S**, **Hackett LP**, **Kristensen JH**, **Ilett KF**. A pilot study of newer antidepressant concentrations in cord and maternal serum and possible effects in the neonate. *Int J Neuropsychopharmacol* 7: 329–334, 2004.

220. **Ranjan V**, **Xiao Z**, **Diamond SL**. Constitutive NOS expression in cultured endothelial cells is elevated by fluid shear stress [Online]. *Am J Physiol Hear Circ Physiol* 269: H550–H555, 1995. http://www.ncbi.nlm.nih.gov/pubmed/7544542.

221. **Rashid N**, **Morin FC**, **Swartz DD**, **Ryan RM**, **Wynn KA**, **Wang H**, **Lakshminrusimha S**, **Kumar VH**. Effects of prostacyclin and milrinone on pulmonary hemodynamics in newborn lambs with persistent pulmonary hypertension induced by ductal ligation. *Pediatr Res* 60: 624–629, 2006.

222. **Rathore R**, **Zheng YM**, **Niu CF**, **Liu QH**, **Korde A**, **Ho YS**, **Wang YX**. Hypoxia activates NADPH oxidase to increase [ROS]i and [Ca2+]i through the mitochondrial ROS-PKCe signaling axis in pulmonary artery smooth muscle cells. *Free Radic Biol Med* 45: 1223–1231, 2008.

223. **Resnik ER**, **Keck M**, **Sukovich DJ**, **Herron JM**, **Cornfield DN**. Chronic intrauterine pulmonary hypertension increases capacitative calcium entry in fetal pulmonary artery smooth muscle cells. *Am J Physiol Lung Cell Mol Physiol* 292: L953–L959, 2007.

224. **Resta TC**, **Gonzales RJ**, **Dail WG**, **Sanders TC**, **Walker BR**. Selective upregulation of arterial endothelial nitric oxide synthase in pulmonary hypertension [Online]. *Am J Physiol Hear Circ Physiol* 272: H806–H813, 1997. http://www.ncbi.nlm.nih.gov/pubmed/9124442.

225. **Resta TC**, **O'Donaughy TL**, **Earley S**, **Chicoine LG**, **Walker BR**. Unaltered vasoconstrictor responsiveness after iNOS inhibition in lungs from chronically hypoxic rats. *Am J Physiol Lung Cell Mol Physiol* 276: L122–L130, 1999.

226. **Resta TC**, **Walker BR**. Chronic hypoxia selectively augments pulmonary arterial vasodilation. *Am J Physiol Hear Circ Physiol* 270: H888–H896, 1996.

227. **Robertson TP**, **Hague D**, **Aaronson PI**, **Ward JPT**. Voltage-independent calcium entry in hypoxic pulmonary vasoconstriction of intrapulmonary arteries of the rat. *J Physiol* 525: 669–680, 2000.

228. **Rosenberg AA**, **Kennaugh J**, **Koppenhafer SL**, **Loomis M**, **Chatfield BA**, **Abman SH**. Elevated immunoreactive endothelin-1 levels in newborn infants with persistent pulmonary hypertension [Online]. *J Pediatr* 123: 109–114, 1993. http://www.sciencedirect.com/science?_ob=ArticleURL&_udi=B6WKR-4JGGF4T-10&_user=10&_coverDate=07/31/1993&_rdoc=1&_fmt=&_orig=search&_sort=d&view=c&_acct=C000050221&_version=1&_urlVersion=0&_userid=10&md5=b3920f867b1b589e92b47808ff430ce4.

229. **Rossi GP**, **Seccia TM**, **Nussdorfer GG**. Reciprocal regulation of endothelin-1 and nitric oxide: relevance in the physiology and pathology of the cardiovascular system. [Online]. *Int Rev Cytol* 209: 241–72, 2001. http://www.ncbi.nlm.nih.gov/pubmed/11580202 [3 Jan. 2018].

230. **Russ RD**, **Walker BR**. Maintained endothelium-dependent pulmonary vasodilation following chronic hypoxia in the rat. *J Appl Physiol* 74: 339–344, 1993.

231. **Ruth V**, **Fyhrquist F**, **Clemons G**, **Raivio KO**. Cord plasma vasopressin, erythropoietin, and hypoxanthine as indices of asphyxia at birth. *Pediatr Res* 24: 490–494, 1988.

232. **Ruth V**, **Widness JA**, **Clemons G**, **Raivio KO**. Postnatal changes in serum immunoreactive erythropoietin in relation to hypoxia before and after birth. *J Pediatr* 116: 950–954, 1990.

233. **Santhosh KT**, **Sikarwar AS**, **Hinton M**, **Chelikani P**, **Dakshinamurti S**.

Thromboxane receptor hyper-responsiveness in hypoxic pulmonary hypertension requires serine 324. *Br J Pharmacol* 171: 676–687, 2014.

234. **Sharma S**, **Sud N**, **Wiseman DA**, **Lee Carter A**, **Kumar S**, **Hou Y**, **Rau T**, **Wilham J**, **Harmon C**, **Oishi P**, **Fineman JR**, **Black SM**. Altered carnitine homeostasis is associated with decreased mitochondrial function and altered nitric oxide signaling in lambs with pulmonary hypertension. *Am J Physiol Lung Cell Mol Physiol* 294: 46–56, 2008.

235. **Shaul PW**. Regulation of vasodilator synthesis during lung development. *Early Hum Dev* 54: 271–294, 1999.

236. **Shaul PW**, **Afshar S**, **Gibson LL**, **Sherman TS**, **Kerecman JD**, **Grubb PH**, **Yoder BA**, **McCurnin DC**. Developmental changes in nitric oxide synthase isoform expression and nitric oxide production in fetal baboon lung. *Am J Physiol Lung Cell Mol Physiol* 283: L1192–L1199, 2002.

237. **Shaul PW**, **North AJ**, **Brannon TS**, **Ujiie K**, **Wells LB**, **Nisen PA**, **Lowenstein CJ**, **Snyder SH**, **Star RA**. Prolonged in vivo hypoxia enhances nitric oxide synthase type I and type III gene expression in adult rat lung. *Am J Respir Cell Mol Biol* 13: 167–174, 1995.

238. **Shaul PW**, **Yuhanna IS**, **German Z**, **Chen Z**, **Steinhorn RH**, **Morin, Frederick C. 3rd**. Pulmonary endothelial NO synthase gene expression is decreased in fetal lambs with pulmonary hypertension. *Am J Physiol Lung Cell Mol Physiol* 16: L1005–L1012, 1997.

239. **Sheetz MJ**, **Aiello LP**, **Davis MD**, **Danis R**, **Bek T**, **Cunha-Vaz J**, **Shahri N**, **Berg PH**. The effect of the Oral PKC β inhibitor ruboxistaurin on vision loss in two phase 3 studies. *Investig Ophthalmol Vis Sci* 54: 1750–1757, 2013.

240. **Sherwood JB**. The chemistry and physiology of erythropoietin [Online]. *Vitam Horm* 41: 161–211, 1984. http://www.ncbi.nlm.nih.gov/pubmed/6397910 [6 Mar. 2017].

241. **Smith RAJ**, **Murphy MP**. Animal and human studies with the mitochondria-targeted antioxidant MitoQ. *Ann N Y Acad Sci* 1201: 96–103, 2010.

242. **Snow JB**, **Gonzalez Bosc L V.**, **Kanagy NL**, **Walker BR**, **Resta TC**. Role for PKC in enhanced endothelin-1-induced pulmonary vasoconstrictor reactivity following intermittent hypoxia. *Am J Physiol Lung Cell Mol Physiol* 301: L745–L754, 2011.

243. **Snow JB**, **Kitzis V**, **Norton CE**, **Torres SN**, **Johnson KD**, **Kanagy NL**, **Walker BR**, **Resta TC**. Differential effects of chronic hypoxia and intermittent hypocapnic and eucapnic hypoxia on pulmonary vasoreactivity. *J Appl Physiol* 104: 110–118, 2008.

244. **Soliman H**, **Gador A**, **Lu Y-H**, **Lin G**, **Bankar G**, **MacLeod KM**. Diabetes-induced increased oxidative stress in cardiomyocytes is sustained by a positive feedback loop involving Rho kinase and PKC 2. *Am J Physiol Hear Circ Physiol* 303: H989–H1000, 2012.

245. **Somlyo AP**, **Somlyo A V**. Ca2+ sensitivity of smooth muscle and nonmuscle myosin II: modulated by G proteins, kinases, and myosin phosphatase. *Physiol Rev* 83: 1325–58, 2003.

246. **Steinhorn RH**. Pharmacotherapy for pulmonary hypertension. *Pediatr Clin North Am* 59: 1129–1146, 2012.

247. **Stelzner TJ**, **O'Brien RF**, **Yanagisawa M**, **Sakurai T**, **Sato K**, **Webb SA**, **Zamora M**, **McMurtry IF**, **Fisher JH**. Increased lung endothelin-1 production in rats with idiopathic pulmonary hypertension [Online]. *Am J Physiol Lung Cell Mol Physiol* 262: L614–L620, 1992. http://www.ncbi.nlm.nih.gov/pubmed/1534203.

248. **Steudel W**, **Scherrer-Crosbie M**, **Bloch KD**, **Weimann J**, **Huang PL**, **Jones RC**, **Picard MH**, **Zapol WM**. Sustained pulmonary hypertension and right ventricular hypertrophy after chronic hypoxia in mice with congenital deficiency of nitric oxide synthase. *J Clin Invest* 101: 2468–2477, 1998.

249. **Storme L**, **Aubry E**, **Rakza T**, **Houeijeh A**, **Debarge V**, **Tourneux P**, **Deruelle P**, **Pennaforte T**. Pathophysiology of persistent pulmonary hypertension of the newborn: Impact of the perinatal environment. *Arch Cardiovasc Dis* 106: 169–177, 2013.

250. **Storme L**, **Parker TA**, **Kinsella JP**, **Rairigh RL**, **Abman SH**. Chronic hypertension impairs flow-induced vasodilation and augments the myogenic response in fetal lung [Online]. *Am J Physiol Lung Cell Mol Physiol* 282: L56–L66, 2002. http://www.ncbi.nlm.nih.gov/pubmed/11741816.

251. **Storme L**, **Rairigh RL**, **Parker TA**, **Kinsella JP**, **Abman SH**. In vivo evidence for a myogenic response in the fetal pulmonary circulation. *Pediatr Res* 45: 425–431, 1999.

252. **Su K**, **Bourdette D**, **Forte M**. Mitochondrial dysfunction and neurodegeneration in multiple sclerosis. *Front Physiol* 4 JUL: 1–10, 2013.

253. **Su Z**, **Tan W**, **Shandas R**, **Hunter KS**. Influence of distal resistance and proximal stiffness on hemodynamics and RV afterload in progression and treatments of pulmonary hypertension: A computational study with validation using animal models. *Comput Math Methods Med* 2013, 2013.

254. **Sud N**, **Sharma S**, **Wiseman DA**, **Harmon C**, **Kumar S**, **Venema RC**, **Fineman JR**, **Black SM**. Nitric oxide and superoxide generation from endothelial NOS: modulation by HSP90. *Am J Physiol Lung Cell Mol Physiol* 293: L1444–L1453, 2007.

255. **Sud N**, **Wells SM**, **Sharma S**, **Wiseman DA**, **Wilham J**, **Black SM**. Asymmetric dimethylarginine inhibits HSP90 activity in pulmonary arterial endothelial cells: role of mitochondrial dysfunction. *Am J Physiol Cell Physiol* 294: C1407–C1418, 2008.

256. **Sweazea KL**, **Walker BR**. Impaired myogenic tone in mesenteric arteries from overweight rats. *Nutr Metab (Lond)* 9: 18–27, 2012.

257. **Tábara LC**, **Poveda J**, **Martin-Cleary C**, **Selgas R**, **Ortiz A**, **Sanchez-Niño MD**. Mitochondria-targeted therapies for acute kidney injury. *Expert Rev Mol Med* 16: e13, 2014.

258. **Tang DD**, **Anfinogenova Y**. Physiologic properties and regulation of the actin cytoskeleton in vascular smooth muscle. *J Cardiovasc Pharmacol Ther* 13: 130–140, 2008.

259. **Tang DD**, **Gunst SJ**. The small GTPase Cdc42 regulates actin polymerization and tension development during contractile stimulation of smooth muscle. *J Biol Chem* 279: 51722–51728, 2004.

260. **Thébaud B**, **Abman SH**. Bronchopulmonary dysplasia: where have all the vessels gone? Roles of angiogenic growth factors in chronic lung disease. *Am J Respir Crit Care Med* 175: 978–85, 2007.

261. **Thébaud B**, **Ladha F**, **Michelakis ED**, **Sawicka M**, **Thurston G**, **Eaton F**, **Hashimoto K**, **Harry G**, **Haromy A**, **Korbutt G**, **Archer SL**. Vascular endothelial growth factor gene therapy increases survival, promotes lung angiogenesis, and prevents alveolar damage in hyperoxia-induced lung injury: Evidence that angiogenesis participates in alveolarization. *Circulation* 112: 2477–2486, 2005.

262. **Tourneux P**, **Chester M**, **Grover T**, **Abman SH**. Fasudil inhibits the myogenic response in the fetal pulmonary circulation. *Am J Physiol Hear Circ Physiol* 295: H1505–H1513, 2008.

263. **Townsley MI**. Structure and composition of pulmonary arteries, capillaries and veins. *Compr Physiol* 2: 675–709, 2012.

264. **Vallance P**, **Leiper J**. Cardiovascular biology of the asymmetric dimethylarginine:dimethylarginine dimethylaminohydrolase pathway. *Arterioscler Thromb Vasc Biol* 24: 1023–1030, 2004.

265. **Vallentin A**, **Prévostel C**, **Fauquier T**, **Bonnefont X**, **Joubert D**. Membrane targeting and cytoplasmic sequestration in the spatiotemporal localization of human protein kinase C alpha [Online]. *J Biol Chem* 275: 6014–6021, 2000. http://www.ncbi.nlm.nih.gov/pubmed/10681596.

266. **Vilos GA**, **Liggins GC**. Intrathoracic pressures in fetal sheep [Online]. *J Dev Physiol* 4: 247–56, 1982. http://www.ncbi.nlm.nih.gov/pubmed/7175122 [11 Mar. 2017].

267. **Vintzileos AM**, **Smulian JC**. Variability: Have We Overlooked the Significance of Longitudinal Fetal Heart Rate Changes for Detecting Intrapartum Fetal Hypoxia? *Am J Obstet Gynecol* 215: 261–264, 2016.

268. **Violin JD**, **Newton AC**. Pathway illuminated: visualizing protein kinase C signaling. *IUBMB Life* 55: 653–60, 2003.

269. **Voris JP**, **Sitailo LA**, **Rahn HR**, **Defnet A**, **Gerds AT**, **Sprague R**, **Yadav V**, **Caroline Le Poole I**, **Denning MF**. Functional alterations in protein kinase C beta II expression in melanoma. *Pigment Cell Melanoma Res* 23: 216–224, 2010.

270. **Wang G**, **Chen Z**, **Zhang F**, **Jing H**, **Xu W**, **Ning S**, **Li Z**, **Liu K**, **Yao J**, **Tian X**. Blockade of PKCβ protects against remote organ injury induced by intestinal ischemia and reperfusion via a p66shc-mediated mitochondrial apoptotic pathway. *Apoptosis* 19: 1342–1353, 2014.

271. **Wang J**, **Weigand L**, **Lu W**, **Sylvester JT**, **Semenza GL**, **Shimoda LA**. Hypoxia Inducible Factor 1 Mediates Hypoxia-Induced TRPC Expression and Elevated Intracellular Ca2+ in Pulmonary Arterial Smooth Muscle Cells. *Circ Res* 98: 1528–1537, 2006.

272. **Wang Q-S**, **Zheng Y-M**, **Dong L**, **Ho Y-S**, **Guo Z**, **Wang Y-X**. Role of mitochondrial reactive oxygen species in hypoxia-dependent increase in intracellular calcium in pulmonary artery myocytes. *Free Radic Biol Med* 42: 642–53, 2007.

273. **Watson RS**, **Clermont G**, **Kinsella JP**, **Kong L**, **Arendt RE**, **Cutter G**, **Linde-Zwirble WT**, **Abman SH**, **Angus DC**. Clinical and economic effects of iNO in premature newborns with respiratory failure at 1 year. *Pediatrics* 124: 1333–43, 2009.

274. **Watts SW**, **Yang P**, **Banes AK**, **Baez M**. Activation of Erk mitogen-activated protein kinase proteins by vascular serotonin receptors. *J Cardiovasc Pharmacol* 38: 539–551, 2001.

275. **Waypa GB**, **Schumacker PT**. Hypoxic pulmonary vasoconstriction: redox events in oxygen sensing. *J Appl Physiol* 98: 404–414, 2005.

276. **Wedgwood S**, **Bekker JM**, **Black SM**. Shear stress regulation of endothelial NOS in fetal pulmonary arterial endothelial cells involves PKC. *Am J Physiol Lung Cell Mol Physiol* 281: L490–L498, 2001.

277. **Wedgwood S**, **Black SM**. Endothelin-1 decreases endothelial NOS expression and activity through ETA receptor-mediated generation of hydrogen peroxide. *Am J Physiol Lung Cell Mol Physiol* 288: L480–L487, 2005.

278. **Wedgwood S**, **Lakshminrusimha S**, **Schumacker PT**, **Steinhorn RH**. Cyclic stretch stimulates mitochondrial reactive oxygen species and Nox4 signaling in pulmonary artery smooth muscle cells. *Am J Physiol Lung Cell Mol Physiol* 309: L196–L203, 2015.

279. **Wedgwood S**, **Mitchell CJ**, **Fineman JR**, **Black SM**. Developmental differences in the shear stress-induced expression of endothelial NO synthase: changing role of AP-1. *Am J Physiol Lung Cell Mol Physiol* 284: L650–L662, 2003.

280. **Wedgwood S**, **Steinhorn RH**. Role of Reactive Oxygen Species in Neonatal Pulmonary Vascular Disease. *Antioxid Redox Signal* 21: 1926–1942, 2014.

281. **Wedgwood S**, **Steinhorn RH**, **Bunderson M**, **Wilham J**, **Lakshminrusimha S**, **Brennan LA**, **Black SM**. Increased hydrogen peroxide downregulates soluble guanylate cyclase in the lungs of lambs with persistent pulmonary hypertension of the newborn. *Am J Physiol Lung Cell Mol Physiol* 289: L660–L666, 2005.

282. **Weir EK**, **Archer SL**. The mechanism of acute hypoxic pulmonary vasoconstriction: the tale of two channels [Online]. *FASEB J* 9: 183–9, 1995. http://www.ncbi.nlm.nih.gov/pubmed/7781921.

283. **Widness JA**, **Teramo KA**, **Clemons GK**, **Garcia JF**, **Cavalieri RL**, **Piasecki GJ**, **Jackson BT**, **Susa JB**, **Schwartz R**. Temporal response of immunoreactive erythropoietin to acute hypoxemia in fetal sheep. *Pediatr Res* 20: 15–19, 1986.

284. **Wojciak-Stothard B**, **Tsang LYF**, **Paleolog E**, **Hall SM**, **Haworth SG**. Rac1 and RhoA as regulators of endothelial phenotype and barrier function in hypoxia-induced neonatal pulmonary hypertension. *Am J Physiol Lung Cell Mol Physiol* 290: L1173–L1182, 2006.

285. **Xiao D**, **Huang X**, **Zhang L**. Chronic hypoxia differentially up-regulates protein kinase C-mediated ovine uterine arterial contraction via actin polymerization signaling in pregnancy. *Biol Reprod* 87: 142, 2012.

286. **Xiao D**, **Zhang L**. Adaptation of uterine artery thick- and thin-filament regulatory pathways to pregnancy. *Am J Physiol Hear Circ Physiol* 288: H142–H148, 2005.

287. **Xu EZ**, **Kantores C**, **Ivanovska J**, **Engelberts D**, **Kavanagh BP**, **McNamara PJ**, **Jankov RP**. Rescue treatment with a Rho-kinase inhibitor normalizes right ventricular function and reverses remodeling in juvenile rats with chronic pulmonary hypertension. *Am J Physiol Hear Circ Physiol* 299: H1854–H1864, 2010.

288. **Xu H**, **Jackson WF**, **Fink GD**, **Galligan JJ**. Activation of potassium channels by tempol in arterial smooth muscle cells from normotensive and deoxycorticosterone acetate-salt hypertensive rats. *Hypertension* 48: 1080–1087, 2006.

289. **Yamauchi K**, **Stone AJ**, **Stocker SD**, **Kaufman MP**. Blockade of ATP-sensitive potassium channels prevents the attenuation of the exercise pressor reflex by tempol in rats with ligated femoral arteries. *Am J Physiol Hear Circ Physiol* 303: H332–H340, 2012.

290. **Yanagisawa M**, **Kurihara H**, **Kimura S**, **Tomobe Y**, **Kobayashi M**, **Mitsui Y**, **Yazaki Y**, **Goto K**, **Masako T**. A novel potent vasoconstrictor peptide produced by vascular endothelial cells [Online]. *Nature* 332: 411–415, 1988. http://web.mit.edu/hst527/www/readings/Lecture 11/Nature.pdf [8 Mar. 2014].

291. **Zeller KS**, **Idevall-Hagren O**, **Stefansson A**, **Velling T**, **Jackson SP**, **Downward J**, **Tengholm A**, **Johansson S**. PI3-kinase p110alpha mediates beta1 integrin-induced Akt activation and membrane protrusion during cell attachment and initial spreading. *Cell Signal* 22: 1838–1848, 2010.

292. **Zeller KS**, **Riaz A**, **Sarve H**, **Li J**, **Tengholm A**, **Johansson S**. The Role of Mechanical Force and ROS in Integrin-Dependent Signals. *PLoS One* 8, 2013.

293. **Zhang W**, **Gunst SJ**. Interactions of airway smooth muscle cells with their tissue matrix: implications for contraction. *Proc Am Thorac Soc* 5: 32–39, 2008.

294. **Zhong XZ**, **Abd-Elrahman KS**, **Liao C-H**, **El-Yazbi AF**, **Walsh EJ**, **Walsh MP**, **Cole WC**. Stromatoxin-sensitive, heteromultimeric Kv2.1/Kv9.3 channels

contribute to myogenic control of cerebral arterial diameter. *J Physiol* 588: 4519–37, 2010.

295. **Zorov DB**, **Juhaszova M**, **Sollott SJ**. Mitochondrial Reactive Oxygen Species (ROS) and ROS-Induced ROS Release. *Physiol Rev* 94: 909–950, 2014.